Universidade de Lisboa

Faculdade de Farmácia

Evaluation of the therapeutic potential of several compounds in Human Herpesvirus 8 using a Chimera Virus Mouse Infection Model

Tânia Alexandra da Cruz Rodrigues

Dissertation supervised by Professor Doctor João Pedro Monteiro e Louro Machado de Simas and co-supervised by Professor Doctor José Miguel Azevedo Pereira

Master in Biopharmaceutical Sciences

2019

Universidade de Lisboa

Faculdade de Farmácia

Evaluation of the therapeutic potential of several compounds in Human Herpesvirus 8 using a Chimera Virus Mouse Infection Model

Tânia Alexandra da Cruz Rodrigues

Dissertation supervised by Professor Doctor João Pedro Monteiro e Louro Machado de Simas and co-supervised by Professor Doctor José Miguel Azevedo Pereira

Master in Biopharmaceutical Sciences

2019

Abstract

Kaposi's sarcoma-associated herpesvirus (KSHV), also known as human herpesvirus 8, is an infectious agent able to establish a lifelong infection in B cells of the host. KSHV is associated with several malignancies such as Kaposi's sarcoma (KS), primary effusion lymphoma (PEL), multicentric Castleman disease (MCD) and KSHV-associated inflammatory cytokine syndrome (KICS). The latent phase of the life cycle is responsible for the long-term persistence of the virus. KSHV latency-associated nuclear antigen (LANA) is an essential protein in the latent phase, regulating the transcription of both virus and host, genome replication and tumorigenesis and, given this, it is a potential target to clear latent infection. Nowadays, the conventional treatment of KSHV-associated malignancies is based on anti-tumour agents, which control the evolution of the disease but do not eliminate the KSHV infection. Since the discovery of effective drugs is imperative, a chimeric virus in which KSHV LANA (kLANA) was cloned in a murine herpesvirus 68 background, the mouse homologue of KSHV, was used to study kLANA as a target, to assess whether sulfathiazole, sulfanilamide, glybenclamide and JQ1 were able to eliminate persistence of the virus *in vivo*. Frequency of infection, capacity to establish latency by *ex vivo* reactivation assay and the infection on germinal centre (GC) B cells assessed by yellow fluorescent protein (YFP) expression were determined and analysed, after infection of mice and treatment with these drugs. Sulfathiazole, a drug that has been used as an antibiotic, showed to be very effective by impairing the formation of the murine double minute 2 (MDM2)-p53 complex, detaching the viral genome from the cellular DNA and diminishing viral infection *in vivo* using the chimeric mouse model of infection. Sulfanilamide has also been used as an antibiotic and, even though it has the same mechanism of action of sulfathiazole, it did not show a significant effect in clearing the viral infection but reduced the capacity of viral reactivation. Glybenclamide is broadly used in the management of diabetes mellitus type 2. It also reduces KSHV infection *in vitro*, possibly using a mechanism similar to that of both sulfathiazole and sulfanilamide. At the studied dose, glybenclamide did not display any effect and the viral infection was not affected. JQ1 is an inhibitor of bromodomain proteins, a family of proteins that allows the establishment of latency by the association of the viral genome with cellular chromatin and the transcription of the proto-oncogene *c-myc*, important to cell cycle progression, as well as to germinal centre formation and maintenance. JQ1 confirmed to be effective in reducing the GC B cells, but not specifically targeting latent virus. Since it decreased the number of GC B cells, including the infected cells, JQ1 was able to significantly reduce the level of systemic infection. In this study, two new effective approaches against the viral infection *in vivo*, sulfathiazole and JQ1, were discovered. Although the known molecular mechanism of action of the drugs is different, both drugs revealed to be promising for treating patients with KSHV infection.

Keywords: KSHV; LANA; Latency; Antivirals; *In vivo*.

Resumo

O herpesvírus associado ao sarcoma de Kaposi (KSHV, em inglês), também denominado por herpesvírus humano 8, é um agente infeccioso com a capacidade de estabelecer uma infeção latente vitalícia nas células B do hospedeiro. Este vírus está associado a várias doenças, tais como o sarcoma de Kaposi e a doença de Castleman, e está amplamente disperso pelo mundo. O ciclo de vida é constituído por duas fases: lítica e latente. A fase latente é responsável pela persistência vitalícia do vírus. Embora nesta fase a expressão génica seja bastante limitada, o antigénio nuclear associado à latência (LANA, em inglês) do KSHV (kLANA, em inglês), é expresso abundantemente, sendo uma proteína essencial da fase latente. kLANA é responsável por regular vários processos a nível celular, tais como a transcrição, tanto do vírus como do hospedeiro, a replicação do genoma viral, a reativação lítica, entre outros. Desta forma, kLANA controla a latência do KSHV.

Atualmente, o tratamento convencional para as doenças associadas ao KSHV é baseado em agentes anti-tumorais que, apesar de controlarem a evolução da doença, não eliminam a infeção viral. Tendo em conta a epidemiologia e a severidade das doenças associadas ao KSHV, novos fármacos que tenham a capacidade de eliminar a infeção são urgentes. No entanto, a inexistência de um modelo adequado *in vivo* tem limitado o estudo do KSHV. Face a isto, em 2017 foi desenvolvido um vírus quimérico em que, no genoma do herpesvírus murino 68 (MHV-68), o vírus homólogo de murganho do KSHV, foi substituído o MHV-68 LANA (mLANA) pelo kLANA. Este vírus quimérico permite estudar kLANA como um alvo terapêutico para eliminar a persistência do vírus *in vivo*.

Sulfatiazol e sulfanilamida são dois fármacos que têm sido utilizados como antibióticos. Foi descoberto, *in vitro*, que podem ser eficazes na eliminação da infeção pelo KSHV, afetando a formação do complexo murino duplo minuto 2 (MDM2)-p53, que inativa a p53 e permite a ligação e estabilização do kLANA ao DNA celular.

Glibenclamida é um fármaco atualmente muito utilizado para controlar a diabetes mellitus tipo 2 e que demonstrou ter efeito no KSHV, *in vitro*, sendo também capaz de eliminar a infeção. Embora ainda sejam necessários estudos para esclarecer o mecanismo de ação da glibenclamida, pensa-se que atua da mesma forma que o sulfatiazol e a sulfanilamida, no complexo MDM2-p53.

JQ1 é inibidor de bromodomínios (BRD), uma família de proteínas que está envolvida na transcrição de *c-myc*. *c-myc* é um proto-oncogene importante para a formação e manutenção de centros germinais, assim como para o ciclo celular. Para além disso, as proteínas BRD permitem o estabelecimento de latência, associando o genoma viral à cromatina celular.

Após a infeção dos murganhos com o vírus quimérico, a eficácia dos fármacos foi avaliada através da determinação da frequência de infeção, quantificação da infeção em centros germinais por expressão da proteína amarela fluorescente (YFP, em inglês) e análise da capacidade de estabelecer latência através de ensaio de reativação *ex vivo*.

Neste estudo, sulfatiazol foi testado em três doses diferentes, 0,25 mg/g de peso corporal, 0,5 mg/g e 1 mg/g. A dose de 0,25 mg/g apresentou uma taxa de sobrevivência de 100%, sem sinais de toxicidade A frequência de infeção, a percentagem de células infetadas nas células GC B pela expressão de YFP e a capacidade de estabelecer latência apresentaram uma diminuição significativa, demonstrando que, nessa dose, o sulfatiazol é eficaz na eliminação da infeção viral. O aumento da dose para 0,5 mg/g apresentou uma diminuição da latência nos três ensaios realizados, em comparação com

o controlo, e uma taxa de sobrevivência de 100%, também sem sinais de toxicidade. Apenas na frequência de infeção foi observado um decréscimo menor do que com 0,25 mg/g, sendo que nos outros ensaios esta dose demonstrou ser mais eficaz que a dose de 0,25 mg/g. No entanto, com 1 mg/g, a taxa de sobrevivência desceu para 30%, sendo esta dose altamente tóxica. Os resultados obtidos demonstraram uma diminuição significativa da latência viral face ao controlo, apesar da referida redução ser menor do que com 0,5 mg/g, exceto a frequência de infeção. Desta forma, foi concluído que o sulfatiazol é um fármaco eficaz em diminuir a infeção do vírus kLANA.yfp em todas as doses testadas. Na medida em que a dose deve ser obrigatoriamente menor que 1 mg/g, dada a toxicidade associada, e de acordo com os resultados significativos obtidos em 0,25 mg/g e 0,5 mg/g, a dose ideal será igual ou superior a 0,25 mg/g e menor que 1 mg/g.

Sulfanilamida foi testada a 0,25 mg/g e a 1 mg/g. A 0,25 mg/g, não se registou nenhum sinal de toxicidade, bem como nenhuma alteração face ao controlo, em todos os ensaios. O aumento para 1 mg/g diminuiu a taxa de sobrevivência para 90%, no entanto os resultados foram significativamente melhores do que com apenas 0,25 mg/g, tendo sido observada uma diminuição significativa face ao controlo, no ensaio de reativação. Por outro lado, a frequência de infeção apresentou uma pequena diminuição e o percentual de células infetadas nas células GC B também teve uma redução, apesar de não ter atingido significância estatística. Assim sendo, pensa-se que a sulfanilamida não tenha efeito na eliminação da infeção viral, sendo apenas capaz de afetar a capacidade de reativação do vírus. Concluiu-se, também, que a dose apropriada para ensaios futuros terá de ser maior que 0,25 mg/g e, dada a toxicidade, obrigatoriamente menor que 1 mg/g.

A glibenclamida foi testada a 0,005 mg/g de modo a evitar um efeito letal, dado ser um fármaco hipoglicémico. Embora a taxa de sobrevivência tenha sido 100%, foram observados sinais de toxicidade nesta dose. Para além disso, não foram obtidos resultados significativos nos três ensaios, concluindo que o fármaco não teve efeito na infeção latente.

JQ1 foi administrado a 0,05 mg/g e a taxa de sobrevivência obtida foi 100%. Foi observada uma diminuição estatisticamente significativa na capacidade do vírus em estabelecer latência, demonstrada em todos os ensaios realizados. Foi também detetada uma redução no número de esplenócitos totais e de centros germinais. No entanto, ao avaliar a percentagem de células infetadas do centro germinal, observou-se uma diminuição estatisticamente não significativa, e a percentagem de células infetadas com fenótipo de centro germinal permaneceu semelhante. Com base nisso, e sabendo que JQ1 afeta a transcrição de *c-myc*, essencial para a formação e manutenção de centros germinais, os centros germinais foram isolados e foi determinada a frequência de células positivas para DNA viral em centros germinais. O resultado obtido foi concordante e confirmou o que tinha sido concluído nos primeiros ensaios, não tendo sido observado um decréscimo muito elevado na frequência de infeção em centros germinais. Foi também realizada uma hibridação *in situ*, de forma a analisar as células infetadas. Foi observada uma diminuição no tamanho das secções do baço de murganho tratados com JQ1, afetando a área, embora o perímetro não tenha sido afetado, uma vez que a diminuição é maior na largura. Apesar de o número de folículos registados ter sido semelhante ao controlo, o tamanho foi significativamente menor (tanto na área como no perímetro), tal como esperado, uma vez que os murganhos tratados com JQ1 apresentam menos centros germinais. Por fim, observou-se uma diminuição estatisticamente significativa nos folículos positivos para RNA viral (com, pelo menos, uma célula infetada), mostrando que a infeção está diminuída devido ao facto de haver

menos centros germinais. Desta forma, concluiu-se que o JQ1 aparenta afetar somente o número de centros germinais, o que leva a uma consequente diminuição generalizada da infeção, embora não afete o vírus nem a infeção latente.

Neste estudo, duas novas abordagens eficazes contra a infeção viral foram descobertas. Embora o mecanismo de ação dos fármacos seja diferente, tanto o sulfatiazol como o JQ1 revelaram ser promissores para o tratamento de pacientes infetados pelo KSHV.

Palavras-Chave: KSHV; LANA; Latência; Antivirais; *In vivo.*

Acknowledgements (Agradecimentos)

Primeiramente, ao Professor Pedro, meu orientador, por ter permitido que exercesse a minha paixão por farmacologia, ainda que esta abordagem não se inserisse nos objetivos do laboratório. Obrigada pela oportunidade, por todos os ensinamentos e disponibilidade. Foi incrível desenvolver esta tese!

Ao Miguel. Por toda a paciência e apoio, por todas as vezes em que acreditaste em mim quando eu não acreditei. Por teres estado lá, às 3h da manhã, ao meu lado, quando só me apetecia desistir e ir para casa. Por me animares em todos os finais de tarde quando saía desnorteada do lab. Por todas as vezes em que me limpaste as lágrimas. Por teres sempre a única palavra amiga que me consegue levantar. Por tudo, obrigada! Juro por nós que, sem ti, não tinha conseguido. Metade desta tese é tua.

Ao Fael e aos meus pais. Obrigada por me terem aturado quando estava insuportável, por terem continuado a perguntar sobre a tese quando a minha resposta era sempre "não me apetece falar sobre isso agora" e por aceitarem tão bem a possibilidade de só sair de casa aos 30 por me meter em áreas em que vou para o desemprego, são os maiores! (Ah, e obrigada por pagarem as propinas, sem isso de certeza que não tinha sido possível).

Ao resto da minha família, principalmente ao meu avô Augusto, muito obrigada por todo o apoio e carinho, e por reconhecer sempre todo o esforço envolvido nisto.

À Anita, Catarina e Andreia, não há palavras para vocês! Obrigada por terem sido a melhor companhia este ano! Por toda a ajuda, gargalhadas, conversas e choro partilhado. Por não me terem levado a sério quando fui pessimista e por terem deixado bilhetes encorajadores ao sábado de manhã. Sem vocês não tinha conseguido aguentar este ano!

À Marta Miranda, por toda a ajuda, orientação, paciência e ensinamentos ao longo deste ano.

Ao Fabrizio Angius, por esclarecer todas as dúvidas e estar sempre disponível, tal como um orientador.

Ao professor José Pereira, meu co-orientador, por ter sido sempre tão amável e disponível.

A todos os meus amigos, a todos vocês que mereciam tanto que escrevesse o nome individual de cada um. A todos os que me ajudaram a abstrair fim-de-semana após fim-de-semana e que, mesmo sem perceberem o que eu dizia, perguntavam sempre como estava a correr. A todos o que me ouviram a lamentar vezes sem conta e disseram sempre "já está quase, vai correr tudo bem". A todos os que me obrigaram a escrever a tese e a todos os que foram para a biblioteca comigo. A todos os que a primária, o básico, o secundário, a FCUL e a FFUL me deram, e a todos os aleatórios que não sei de onde vieram, e que continuam cá, ao meu lado. E a todos os ativistas que puseram a nossa amizade acima do que eu fazia aos ratinhos. Cliché, mas vocês são os melhores amigos do mundo! Sem vocês e as vossas palavras de motivação eu não tinha conseguido chegar ao fim deste mestrado.

♥ A todos vocês, um obrigada gigante do fundo do coração.

Tânia

Contents

List of Figures

List of Tables

List of Abbreviations

AIDS	Acquired immunodeficiency syndrome
AKT	Protein kinase B
AP	Alkaline phosphatase
ATP	Adenosine triphosphate
BET	Bromodomain and extraterminal domain
BHK	Baby hamster kidney
BHK-21	BHK strain 21
BRD	Bromodomain
cART	Combination antiretroviral therapy
CSR	Class switch recombination
CWS	Cell working stock
DBD	DNA binding domain
DE	Delayed-early
dH_2O	Distilled H_2O
DIG	Digoxigenin
DMSO	Dimethyl sulfoxide
DNA	Deoxyribonucleic acid
Dpi	Days post-infection
DSB	DNA double-strand break
dsDNA	Double-stranded DNA
DTT	Dithiothreitol
EBV	Epstein-Barr virus
EDTA	Ethylenediamine tetraacetic acid
FBS	Fetal bovine serum
G+C	Guanine and cytosine
GC	Germinal centre
GFP	Green fluorescent protein
GMEM	Glasgow minimum essential medium
HCMV	Human cytomegalovirus
HHV-6	Human herpesvirus 6
HHV-7	Human herpesvirus 7
HHV-8	Human herpesvirus 8
HIV	Human immunodeficiency virus

HRP	Horse radish peroxidase
HSV-1	Herpes simplex virus type 1
HSV-2	Herpes simplex virus type 2
HVS	Herpesvirus saimiri
ICA	Infectious centre assay
ICTV	International Committee on Taxonomy of Viruses
IE	Immediate-early
IFN-α	Interferon alpha
IRIS	Immune reconstitution inflammatory syndrome
KICS	KSHV-associated inflammatory cytokine syndrome
kLANA	KSHV latency-associated nuclear antigen
KS	Kaposi's sarcoma
KSHV	Kaposi's sarcoma-associated herpesvirus
L	Late
LANA	Latency-associated nuclear antigen
LBS	kLANA binding site
LUR	Long unique coding region
LZ	Leucine zipper
MCD	Multicentric Castleman disease
MDM2	Murine double minute 2
MHV-68	Murine herpesvirus 68
mLANA	MHV-68 latency-associated nuclear antigen
MOI	Multiplicity of infection
miRNA	Micro RNA
MZ	Marginal zone
NBT	Nitroblue tetrazolium chloride
ncRNA	Non-coding RNA
NHEJ	Non-homologous end joining
ns	Non-significant
O/N	Overnight
ORF	Open reading frame
Ori-P	Origin of replication
PABA	*Para*-aminobenzoic acid
PBS	Phosphate buffered saline
PBS-T	PBS+0.05% Tween-20

PCR	Polymerase chain reaction
PEL	Primary effusion lymphoma
PFU	Plaque forming unit
RBL	Red blood cell lysis buffer
RE	Replication element
RNA	Ribonucleic acid
RNase	Ribonuclease
rpm	Revolutions per minute
RT	Room temperature
RTA	Replication and transcription activator
SDS	Sodium dodecyl sulphate
SDS-PAGE	Sodium dodecyl sulphate-polyacrylamide gel electrophoresis
SHM	Somatic hypermutation
SHPM	Single-hit Poisson model
siRNA	Small interfering RNA
SSC	Saline sodium citrate
TEMED	Tetramethylethylenediamine
TGS	Tris-Glycine-SDS
TPB	Tryptose phosphate broth
TR	Terminal repeat
tRNA	Transfer RNA
v-cyclin	Viral cyclin
v-FLIP	Viral Fas-associated death domain-like interleukin-1β-converting enzyme-inhibitory protein
v-GPCR	Viral G protein-coupled receptor
v-miRNA	Viral micro RNA
v-ORF	Viral open-reading frame
v-tRNA	Viral transfer RNA
VEGF	Vascular endothelial growth factor
VZV	Varicella-zoster virus
WSM	Working stock media
YFP	Yellow fluorescent protein

1. Introduction

1.1. Virus

A virus is an infectious agent that needs living cells to replicate. According to Baltimore classification, viruses are divided in seven groups, varying in several properties, such as the type of nucleic acid (deoxyribonucleic acid (DNA), ribonucleic acid (RNA) or both, at different stages of the life cycle), shape (linear, circular or segmented), strandedness (single, double or both), sense (positive, negative or both – ambisense), and the use or not of reverse transcriptase (Baltimore, 1971).

Virion is the infectious particle designed for the transmission of the viral genome. A typical virion consists in an external protein shell, capsid, and an internal core of nucleic acid. While the capsid adds specificity to the virus, the genetic material provides infectivity (Forterre, 2010). The characteristics of the virion vary according to the virus (Forterre, 2010).

1.2. *Herpesviridae*

Herpesviridae is a family of viruses characterized by a large double-stranded DNA (dsDNA) genome and the capacity of maintaining their genomes in a latent state in the nucleus of distinct cells for the life of the host (Mettenleiter *et al*., 2009). An architecturally similar virion is another characteristic that herpesviruses, denomination given to the members of *Herpesviridae* family, have in common. A typical herpesvirus virion consists in a core containing a linear double stranded DNA, an extremely ordered icosahedral shape nucleocapsid, surrounded by a semi-ordered tegument (the space between the envelope and nucleocapsid which contains proteins and RNAs), and a lipid bilayer envelope containing viral glycoprotein spikes on its surface, accountable for viral connection and entry to host cells (Figure 1.1.) (Bândea, 1983; Forterre, 2010).

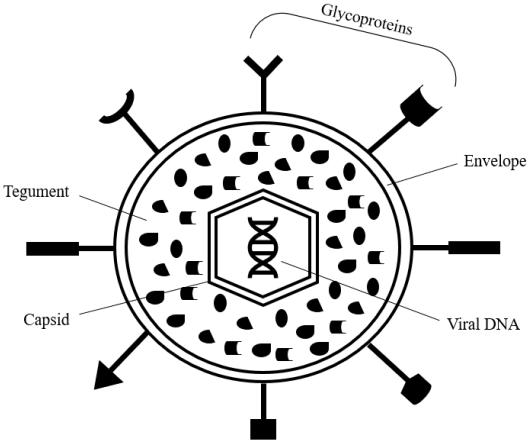

Figure 1. 1. Schematic representation of the multilayer organization of herpesvirus (Adapted from Prasad and Schmid, 2012).

Herpesvirus are largely disseminated in nature and there are more than a hundred herpesviruses identified. Eight herpesviruses have been isolated from humans (Table 1.1.). It is known that there was a co-evolution of herpesviruses and their hosts, so they are very well adapted to each one of them (Davison *et al*., 2002).

One of the characteristics of herpesviruses is the transition of their life cycle between the latent and the lytic phase (Jenner *et al*., 2001). The virus has the ability to establish a quiescent infection, in which it stays dormant within the host cell and there is no replication – latent phase. The virus can reactivate and start producing huge quantities of viral progeny without the host being infected by new external virus – lytic phase (Traylen *et al*., 2011). However, this phase is deleterious for the virus, since a dynamic replication will tend to induce the immune system of the host or internal cell signalling that lead to the death of the infected cell. The transition between phases involves several changes at cellular level. The latent phase is characterized by circularized viral genome that forms episomal DNA element packed in histones (Deshmane and Fraser, 1989; Grinde, 2013). Furthermore, the viral DNA is copied by cellular DNA polymerases along with the chromosomes when the cell engages in mitosis. There are also some mechanisms for the silencing of viral genes, such as specific methylation programs and packaging of the DNA in particular types of histones (Wilson and Mohr, 2012). So, the production of viral proteins stays reduced to a minimum in order to escape from the immune system of the host. However, the genome is not completely silenced due to its necessity to maintain long-term latency (Amon and Farrell, 2005; Calderwood *et al*., 2007; Klein *et al*., 2007). On the other hand, there is an evident takeover of the cell in the lytic phase: viral genome is linearized, viral DNA is copied by the viral DNA polymerase and viral proteins are largely produced (Wilson and Mohr, 2012). Nevertheless, during chronic infection there may also occur the production of infectious viruses at the sites of persistent infection, allowing transmission to new hosts.

According to the International Committee on Taxonomy of Viruses (ICTV), the *Herpesviridae* family belongs to the order *Herpesvirales*, along with *Alloherpesviridae* and *Malacoherpesviridae* families. *Herpesviridae* family is divided in three subfamilies (i) *Alphaherpesvirinae*, (ii) *Betaherpesvirinae* and (iii) *Gammaherpevirinae*, that vary in the main site of latent infection, as listed in Table 1.1..

Table 1. 1. Human herpesvirus and some of their characteristics (Adapted from Davison, 2010).

Virus	Abbreviation	ICTV species name	Subfamily	Main site of latent infection	Genome size (kbp)
Herpes simplex virus type 1	HSV-1	Human herpesvirus 1	*Alpha Herpesvirinae*	Sensory nerve ganglia	≅ 152
Herpes simplex virus type 2	HSV-2	Human herpesvirus 2			≅ 154
Varicella-zoster virus	VZV	Human herpesvirus 3			≅ 125
Human Cytomegalovirus	HCMV	Human herpesvirus 5	*Beta Herpesvirinae*	Secretory glands, kidneys and cells of the reticuloendothelial system	≅ 230
Human herpesvirus 6	HHV-6	Human herpesvirus 6			≅ 159
Human herpesvirus 7	HHV-7	Human herpesvirus 7			≅ 144
Epstein-Barr virus	EBV	Human herpesvirus 4	*Gamma Herpesvirinae*	B cells	≅ 171
Kaposi's sarcoma-associated herpesvirus	KSHV	Human herpesvirus 8			≅ 140

Besides the site of latent infection, the members of this family also differ significantly in some properties such as the features of their DNAs, content and linear arrangement of the genes in viral genomes, host range, duration of the replication cycle and the mechanism by which the viruses maintain the latent state in the host (Davison, 2010).

1.3. The *Gammaherpesvirinae* subfamily

The *Gammaherpesvirinae* subfamily includes four genera based on genomic organization and DNA homology: *Lymphocryptovirus* (gamma-1-herpesvirus), *Rhadinovirus* (gamma-2-herpesvirus), *Macavirus* and *Percavirus* (Simas and Efstathiou, 1998). In humans, two gammaherpesviruses have been identified: Epstein-Barr virus (EBV), that belongs to genus *Lymphocryptovirus*, and Kaposi's sarcoma-associated herpesvirus (KSHV), included in genus *Rhadinovirus* (Baer *et al*., 1984; Davison *et al*., 2009). Likewise, the murine herpesvirus 68 (MHV-68), the mouse homologue of KSHV, also belongs to *Rhadinovirus* (Virgin IV *et al*., 1997).

Gammaherpesvirinae, similarly to all the herpesvirus, encodes several genes that can manipulate the host cell machinery and establish a lifelong infection. The main site of latent infection of gammaherpesviruses is the nucleus of lymphoid cell populations, particularly B cells, where the viral episome is maintained in the nucleus and replicated along with cellular mitosis (Damania, 2004; Barton *et al*., 2011). Thereby, both EBV and KSHV induce lymphoproliferative diseases and lymphomas in hosts with a compromised immune system (Nash *et al*., 2001; Cesarman, 2011). EBV and KSHV are also related with the development of human cancers, which distinguishes themselves from other viruses (Wen and Damania, 2010).

1.3.1. Kaposi's sarcoma-associated herpesvirus

Kaposi's sarcoma-associated herpesvirus, also known as human herpesvirus 8, is a member of *Gammaherpesvirinae* subfamily and the infectious agent responsible for Kaposi's sarcoma (KS).

KS is a tumour of endothelial cell lineage with an inflammatory component and characterized by cutaneous, visceral, and mucosal lesions. Due to the characteristic lesions, KS was first described in 1872 by Moritz Kaposi as an idiopathic multiple pigmented sarcoma. More than a century later, in 1994, KSHV was discovered by Chang and colleagues and only then described as the cause of KS (Chang *et al*., 1994).

KSHV has a genome of approximately 165 kbp that consists in nearly 140 kbp of a long unique coding region (LUR) that is flanked by a guanine and cytosine (G+C)-rich long terminal repeat (TR) sequence with 801 bp, that encodes for approximately 86 viral open-reading frames (v-ORF), 12 microRNAs (miRNA), non-coding RNAs (ncRNA) and antisense RNAs (Figure 1.2.) (Renne *et al*., 1996; Russo *et al*., 1996; Juillard *et al*., 2016).

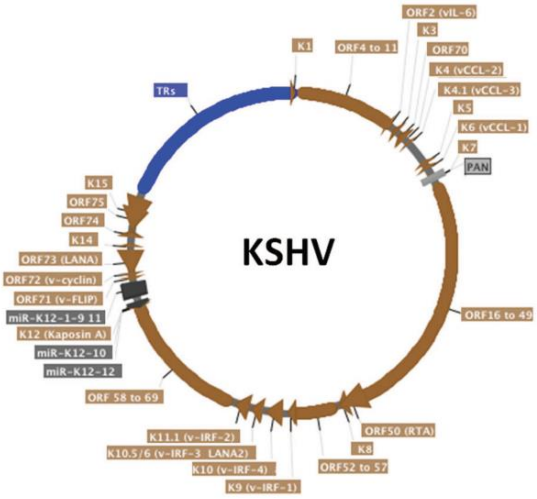

Figure 1. 2. Schematic representation of the KSHV genome. TRs (blue), v-ORFs (brown), miRNAs (dark gray) and ncRNAs (light gray) are represented. Alternative protein names are written in parenthesis. Arrows indicate transcription direction (From Juillard *et al*., 2016).

Like other herpesvirus, the virion has an icosahedral capsid, a tegument and an envelope that contains glycoproteins that interact with cell-type specific cellular entry receptors (Damania and Cesarman, 2013; Kumar and Chandran, 2016).

Since KSHV is able to infect more than one cell type (mainly B cells, but also endothelial cells, monocytes, epithelial cells and keratinocytes), it is thought that KSHV interacts with ubiquitous cellular molecules (Chakraborty *et al*., 2012). From this interaction results the delivery of the virion capsid into the cytoplasm, after viral envelope fusion with plasma or endosome membrane where it is uncoated. Then, the genome is transferred to the nucleus where its circularization occurs using the cellular enzymatic machinery. It remains as an episome, entering in a latent state and, consequently, escaping from the DNA-sensing mechanisms of the host (Spear and Longnecker, 2003; Uppal *et al*., 2015). Sporadically, the virus has bouts of lytic reactivation (Bechtel *et al*., 2003).

1.3.1.1. Lytic phase

The lytic phase allows the replication of the viral genome as well as the production of infectious viral progeny. During the reactivation, the viral genome is linearized, the viral DNA is copied and there are viral genes that are expressed in a chronological order and that can be divided in three groups: immediate-early (IE) genes, delayed-early (DE) genes and late (L) genes (Wilson and Mohr, 2012; Damania and Cesarman, 2013; Purushothaman *et al.*, 2016). IE genes are responsible for controlling transcription. Furthermore, the principal lytic protein, replication and transcription activator (RTA), is encoded by an IE gene. RTA is a transcription factor, encoded by open reading frame (ORF) 50, that triggers several cellular and viral promoters and guarantees the expression of essential viral genes for viral replication (Damania and Cesarman, 2013; Thakker and Verma, 2016). DE genes are expressed after IE genes and encode proteins related with viral DNA replication, a mechanism that occurs after the DE genes phase and produces linear genomes that are packaged into capsids (Damania and Cesarman, 2013). L genes encode all the viral structural proteins, concluding the process of the production of infectious viruses.

Some genes are responsible for blocking innate and adaptative recognitions of the host (Kwun *et al.*, 2007). There are also genes that contribute to tumorigenesis, encoding proteins that damage non-homologous end joining (NHEJ) repair mechanism or inducing DNA double-strand breaks (DSB) (Damania and Cesarman, 2013; Xiao *et al.*, 2013; Purushothaman *et al.*, 2016).

1.3.1.2. Latent phase

The capacity of entering in a latent phase is the characteristic that allows KSHV to maintain a lifelong infection, remaining hidden from the host. To achieve this, the virus keeps the genome circularized, downregulates some cell surface markers typically detected by the immune system of the host, and maintains an extremely limited gene expression (only the genes located in the latency locus are expressed) (Cai *et al.*, 2010; Cesarman *et al.*, 2019). The latency locus is composed by four ORF: ORF71, also called ORFK13, that encodes the viral Fas-associated death domain-like interleukin-1β-converting enzyme-inhibitory protein (v-FLIP); ORF72, that encodes the viral cyclin (v-cyclin) D homolog; ORF73, that encodes latency-associated nuclear antigen (LANA); and ORFK12, that encodes kaposins (A, B and C), signalling proteins. Besides these, there are also some miRNAs that are expressed in this phase, promoting endothelial cell reprogramming, migration and invasion of endothelial cells by activating protein kinase B (AKT) - miR-K12-3 – and impairing the synthesis of RTA to prevent reactivation from latency - miRK9* - (Sarid *et al.*, 1998; Cai *et al.*, 2005; Bellare and Ganem, 2009; Cai *et al.*, 2010; Hansen *et al.*, 2010; Hu *et al.*, 2015). Since miRNAs cannot be identified by the immune system, their expression represents an efficient mechanism for the persistence of KSHV (Coscoy, 2007; Mesri *et al.*, 2010).

LANA, v-cyclin and v-FLIP promote tumorigenesis by interfering with some pathways responsible for cell growth and apoptosis, and by inhibiting tumour suppressors. These mechanisms are essential for the persistence of the virus, once the replication of viral genome occurs at the same time of the replication of cellular genome, so the G1/S checkpoint arrest and apoptotic programs have to be inhibited in order to allow the persistence of the viral infection (Dittmer, 1998; Moore and Chang, 2003). v-FLIP promotes vascular proliferation, as well as an inflammatory phenotype in endothelial cells (Ballon *et al*., 2015). However, in contrast to lytic genes being expressed in a very low proportion of tumour cells, latent genes are expressed in all tumour cells (Damania and Cesarman, 2013).

The interchange between latent and lytic phases is triggered by certain physiological and environmental factors, such as oxidative stress, hypoxia, co-infection, inflammation, host immune suppression and pharmacological agents, being controlled by the interplay of RTA and LANA (Figure 1.3.) (Cai *et al*., 2010; Purushothaman *et al*., 2016). A perfect balance between the two life cycle phases is essential for the lifelong persistence of the virus (Ohsaki and Ueda, 2012; Purushothaman *et al*., 2016).

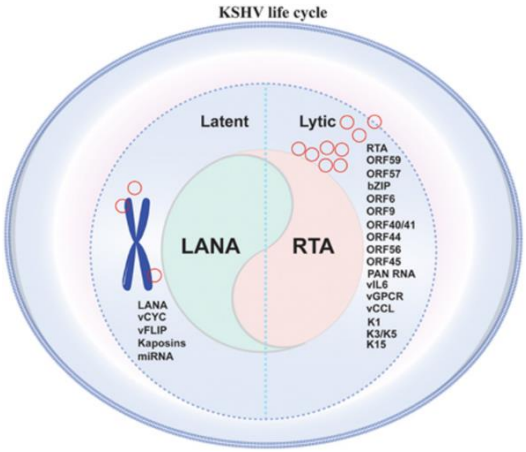

Figure 1. 3. Representation of the two phases of KHSV life cycle, regarding the genes expressed in each phase (From Purushothaman *et al*., 2016).

1.3.1.2.1. KSHV latency-associated nuclear antigen

KSHV latency-associated nuclear antigen (kLANA) is a dimer protein encoded by the ORF73 and it is an essential protein expressed during latent phase (Purushothaman *et al.*, 2016). It is a 1162 amino acid protein constituted by several parts: a proline-rich N-terminal domain; an internal repeat region constituted by aspartate-glutamate, glutamine, and glutamate-glutamine regions; a predicted leucine zipper; and a C-terminal DNA binding domain (Figure 1.4.) (Komatsu *et al.*, 2004; Uppal *et al*., 2014).

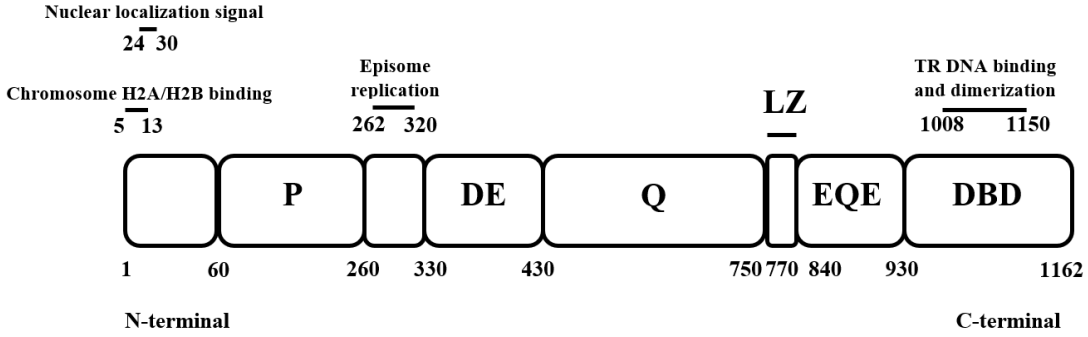

Figure 1. 4. Schematic representation of kLANA protein, divided by the different parts which constitute it, namely the proline-rich (P), the aspartate and glutamate (DE), the glutamine (Q), the leucine zipper (LZ), the glutamate and glutamine (EQE) and the DNA binding domain (DBD) regions. Numbers indicate amino acid residues (Adapted from Piolot *et al.*, 2001, De Leon Vazquez *et al*., 2013, Ponnusamy *et al.*, 2015).

kLANA is vital for the long-term persistence of viral episome, being responsible for the segregation and replication of TR-containing plasmids in proliferating cells by acting directly on the TR of the virus (Ballestas *et al*., 1999; Ye *et al.*, 2004). Through its N-terminal domain, a flexible and disordered region, kLANA is attached to the cell chromosomes via histones H2A and H2B, on the surface of the nucleosome (Figure 1.5.) (Decker *et al.*, 1996; Ballestas *et al*., 1999; Ballestas & Kaye, 2001; Barbera *et al.*, 2006). C-terminal, a stable and ordered region, contains a DNA binding domain that recognizes two kLANA binding sites (LBS) located in the terminal repeats of the episome – LBS-1 and LBS-2 – to which kLANA binds. There is LBS-3, also designated by replication element (RE). It is thought that the LBS-RE constitutes the latent DNA origin of replication (ori-P) (Ueda, 2012). The internal region is the less studied, but it was found that it adds stability to kLANA, decelerates protein synthesis, suppresses proteosomal degradation and it is also related with the efficiency of DNA replication (Kwun *et al*., 2007; De Leon Vazquez *et al.*, 2013). Among KSHV strains, the length of the internal repeat region varies, resulting in kLANA molecules with different sizes (Gao *et al.*, 1999).

The interaction with both mitotic chromosomes and viral episome is essential for viral persistence, since it allows passive segregation of viral DNA to progeny nuclei during mitosis and maintenance of a stable copy number in latently infected cells (Figure 1.5.) (Ballestas & Kaye, 2001; Uppal *et al.*, 2014). kLANA is also essential for several processes that involve cellular machinery, such as the replication of the episome, recruiting host cell DNA replication system (Sun *et al.*, 2014); modulation of host cell gene expression, interacting with transcription factors (Uppal *et al.*, 2014); and regulation of cell growth and survival, interacting with cellular proteins (Verma *et al.*, 2007). Moreover, the maintenance of viral latency is responsibility of kLANA, that acts by repressing the transcriptional activity of RTA. kLANA can regulate these processes by modulating both cellular and viral gene expression (Lan *et al.*, 2004).

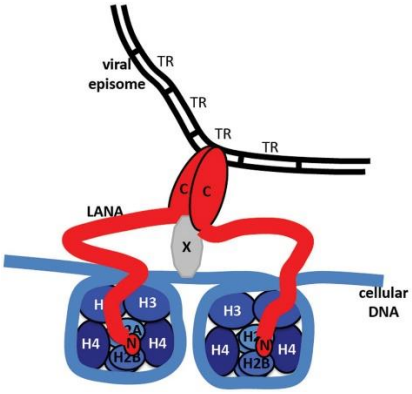

Figure 1. 5. Schematic representation of tethering mechanism of kLANA to a chromosome. N-terminal (N) associates with histones H2A and H2B while C-terminal (C) binds to terminal repeats (TR) of KSHV episome and to a putative protein (X) that associates with the mitotic chromosome (From Juillard *et al*., 2016).

Tumorigenesis is also related with kLANA, which is expressed at high levels in tumours cells (Komatsu *et al*., 2001). kLANA interacts with p53, a tumour suppressor protein, whose stability is regulated by the ubiquitin ligase activity of the murine double minute 2 (MDM2), a negative regulator of p53, that is also a target for kLANA. MDM2 inhibits the function of p53 in two distinct ways. It blocks the transcriptional activity of p53 by binding directly to the transcriptional activation domain of p53. Additionally, as an E3 ligase, MDM2 ubiquitinates p53, inducing its nuclear export and proteosomal degradation (Moll and Petrenko, 2003). Thus, the formation of the MDM2-p53 complex inhibits p53, leading to the suppression of cellular apoptosis and development of a tumour (Petre *et al*., 2007; Di Domenico *et al*., 2016). In addition, this complex is very important for KSHV latency, as it allows kLANA to bind to cellular DNA and to stabilize itself (Paul *et al*., 2011).

Essentially, kLANA is a multifunctional protein that regulates both virus and host DNA transcription, as well as the episomal maintenance and lytic reactivation, viral genome replication, tumorigenesis and KSHV latency (Verma *et al*., 2007). Therefore, kLANA is potentially a good target to clear the viral infection.

1.3.1.3. KSHV-related Diseases

1.3.1.3.1. Kaposi's sarcoma

KS, the principal malignancy associated to KSHV infection, can be divided in four subtypes, according to the epidemiology and clinical manifestations: classic, characterized by few lesions and restricted to lower limbs, found in ethnic groups from regions where KSHV highly occurs; iatrogenic, that occurs after a solid-organ allograft and presents, essentially, cutaneous lesions; endemic, in which children (mostly sub-Saharan Africa) present lymph nodes and a very violent form of the disease; and acquired immunodeficiency syndrome (AIDS)-associated, that presents cutaneous lesions on the limbs, face and trunk and often mucosal and visceral lesions, as well as tumour-associated oedema (Cai *et al*., 2010; Wen and Damania, 2010). KSHV can be transmitted by sexual and non-sexual modes, including saliva, blood and organ transplant (Vitale *et al.*, 2001; Mbulaiteye *et al.*, 2006; Bagni and Whitby, 2009; Uppal *et al*., 2014).

1.3.1.3.2. Other diseases associated to KSHV

Although the most common disease caused by KSHV is KS, primary effusion lymphoma (PEL), multicentric Castleman disease (MCD) and KSHV-associated inflammatory cytokine syndrome (KICS) are also consequences of KSHV infection. PEL, originally called body cavity lymphoma, is a B cell lymphoma that affects mostly body cavities, such as peritoneal and pericardial, and can also be manifested as solid lesions outside of cavities. This disease is commonly related with co-infection with EBV (Nador *et al*., 1996; Chadburn *et al*., 2004; Narkhede *et al*., 2018). MCD is a lymphoproliferative disorder characterized by abnormal lymph nodes (in size, number or consistency) and systemic symptoms. It is thought that the symptoms are a consequence of excessive production of inflammatory cytokines, such as IL-6. MCD is highly found in patients with human immunodeficiency virus (HIV) infection (Polizzotto *et al*., 2013). KICS is a systemic disease, displaying symptoms of systemic inflammation and cytokine release without any indicator of generalized lymphadenopathy or histological features of MCD. Patients with KICS recurrently have other KSHV- associated tumours (Polizzotto *et al*., 2016a). KSHV are also related with rare cases of bone marrow failure, hepatitis, acute inflammatory syndromes and KSHV immune reconstitution inflammatory syndrome (IRIS) (Giffin and Damania, 2014; Mariggiò *et al*., 2017).

1.3.1.4. Epidemiology

Currently, the highest seroprevalence of KSHV is in sub-Saharan Africa, where the occurrence can get up to 90% in adults of some populations. Although the virus can be found in 20-30% of the Mediterranean population, in Asia, northern Europe and United States of America, it affects less than 10%. The geographical variation is not completely understood, but environmental factors, like co-infection with malaria and other parasitic infections, might increase shedding of KSHV in saliva, increasing transmission rates (Wakeham *et al*., 2011). The geographical variance in the occurrence of KS reflects differences in the prevalence of KSHV (Figure 1.6.) (Mesri *et al*., 2010). It is known that KS was rare before the AIDS epidemic, in the 1980s, when the occurrence of KS increased, reflecting the impact of sexual transmission (Grulich *et al*., 1992).

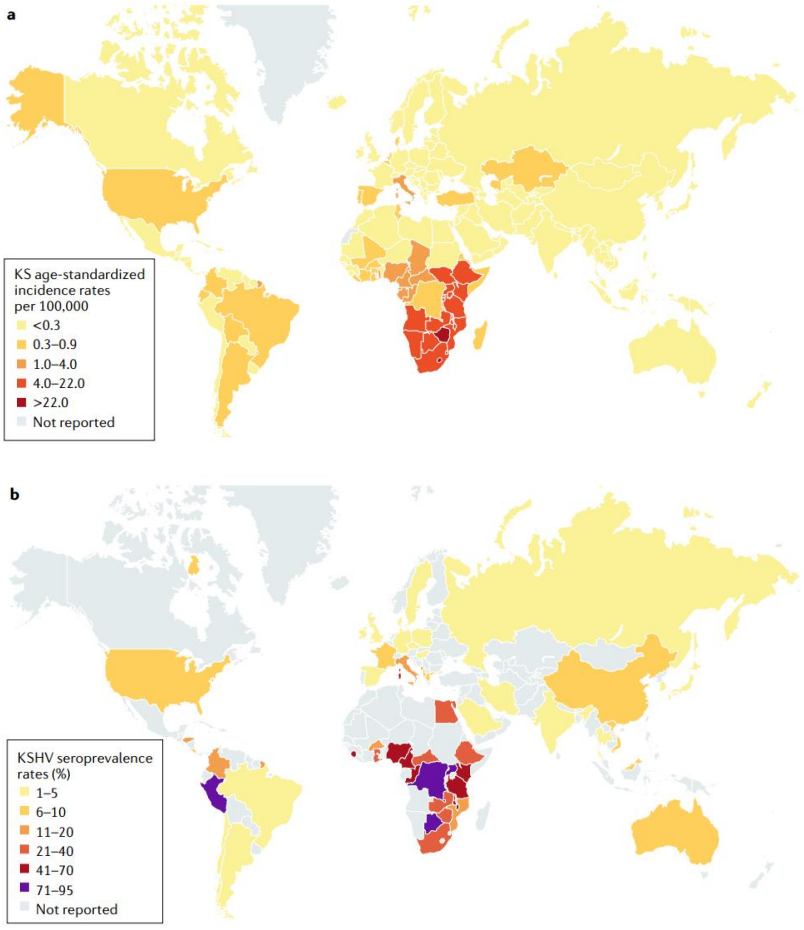

Figure 1. 6. Geographical prevalence of KS age-standardized incidence rates per 100.000 (a) and percentage of seroprevalence of KSHV (b) (From Cesarman *et al*., 2019).

1.3.2. Murine herpesvirus 68

MHV-68 is a gamma-2-herpesvirus and is the mouse homologue of KSHV. MHV-68 is able to establish a lifelong latent infection (Sunil-Chandra *et al*., 1992a). It was first isolated from free-living rodents like bank voles (*Myodes glareolus*) and yellow-necked field mice (*Apodermus flavicollis*), in Slovakia (Blaskovic *et al*., 1980). However, the wood mice (*Apodermus sylvaticus*) is the natural reservoir of this virus (Blasdell *et al*., 2003).

The MHV-68 genome is composed by a 118 kbp of a unique sequence of DNA flanked by multiple copies of 1213 bp terminal repeats and has a G+C content of approximately 45% (Efstathiou *et al*., 1990). The virus encodes around 80 genes, 63 of them collinear with herpesvirus saimiri (HVS) and KSHV, and some of them homologous to cellular genes (Simas and Efstathiou, 1998; Nash *et al*., 2001).

MHV-68 is capable of infecting laboratory mice (*Mus musculus*), contrarily to KSHV (Speck and Ganem, 2010).

1.3.2.1. MHV-68 latency-associated nuclear antigen

MHV-68 latency-associated nuclear antigen (mLANA), also encoded by ORF73, is homologous to human KSHV LANA, both in function and sequence, namely in the C-terminal domain and N-terminal proline rich region (Figure 1.7.) (Correia *et al*., 2013). However, since mLANA has a lack of internal acidic and glutamine-rich repeat elements, it is smaller than kLANA, being composed by 314 amino acids (Barton *et al*., 2011; Habison *et al*., 2012).

mLANA is expressed in germinal centre (GC) B cells and it is essential for MHV-68 to establish an efficient latent infection in mice, since it has a DNA binding domain that acts on the TRs elements of the MHV-68 genome and both N- and C-terminals that interact with cellular proteins (Fowler *et al*., 2003; Marques *et al*., 2003; Moorman *et al*., 2003; Habison *et al*., 2012; Correia *et al*., 2013).

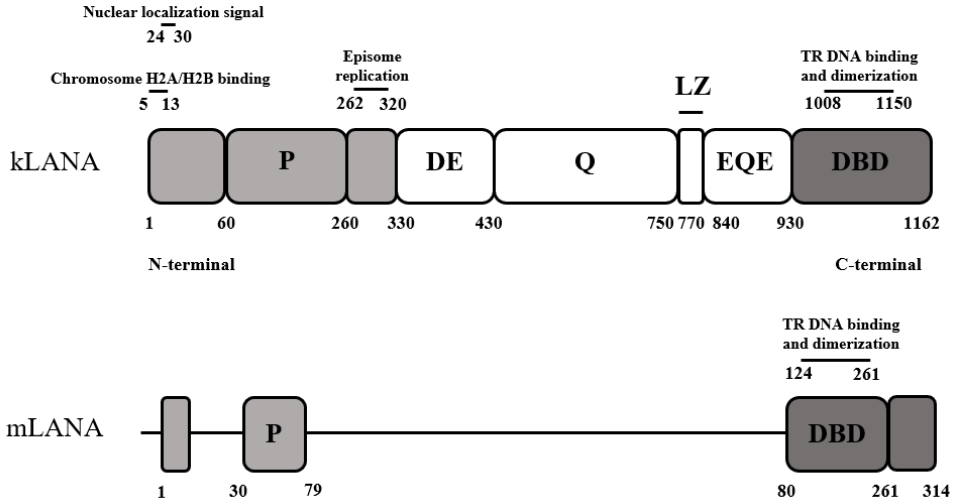

Figure 1. 7. Schematic representation of the comparison between kLANA and mLANA proteins. Shaded regions represent homology between proteins and unshaded regions lack homology. The intensity of the shade refers to the level of homology (dark means more homology). Proline-rich (P), the aspartate and glutamate (DE), the glutamine (Q), the leucine zipper (LZ), the glutamate and glutamine (EQE) and the DNA binding domain (DBD) regions. Numbers indicate amino acid residues (Adapted from Habison *et al.*, 2012; Ponnusamy *et al.*, 2015).

1.3.2.2. MHV-68 infection

After MHV-68 infection, mice develop an acute lytic infection in the lungs, affecting alveolar epithelial cells, which is cleared by the immune system of the host from 9 to 12 days post-infection (dpi) (Sunil-Chandra *et al.*, 1992a; Sunil-Chandra *et al.*, 1992b).

Then, the virus infects naïve B cells and disseminates to lymph nodes via dendritic cells and helper T cells. After that, it reaches the spleen by infecting marginal zone (MZ) macrophages first, and then MZ B cells, followed by GC B cells (Frederico *et al*., 2014). There occurs an expansion of latently infected B cells trough GC reaction. This reaction is marked by fast proliferation, somatic hypermutations (SHM) and class switch recombination (CSR), in order to increase the antibody/antigen affinity. Then, an interaction with follicular dendritic and T cells occurs, in which cells with low affinity suffer apoptosis, and the ones that survive can differentiate into memory B cells, the principal long-term reservoir of the virus (Figure 1.8.) (Sunil-Chandra *et al*., 1992b; Simas *et al*., 1999; Flaño *et al.*, 2002). The peak of latency (approximately 14 dpi) is coupled with splenomegaly and followed by a decrease in the number of infected cells that ultimately reach a steady-state level (Simas and Efstathiou, 1998). MHV-68 latent infection is established predominantly in B cells, but macrophages, dendritic and epithelial cells can also be latently infected (Stewart *et al*., 1998; Weck *et al*., 1999; Flaño *et al.*, 2000; Marques *et al.*, 2003).

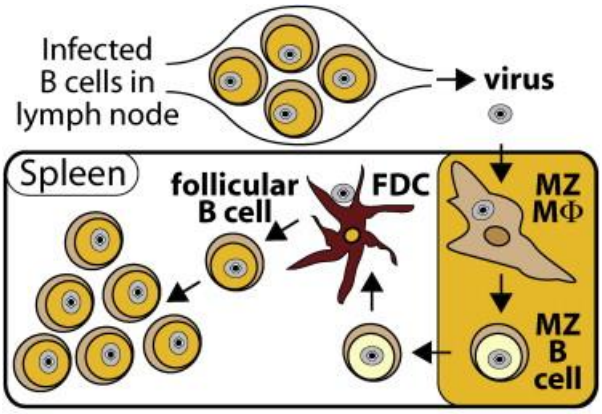

Figure 1. 8. Schematic representation of MHV-68 infection. The virus infects marginal zone (MZ) macrophages and MZ B cells, thus reaching the spleen. MZ B cells move to the white pulp of the spleen, where the transference of the virus to follicular dendritic cells (FDC) occurs. After this, the virus reaches GC B cells (From Frederico *et al*., 2014).

1.3.3. Chimeric virus to study kLANA functions *in vivo*

The infection of gammaherpesviruses does not only depend on the virus itself but also on the host, both the animal species and the cell type infected (Ackermann, 2006). Therefore, the study of KSHV has been limited by the inexistence of an appropriate small animal model (Barton *et al*., 2011). Taking into account the homology between MHV-68 and KSHV, and also the easier manipulation of the first one, Habison and collaborators (2017) created a chimeric virus to study both virological and immunological characteristics of infection, as well as possible therapeutics. The chimera consists in the replacement of mLANA by kLANA and its 5'UTR in the MHV-68 genome (v-kLANA). It was demonstrated that kLANA is capable of acting on TRs from MHV-68 as well as mLANA can act on TRs from KSHV. Although the levels of latency of chimeric virus are lower compared with MHV-68, the copy number of the episome is equal in both viruses. Therefore, the chimera is able to establish a latent infection *in vivo*, providing a study model of KSHV (Figure 1.9.) (Habison *et al*., 2017).

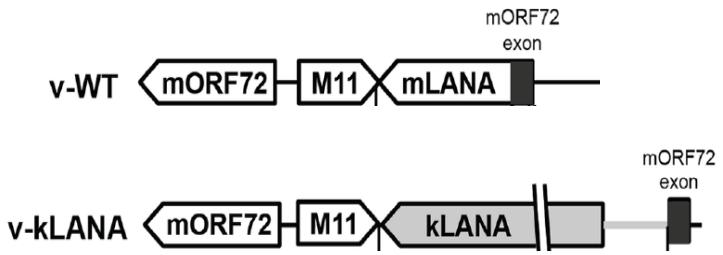

Figure 1. 9. Schematic representation of the construction of v-kLANA. The insertion of the kLANA cassette occurred between the M11 stop codon and the mORF72 exon in place of MHV-68. The mORF72 non-coding exon (black) is positioned within the mLANA coding region (Adapted from Habison *et al*., 2017).

Additionally, some viruses have a genome that expresses the yellow fluorescent protein (YFP), a mutant of green fluorescent protein (GFP), initially derived from the jellyfish *Aequorea victoria*. The excitation peak is at 514 nm, while the emission peak is at 527 nm. YFP is a tracking marker that allows the monitorization of the infection by flow cytometry and fluorescence microscopy, enabling a direct identification of infected cells (Aliye *et al.*, 2015).

1.4. Antivirals and Antiviral Strategies

The necessity of new antivirals is emergent. However, the possession of cellular mechanisms, the replication inside the cell, the small replication cycles, the huge progeny, the fast adaptation and the antiviral resistance lead to a high difficulty in the development of effective drugs to combat the viral agents (De Clercq, 2004; Muller and Krausslich, 2009).

Drugs targeting virus-specific enzymes are one of the most widely used. The enzymes could be inhibited by both allosteric compounds and substrate equivalents, and polymerases and proteases are the main targeted enzymes. Neuraminidases, specific of influenza viruses, and integrases, only used by retroviruses, are also broadly used targets in these specific viruses (Muller and Krausslich, 2009).

Polymerases are enzymes that synthesize nucleic acid chains and the polymerase inhibitors are incorporated into the chain, stopping the synthesis of viral genome. Since several viruses express their own specific nucleic acid polymerase, this class of enzymes is well characterized and this approach is frequently used (Tsai *et al.*, 2006; Shi *et al.*, 2013).

Proteases are enzymes that break peptide bonds of proteins. Viruses regularly produce polyproteins, given the restricted gene expression, requiring the proteolysis of the polypeptides into smaller and functional proteins. Protease inhibitors are substrate analogues which have an uncleavable mimic of a peptide bond flanked by structural elements similar to specific features of cognate cleavage sites (Patick and Potts, 1998; Chang *et al*., 2019).

Furthermore, molecules involved in the virus entry and release, receptors and co-receptors, attachment proteins, the viral capsid, and the capping enzyme (responsible for catalysing the attachment of the 5' cap to messenger RNA molecules in process to be synthesized in the cell nucleus) are also examples of potential viral targets. Although some cellular targets have been explored, this strategy is difficult, since meticulous studies about the virus–host interaction are required (Muller and Krausslich, 2009; Muller *et al*., 2012).

Moreover, antisense RNAs, small interfering RNAS (siRNA) and ribozymes are used to silence the viral gene expression (Feibelman *et al*., 2018). Also, the

administration of interferon is used to stimulate the immune system to face the viral infections (Hengel *et al*., 2005).

1.5. Treatment

Nowadays, there is no treatment for KSHV latent infection. There are only therapies for KS and the only two approved therapies are for AIDS-related KS. Interferon alpha (IFN-α), a cytokine with antiviral and antiproliferative properties, is able to inhibit angiogenesis and control humoral and cellular immune responses. The administration of IFN-α is applicable to AIDS-related KS and induces regression, especially when combined with single inhibitors of HIV-1 nucleotide reverse transcriptase (Krown, 2007). Alitretinoin is a retinoid receptor pan-agonist that regulates the expression of genes that control the process of cellular differentiation and proliferation (Duvic *et al*., 2000; Bodsworth *et al*., 2001). Additionally, there are several recent treatments that showed promising results in small clinical trials, such as imatinib, an antibody that inhibits tyrosine kinase-mediated transmembrane receptor signalling to avoid KS cell angiogenesis and proliferation (Koon, 2014); bevacizumab, a monoclonal antibody against vascular endothelial growth factor (VEGF), an angiogenic growth factor extremely expressed in KS lesions (Uldrick *et al*., 2012); IL-12, a cytokine that improves type 1 immune responses with antiangiogenic effect and that downregulates viral G protein-coupled receptor (v-GPCR) activity (Yarchoan *et al*., 2007); thalidomide, lenalidomide and pomalidomide, imide drugs with immunomodulatory, anti-inflammatory and antiangiogenic properties (Polizzotto *et al*., 2016b); rapamycin, inhibitor of the PI3K–AKT–mTOR pathway (Stallone *et al*., 2005; Krown *et al*., 2012); and timolol and propranolol, inhibitors of autocrine β-adrenergicreceptor-mediated signalling, thought to be the way in which KSHV stimulates the proliferation of transformed cells and supresses the expression of viral lytic genes (McAllister *et al*., 2015).

Although the therapies for all types of KS is based on chemotherapy, only AIDS-related KS has clear evidence of regression (Mui *et al*., 2017; Cesarman *et al*., 2019). Nevertheless, reinforcing the immune system is the first-line approach, even though it may risk graft rejection in iatrogenic KS patients. In cases of AIDS-related KS, previously untreated patients are treated with combination antiretroviral therapy (cART) to target HIV and, recurrently, KS returns (Bower *et al*., 2014). In advanced-stage AIDS-related KS, combining cART with chemotherapy with pegylated liposomal doxorubicin (Caelyx or Doxil) is the most common treatment and over 80% of patients showed tumour regression (Lichterfeld *et al*., 2005). Classic KS uses some tumour-directed therapies for AIDS-related KS in the management of symptoms from lower-extremity oedema, that depends on the number and anatomic distribution of the lesions (Cesarman *et al*., 2019).

For KSHV-associated MCD, rituximab, a monoclonal antibody, is the typical approach (Bower *et al*., 2011; Goncalves *et al*., 2017). Nevertheless, chemotherapy with

etoposide or liposomal anthracycline is added if life-threatening organ failure is a risk (Goncalves *et al.*, 2017). HIV-infected patients are commonly treated with cART and immune-chemotherapy (Harris *et al.*, 2002; Cesarman *et al*., 2019).

In the case of KSHV-associated PEL, the most common treatment is to combine chemotherapy of cyclophosphamide, doxorubicin, etoposide, vincristine and prednisone (generally called EPOCH), even though a therapy with bortezomib, a proteasome inhibitor, can be also used (Bhatt *et al*., 2013; Goncalves *et al*., 2017). While patients without HIV infection are treated with just chemotherapy, in the presence of HIV infection, administration of cART is added to chemotherapy (Harris *et al.*, 2002).

Recently, in 2017, Angius and colleagues showed that sulfathiazole, sulfanilamide and other sulfonamides, as well as glybenclamide (a sulfonylurea), have the capacity to clear latent KSHV infection in BC3 lymphoma cells, latently infected with the virus. The drugs act by impairing the formation of the MDM2-p53 complex, essential for KSHV to sustain latency, as well as to activate tumorigenesis (Angius *et al*., 2017).

1.6. Studied Drugs

1.6.1. Sulfathiazole and Sulfanilamide

Sulfathiazole, 4-amino-*N*-(1,3-thiazol-2-yl)benzenesulfonamide, and sulfanilamide, 4-aminobenzenesulfonamide, are sulfonamides, a class of organic compounds that contain the sulfonamide functional group (Figure 1.10.).

A **B**

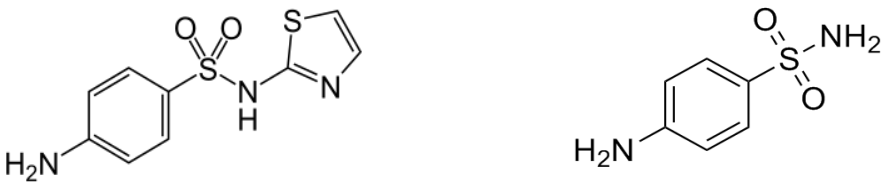

Figure 1. 10. Structural formula of the drugs. a) Sulfathiazole. b) Sulfanilamide (Adapted from Göko and Esra, 2014; Trontelj *et al*., 2019).

Sulfonamides act as bacteriostatic antibiotics with a wide spectrum against most gram-positive and many gram-negative organisms. They are competitive inhibitors of the bacterial enzyme dihydropteroate synthase, which converts *para*-aminobenzoic acid (PABA) in folic acid, essential for bacterial replication (Skold, 2000).

In the KSHV context, the target of these drugs is the MDM2-p53 complex. As referred previously, this complex, formed by the tumour suppressor p53 and its negative regulator, MDM2, has an important function in KSHV infection, helping the maintenance of the latent phase by allowing kLANA to bind to and stabilize on cellular DNA. KSHV sustains the MDM2-p53 complex by binding kLANA to p53. On the other hand, the formation of the complex, by inhibiting p53, promotes tumorigenesis. Thereby, the MDM2-p53 complex is essential to KSHV latency and is also responsible for the malignant cell transformation (Angius *et al*., 2017).

Sulfathiazole and sulfanilamide bind to p53, preventing the formation or disrupting the MDM2-p53 complex. Therefore, impairing the formation of the complex will lead to the activation of p53, allowing cellular apoptosis and also the detachment of viral genome from the cellular DNA, being destroyed by DNA polymerases. Consequently, kLANA stops being transcribed, resulting in the termination of KSHV latency (Figure 1.11.) (Angius *et al*., 2017).

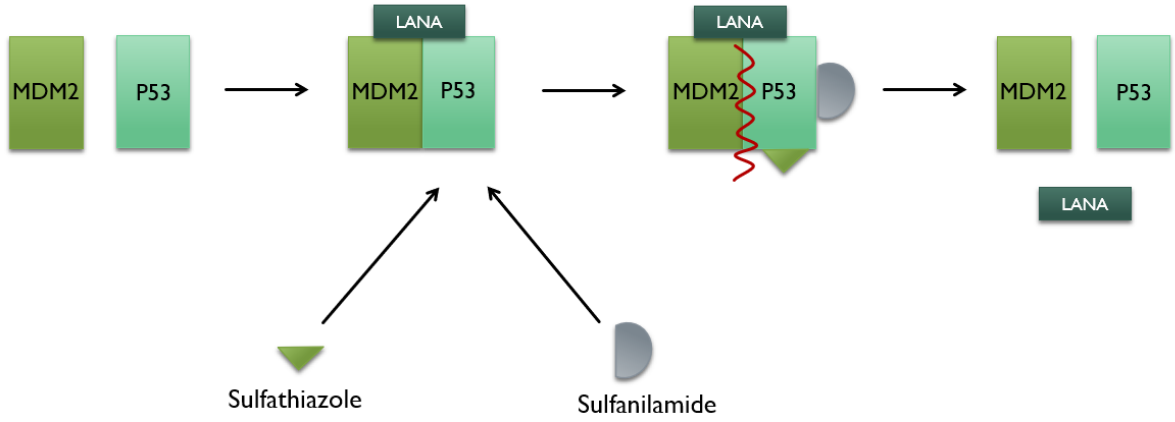

Figure 1. 11. Schematic representation of the mechanism of action of sulfathiazole and sulfanilamide, acting on the MDM2-p53 complex (Adapted from Angius *et al*., 2017).

1.6.2. Glybenclamide

Glybenclamide,5-chloro-*N*-[2-[4-(cyclohexylcarbamoylsulfamoyl)phenyl]ethyl]-2-methoxybenzamide, also known as glibenclamide or glyburide, is a sulfonylurea, a class of organic compounds that contains the sulfonylurea functional group (Figure 1.12.). Glybenclamide is a drug widely used in the management of diabetes mellitus type 2. The mechanism of action in β cells of the pancreas is based on the binding to adenosine triphosphate (ATP)-sensitive potassium channels on the cell surface, reducing potassium conductance and causing depolarization of the membrane. Depolarization stimulates calcium ion influx through voltage-sensitive calcium channels, raising intracellular concentrations of calcium ions, which induces the secretion of insulin (Luzi and Pozza, 1997).

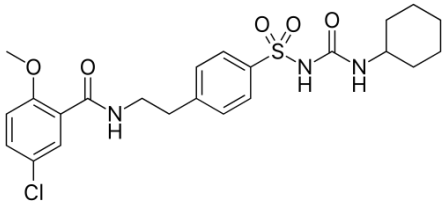

Figure 1. 12. Structural formula of glybenclamide (Adapted from Sanz *et al*., 2012).

Although further mechanistic assays are necessary, it is thought that glybenclamide acts on the MDM2-p53 complex, like sulfonamides. Besides that, glybenclamide is able to inhibit viral protein expression and eliminate KSHV DNA from infected cells (data not published).

1.6.3. JQ1

(+)-JQ1, denoted by JQ1, *tert*-butyl2-[(9S)-7-(4-chlorophenyl)-4,5,13-trimethyl-3-thia-1,8,11,12-tetrazatricyclo[8.3.0.$0^{2,6}$]trideca-2(6),4,7,10,12-pentaen-9-yl]acetate, is a thienotriazolodiazepine (Figure 1.13.A.). It is cell permeable and a potent competitive inhibitor of the bromodomain and extraterminal domain (BET) family of bromodomain (BRD) proteins - BRD2, BRD3, BRD4 and BRDT (Filippakopoulos *et al*., 2010). This family of proteins associates with acetylated lysine residues of histones and controls transcription of gene products that depend on this mechanism for expression, namely *c-myc* (Figure 1.13.B.) (Filippakopoulos *et al*., 2010; Lovén *et al*., 2013). *c-myc* is a proto-oncogene that encodes a nuclear phosphoprotein that plays a role in cell cycle progression, apoptosis and cellular transformation (Wang *et al*., 2018). Besides this, c-Myc is also essential for GC formation and maintenance (Calado *et al*., 2012).

On the other hand, kLANA recruits BET proteins, that allows the viral genome to associate with cellular chromatin and, also, to activate BET-responsive promoters, leading to the establishment of latency (Ottinger *et al*., 2009; Hellert *et al*., 2013; Uppal, 2014; Xu and Vakoc, 2017).

A

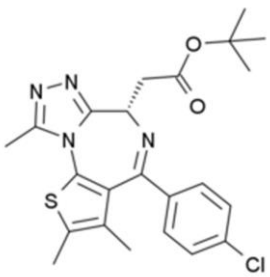

B

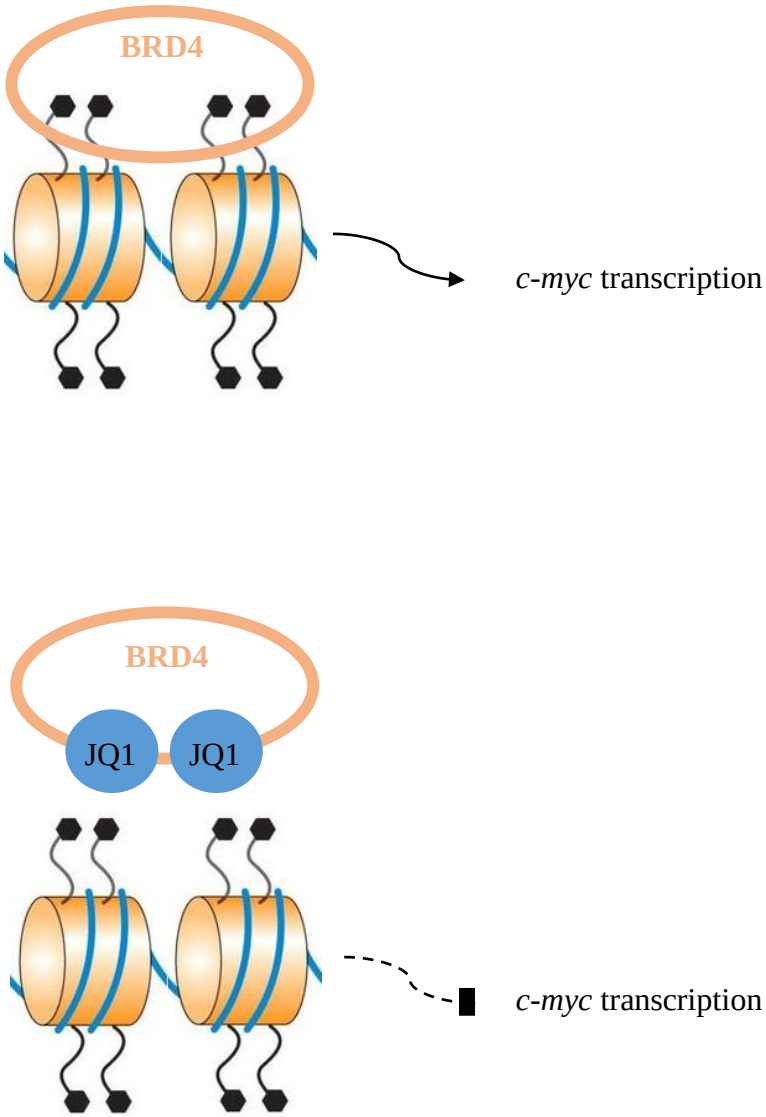

Figure 1. 13. JQ1. a) Structural formula. b) Schematic representation of the mechanism of action, inhibiting *c-myc* transcription. The hexagons represent the acetylated lysine residues of the histones (Adapted from Ferri *et al*., 2015).

Therefore, JQ1 occludes the ligand-binding pockets of BRD proteins, mainly BRD4, and prevents recruitment towards acetylated lysine substrates, leading to the repression of *c-myc* transcription (Ember *et al*., 2014). Thus, when *c-myc* is not transcribed, cell-cycle arrest and cellular senescence are consequences, as well as a decrease of GC (Calado *et al*., 2012; Miller *et al*., 2012; Stanlie *et al*., 2014). However, relatively to the importance of BET proteins in the establishment of latency, Chen and colleagues affirmed that JQ1 is not able to disrupt the interaction of BRD proteins with kLANA, *in vitro* (Chen *et al*., 2017).

2. Aim of the project

KHSV is a virus that can establish a lifelong infection and that is highly disseminated around the world, affecting a large number of people. KSHV is associated with several malignancies, namely KS, and there is no treatment that can eliminate KSHV infection yet. The infection is divided in two phases: lytic and latent, and the latent phase is responsible for the maintenance of the lifelong infection. kLANA is an essential protein expressed in this phase, being a potential target to clear the latent infection.

MHV-68 is the mouse homologue of KSHV, it is easy to manipulate and can infect laboratory mice (*Mus musculus*). Thus, using a chimera virus able to infect laboratory mice in which mLANA was replaced by kLANA, it is possible to study the persistence of the virus *in vivo*.

Previous *in vitro* studies showed that kLANA binds to the MDM2-p53 complex to stabilize on cellular DNA and, consequently, allowing the persistence of KSHV. Sulfathiazole, sulfanilamide and glybenclamide presented promising results in eliminating the infection of KSHV.

JQ1 has previously revealed efficacy in inhibiting BRD proteins, controlling transcription of genes such as *c-myc*, a proto-oncogene. Likewise, it is known that kLANA recruits BET proteins that lead to the establishment of latency.

Therefore, the aim of this project is to test these promising compounds *in vivo* that have already shown effective results *in vitro* and evaluate whether they can clear latent infection of the chimeric virus, giving highlights for the elimination of KSHV infection.

3. Material and Methods

3.1. Cells and Viruses

3.1.1. BHK-21

Baby hamster kidney (BHK) cell line was originally isolated by polyoma transformation of hamster cells and is one of the most used cell lines for the study of biopharmaceuticals and expression of recombinant proteins. BHK strain 21 (BHK-21) fibroblast cell line was derived from baby hamster kidneys of five unsexed, 1-day-old hamsters, *Mesocricetus auratus*, commonly known as syrian golden hamsters, in 1962, by Macpherson and Stoker (Macpherson and Stoker, 1962). BHK-21 cells are susceptible to multiple viruses, including v-kLANA and MHV-68.

The appropriate media for this cell line is supplemented Glasgow minimum essential medium (GMEM). The supplement is 5 mL of glutamine (2 mM), 5 mL of penicillin-streptomycin (100 U/mL), 50 mL of tryptose phosphate broth (TPB) and 50 mL of heat-inactivated fetal bovine serum (FBS). Supplemented GMEM will be denominated GMEM.

Cultures of BHK-21 cells were maintained in a CO_2 incubator at 37ºC.

3.1.2. v-kLANA.yfp

v-kLANA.yfp is a chimeric virus in which mLANA is replaced by kLANA and its 5'UTR in the MHV-68 genome. The levels of latency are lower than the levels of MHV-68, even though the episome copy number is equal in both viruses. Being able to establish a latent infection *in vivo,* this virus provides a study model of KSHV (Habison *et al*., 2017).

The genome of v-kLANA.yfp contains the gene that expresses the YFP, a tracking marker that allows monitorization by flow cytometry and fluorescence microscopy, enabling a direct identification of infected cells.

Being a model to study the persistence of the virus, v-kLANA.yfp is a new way to test drugs *in vivo* and start pre-clinical trials that will give highlights about KSHV inhibition. This virus was used in all the experiments of this thesis.

3.2. *In vitro* assays

3.2.1. Production of viral stocks

Viral stocks were produced through the infection of $5x10^6$ BHK-21 cells at a low multiplicity of infection (MOI), 0.002 plaque forming unit (PFU)/cell, in 175 cm^2 flasks. Then, cells were incubated for 4 days at 37ºC and after the incubation period, cells were scrapped into media and centrifuged at 1500 revolutions per minute (rpm) for 5 minutes at 4ºC. Cell pellet was resuspended in 2 mL of GMEM, aliquoted and stored at -80ºC (Cell Working Stocks, CWS). The supernatant was centrifuged at 12 000 rpm for 2 hours at 4ºC. Pellet was resuspended in 2 mL of GMEM, aliquoted and stored at -80ºC (Working Stock Media, WSM). WSM was used in the infectivity assays.

3.2.2. Virus titration using suspension assay – plaque assay

Suspension assay is a method used to determine the titre of viruses. First, 900 µL of GMEM were distributed to 15 mL falcon tubes, 100 µL of virus were added to the first falcon and 10-fold serial dilutions were performed. The next step was the addition of 1ml $2x10^5$ BHK-21 cells to each falcon and tubes were incubated in a rotating table at room temperature (RT) for 1 hour at 30 rpm. After that, 2 mL of GMEM were added to each tube and mixed by inversion. The suspension was added to 6-well plates, followed by an incubation for 4 days at 37ºC. Media was removed and cells were fixed with 4% formaldehyde (in phosphate buffered saline (PBS)), for 10 minutes. Then, the fixative was removed, and cells were stained with 0.05% toluidine blue in H_2O, for 5 minutes.

Viral plaques were identified and counted using a magnifying glass and titres were calculated accordingly to the formula below:

$$Virus\ titre\ (PFU/mL) = Number\ of\ plaques\ x\frac{1}{Dilution}\ x\frac{1}{Inoculum}$$

3.2.3. Protein expression analysis

$2.5x10^5$ BHK-21 cells per well were seeded in a 12-well plate on the day prior to the infection. Cells were infected with 3 PFU/cell in a total volume of 500 µL. The control was a well with non-infected cells – mock. The inoculum was added to the well and cells were incubated for 2 hours, at 37ºC, with a gentle rock every 30 minutes. After the incubation period, the inoculum was removed, and cells were washed gently with 1 mL of pre-warmed media and 1 mL of fresh media was added to each well. Cells were incubated again for 4 hours at 37ºC. After this time, cells were washed twice with ice-cold PBS and 110 µL of lysis buffer (150 mM NaCl, 10 mM Tris-HCl pH 7.4, 1 mM Na_3VO_4, 1 mM NaF, 1% Triton™ X-100, complete protease inhibitors (Roche), MilliQ

H_2O) were added to each well, cells were harvested into eppendorfs, left for 10 minutes on ice, and frozen at -20ºC. The samples were centrifuged at 13000 rpm for 10 minutes on a refrigerated centrifuge, to remove cell debri, and 100 µL of the supernatant were transferred to a new tube. 100 µL of 2x Laemmli's buffer (100 mM Tris-HCl pH 6.8, 20% glycerol, 4% sodium dodecyl sulphate (SDS), 10% β-mercaptoethanol, 0,1% bromophenol blue, MilliQ H_2O) were added to the cell lysates and these were heated at 95ºC for 3 minutes, in a heat block, before loading into gel.

3.2.3.1. Sodium dodecyl sulphate-polyacrylamide gel electrophoresis (SDS-PAGE)

The technique of polyacrylamide gel electrophoresis under denaturing conditions consists in the separation of proteins of a sample based on their molecular weight, with the application of an electric field. The heavier proteins migrate slower than the lower proteins.

The acrylamide gels are composed by two phases (Table 3.1.):

- Stacking phase: constant phase, used to compact samples, allowing a simultaneous progress of the samples, with 5% acrylamide.
- Resolving phase: phase where the separation of proteins occurs, with 5-15% acrylamide, depending on the molecular weight of the proteins of interest – the higher the percentage of acrylamide, the smaller the mesh size of the pore, allowing better separation of lower molecular weight proteins. In this case, the resolving gel had a percentage of 10% acrylamide.

Table 3. 1. Composition of electrophoresis gels.

	Stacking gel (3 mL)	**Resolving gel (10 mL)**
H_2O	2.1	4.0
30% acrylamide mix	0.5	3.3
1.5 M Tris (pH 8.8)	-	2.5
1.5 M Tris (pH 6.8)	0.38	-
10% SDS	0.03	0.1
10% ammonium persulfate	0.03	0.1
Tetramethylethylenediamine (TEMED)	0.003	0.004

50 µL of each sample and a molecular weight marker (Dual color, Bio-Rad) were loaded into the gels and the electrophoresis was performed in a Bio-Rad tray with Tris-Glycine-SDS (TGS) buffer 1x (25 mM Tris-base, 192 mM glycine, 0.1% SDS pH 8.3) at 180 V constant, for 1 hour.

3.2.3.2. Western blot

After separation of proteins along the acrylamide gel, these were transferred from the gel to a nitrocellulose membrane (Protran, GE Healthcare), by the wet-transfer method, in a transfer buffer (700 mL MilliQ H_2O, 100 mL 10x Tris-Glycine (1x Tris-Glycine: 25 mM Tris pH 8.3, 192 mM Glycine), 200 mL methanol, 3.7 mL 10% SDS), overnight (O/N) at 100 mA, at 4ºC. After the transfer, the nitrocellulose membrane was incubated with Ponceau dye for 2 minutes to visualize proteins in the membrane. The membrane was cut horizontally into three parts: between 250 kDa and 60 kDa marker, for detection of kLANA, between 60 kDa and 30 kDa, for detection of actin, and between 30 kDa and 0 kDa for detection of YFP.

Membranes were blocked using a blocking solution (2.5 g of non-fat powder milk in 50 mL PBS+0.05% Tween-20 (PBS-T) in a rotating table at 10 rpm, for 1 hour, at RT, to reduce non-specific background. Membranes were washed twice with PBS-T (3 minutes each) and then incubated with primary antibodies (Table 3.2.) diluted in blocking solution in sealed bags, in a rotating table at 10 rpm, for 2 hours at RT. After the incubation period, membranes were washed 3 times with PBS-T (5 minutes each) and incubated with blocking solution containing each of the horse radish peroxidase (HRP)-conjugated secondary antibodies (Table 3.3.), specific to the species of the primary antibodies, in a rotating table at 10 rpm, for 1 hour, at RT. The wash step was repeated (3 times for 5 minutes with PBS-T).

Table 3. 2. Primary antibodies used in Western blot.

Antibody	Antigen	Species	Dilution	Supplier
LN53	kLANA	Rat	1:1000	Advanced Biotechnologies
Actin	Actin	Rabbit	1:1000	Sigma
eGFP	eGFP/YFP	Mouse	1:1000	Clontech

Table 3. 3. Secondary antibodies used in Western blot.

Antibody	Species	Dilution	Supplier
Anti-mouse HRP	Goat	1:5000	Jackson Immunoresearch
Anti-rat HRP	Goat	1:5000	Jackson Immunoresearch
Anti-rabbit HRP	Donkey	1:5000	GE Healthcare

Detection of protein-antibody complexes was performed by chemiluminescence using SuperSignal® West Pico Chemiluminescence Substrate (Thermo Scientific). The membrane was covered with the same quantity of hydrogen peroxide and luminol for 1 minute. Chemiluminescence was detected in the Chemidoc XRS$^+$ (Biorad).

3.2.4. One-step growth curves

High multiplicity of infection growth curves were carried out on cell monolayers in 24-well-plates. 5x10^4 BHK-21 cells per well were seeded a day prior to the infection. Media was removed, cells were infected with 5 PFU per cell of v-kLANA.yfp and incubated for 1 hour at 37ºC. After the incubation, inoculum was removed and cells were washed with 1.35 mM NaCl, 10 mM KCl, 40 mM citric acid, pH 3.0, for 1 minute, to inactivate unadsorbed virus. Cells were washed twice with GMEM, and 1 mL of GMEM containing sulfathiazole (25.5 μg/mL), sulfanilamide (17.2 μg/mL), or glybenclamide (5 or 25 μg/mL) was added. The plates were incubated at 37ºC.

At each time point, in hours, after infection (0 - after wash steps, 4, 8, 12, 24 and 48) cells and media were harvested and stored at -80ºC until titration using suspension assay method.

3.3. *In vivo* assays

3.3.1. Mice

Eighty-six 7-week-old female BALB/cByJ mice used in this work were purchased from Charles Rivers Laboratories and were housed and subjected to experimental procedures in specific pathogen-free conditions, at Instituto de Medicina Molecular João Lobo Antunes animal facility.

3.3.2. Ethics statement

This study was done accordingly to the Federation of European Laboratory Animal Science Associations guidelines on laboratory animal welfare and Portuguese Official Veterinary Directorate European Directive 2010/63/EU.

3.3.3. Mice infection

Mice were anaesthetized with isoflurane and inoculated intranasally with v-kLANA.yfp, diluted to 10^4 PFU in 20 μL of PBS.

3.3.4. Treatment with drugs

The treatment was given daily from 9 to 13 dpi. All drugs and control solutions were administered by intraperitoneal injection, in a volume of 200 μL.

3.3.4.1. Sulfathiazole and Sulfanilamide

Sulfathiazole and sulfanilamide used in the experiments were a gift from Fabrizio Angius, University of Cagliari, Italy.

In the first experiment, five mice were administered with 0.25 mg/g of body weight of sulfathiazole in water; and five mice with 0.25 mg/g of sulfanilamide in 17% dimethyl sulfoxide (DMSO)/water, because this drug is insoluble in 100% water. Five control mice were administered with PBS.

In the second experiment, five mice were administered with 0.5 mg/g of sulfathiazole in water; five mice with 1 mg/g of sulfathiazole in water; and five mice with 1 mg/g of sulfanilamide in 17% DMSO/water. Five control mice were administered with PBS.

3.3.4.2. Glybenclamide

Glybenclamide used in the experiments was a gift from Fabrizio Angius, University of Cagliari, Italy.

To study this drug, five mice were administered with 0.005 mg/g of glybenclamide in 17% DMSO/water, because it was not completely soluble in 100% water. Five control mice were administered with PBS. This drug was tested together with sulfathiazole and sulfanilamide in the first experiment.

3.3.4.3. JQ1

JQ1 used in the experiments were a gift from Kenneth M. Kaye, Harvard Medical School, United States of America.

To test JQ1, four mice were treated with 0.05 mg/g of JQ1 in a solution of DMSO and 10% 2-hydropropil-β-ciclodextrin, used to increase the solubility of the drug, in 1:10. To the four mice of the control group it was administered 1:10 DMSO/10% 2-hydropropil-β-ciclodextrin. Each mouse received 200 μL per day.

3.3.5. Preparation of splenocyte suspensions

A. At 14 dpi, mice were sacrificed by cervical dislocation, each spleen was surgically removed to a tube containing 5 mL of complete GMEM and kept on ice until the next step. Collected spleens were mechanically disrupted and filtered through a 100 μm cell strainer to remove stromal debris. Cells were centrifuged at 1200 rpm for 10 minutes at 4ºC and the pellet was resuspended in 1 mL of red blood cell lysis buffer (RBL) (154 mM of ammonium chloride, 14 mM of sodium hydrogen carbonate, 1 mM of ethylenediamine tetraacetic acid (EDTA) (pH 7.3)). Cells were incubated on ice for 5 minutes and then washed with 5 mL of complete GMEM. Cells were centrifuged at 1200 rpm for 5 minutes at 4ºC, the pellet was resuspended in 1 mL of complete GMEM and 4 mL of GMEM were added to a final volume of 5 mL. The splenocyte suspension obtained from each mouse was used to assess viral latency by infectious centre assay (ICA) / *ex vivo* reactivation assay (section 3.3.6.), the frequency of viral DNA positive cells in total splenocytes by limiting dilution assay (section 3.3.7.) and the percentage of infected GC B cells by flow cytometry analysis (section 3.3.8.1.).

B. To assess viral latency by limiting dilution analysis of infected splenocytes (section 3.3.9.), after being sorted by flow cytometry (section 3.3.8.2.), and to perform an *in situ* hybridization (section 3.3.10.), the process was similar to the described above. However, the splenocyte suspensions were made with a pool of spleens from all the mice of the experimental group. The spleens were pooled and processed together, instead of individually. Another difference is the fact that, for these assays, GMEM was replaced by PBS+2% of FBS (PBS+2% FBS) in all the process.

3.3.6. Infectious Centre Assay (ICA)

This assay is an *ex vivo* reactivation assay used to determine latent virus titres. Co-culture of latently infected cells with permissive BHK-21 cells leads to viral reactivation and formation of lytic plaques on a cell monolayer. 10-fold serial dilutions were performed from the splenocyte suspension and plated, in duplicate, in 6 cm^2 plates, along with $4x10^5$ BHK-21 cells. Plates were incubated for 5 days at 37ºC.

To confirm that there were not pre-formed infectious viruses, an assay with freeze-thawed splenocyte suspension was performed. The co-culture was plated and incubated for 4 days, at 37ºC.

After the incubation period, cells were fixed with 4% formaldehyde (in PBS), for 10 minutes, and stained with 0.05% toluidine blue in H_2O for 5 minutes, after the removal of fixative. Viral plaques were counted with the help of a magnifying glass and infectious centres (PFU/spleen) were determined like in the plaque assay (section 3.2.2.), accordingly to the formula below:

$$Virus\ titre\ (PFU/mL) = Number\ of\ plaques\ x\frac{1}{Dilution}\ x\frac{1}{Inoculum}$$

3.3.7. Frequency of viral DNA positive in total splenocytes

To determine the frequency of viral genome positive cells, a pool for each infectious group was prepared (three to five mice per pool) from single cell suspensions from individual mice. The pool was centrifuged at 1300 rpm for 5 minutes at 4ºC and the pellet was resuspended in PBS+2% FBS. This step was repeated twice. After that, the sample was filtered using a 40 µm cell strainer. The splenocytes from each pool were then counted and diluted to $2x10^6$ cells in 100 µL PBS+2% FBS. 2-fold dilutions were performed and eight replicates of each dilution were added to polymerase chain reaction (PCR) tubes containing 10 µL of lysis buffer (10 mM Tris-HCl pH 8.3, 3 mM $MgCl_2$, 50 mM KCl, 0.45% NP-40, 0.45% Tween-20, 0.5 mg/mL proteinase K). PCR tubes were incubated overnight at 37ºC and, in the next day, proteinase K was inactivated at 95ºC for 5 minutes in a thermocycler.

The samples were analysed by real-time PCR, on a Rotor Gene 6000 thermocycler (Corbett Life Science) using a fluorescent Taqman probe and primers specific for the MHV-68 *M9* gene (Table 3.4.). PCR reactions contained 2.5 µL of cell suspension lysate, 200 nM of each primer, 300 nM of M9-T probe (Alfagene), 1x Platinum Quantitative PCR SuperMix-UDG (Invitrogen), 5 mM $MgCl_2$ and nuclease free water, making a total volume of 25 µL. The positive control was a sequence of dilutions of pGBT9-M9, a plasmid that contains the *M9* gene, and the negative control was water. The cycling program initiated with a melting step of 95ºC for 10 minutes, followed by 40 cycles of amplification, starting at 95ºC for 15 seconds and then 60ºC for 1 minute. The acquisition was performed using the green channel with a gain value of 5.33. Real-time PCR results were analysed using Rotor Gene 6000 software. In all dilutions analysed, each replicate was scored positive or negative based on comparison with the negative or the positive controls results.

The frequency of viral DNA positive cells was estimated according to the method developed by Marques and colleagues and described in section 3.4. (Marques *et al.*, 2003).

Table 3. 4. Primers and probe specific for *M9* gene used to detect MHV-68 DNA.

Oligonucleotide	Sequence (5' – 3')
Upper primer	GCCACGGTGGCCCTCTA
Lower primer	CAGGCCTCCCTCCCTTTG
Probe	6-FAM-CTTCTGTTGATCTTCC-MGB[a]

[a] Oligonucleotide with fluorophore (6FAM) and quencher (MGB) covalently attached to the 5' – and 3' – ends, respectively.

3.3.8. Flow Cytometry

3.3.8.1. Determination of the percentage of cells by YFP expression

Each splenocyte suspension from section 3.3.5.A. was filtered through a 40 μm cell strainer and the number of viable cells was estimated by trypan blue exclusion. Then, $10x10^6$ cells were seeded in a round-bottom 96-well plate and incubated for 15 minutes at 4ºC with Fc blocking solution (Table 3.5.), diluted in PBS+2% FBS, to block Fc receptors. Cells were washed with 100 μL of PBS+2% FBS and centrifuged at 2000 rpm for 1 minute at 4ºC. Then, splenocytes were surfaced stained with the appropriate antibodies (Table 3.5.), diluted in PBS+2% FBS, for 25 minutes at 4ºC in the dark. After that, cells were washed twice with PBS+2% FBS, in order to remove unbound antibodies. Thereafter, cells were resuspended in PBS+2% FBS, transferred to tubes and kept on ice and protected from light until analysis. When necessary, cells were fixed in 2% formaldehyde (in PBS), after a centrifugation at 1200 rpm for 1 minute at 4ºC. After 20 minutes on ice, cells were centrifuged at 1200 rpm for 1 minute at 4ºC, the pellet was resuspended in PBS+2% FBS and samples were kept at RT until analysis.

Samples were analysed on LSR Fortessa flow cytometer (BD Biosciences) using FACSDiva software (BD Biosciences) for acquisition and FlowJo (Tree Star, Inc.) for analysis.

Table 3. 5. Antibodies used in flow cytometry assays.

Antigen	Reactivity (fluorochrome)	Specie	Dilution	Company
CD19	APC-H7	Rat	1:400	BD Biosciences
GL7	eF660	Rat	1:200	eBiosciences
CD95	PE	Rat	1:800	BD Biosciences
CD16/32	Anti-CD16/32 (blocking solution)	Rat	1:100	BD Pharmingen

3.3.8.2. Sorting of GC B cells

Each splenocyte suspension from section 3.3.5.B., from the pools of spleens, was centrifuged at 1200 rpm for 10 minutes at 4ºC and the pellet was resuspended in Fc blocking solution (Table 3.5.), diluted in PBS+2% FBS, and incubated for 3 minutes at 4ºC. After washing with PBS+2% FBS, the volume was made up to 10 mL, and cells were centrifuged at 1200 rpm for 5 minutes at 4ºC. Splenocytes were resuspended in the correspondent staining solution (antibodies diluted in PBS+2% FBS) (Table 6) and incubated for 30 minutes at 4ºC. Unbound antibodies were removed by washing with

PBS+2% FBS and centrifuging at 1200 rpm for 5 minutes at 4ºC. Cells were resuspended in PBS+2% FBS, filtered through a 40 µm cell strainer and purified by flow cytometry.

The stained samples were enriched for the GC B cell population $CD19^{+}CD95^{hi}GL7^{hi}$ using BD FACSAria Flow Cytometer (BD Biosciences). Cells were recovered into PBS+50% FBS and kept in ice until further use.

3.3.9. Frequency of viral DNA positive cells in GC B cells

The frequency of viral genome positive cells was determined by limiting dilution combined with real-time PCR. Flow activated cell sorting-purified GC B cells were 2-fold serially diluted in PBS+2% FBS and the following procedure was carried out according to section 3.3.7..

3.3.10. *In situ* hybridization to detect virally infected cells in spleen sections

3.3.10.1. Tissue preparation

Spleens were dissected from mice and fixed in 10% formalin, O/N, at RT, and then embedded in paraffin in the Histology and Comparative Pathology Laboratory of Instituto de Medicina Molecular João Lobo Antunes. Serial 5 µm sections were cut on Minot Microtome Leica RM 2145 and mounted on Superfrost Plus Slides (Menzel-Gläser).

3.3.10.2. *In situ* hybridization

Sections were dewaxed in xylene for 20 minutes, rehydrated through graded ethanol solutions (100% for 5 minutes, 90%, 70% and 50% for 2 minutes each) and then PBS for 5 minutes. After that, sections were fixed in 0.1% v/v glutaraldehyde (in PBS) for 30 minutes at 4ºC, washed twice in PBS for 5 minutes and digested with 100 µg/mL of proteinase K in 20 mM Tris pH 7.5 and 2 mM $CaCl_2$ in distilled H_2O (dH_2O) for 8 minutes at 37ºC. Thereafter, sections were rinsed in PBS for 2 minutes at RT, re-fixed in 0.1% v/v glutaraldehyde for 15 minutes at 4ºC, rinsed in PBS again for 2 minutes at RT, and then acetylated with fresh 0.25% v/v acetic anhydride in 0.1 M triethanolamine pH 8.0 for 10 minutes at RT. Sections were washed in 2x saline sodium citrate (SSC) (300 mM NaCl and 30 mM tri-sodium-citrate) for 5 minutes at 4ºC, before being dehydrated through graded ethanol (50% to 100%) and left to air dry.

A digoxigenin (DIG) uridine-5'-triphosphate-labelled riboprobe specific for viral tRNAs/miRNAs available in the lab was used (Bowden *et al*., 1997). For 600 µL of probe mix, 12 µL of DIG-labelled riboprobe were mixed with 300 µL of formamide, 30 µL of sonicated salmon sperm (10 mg/mL) and 30 µL of tRNA (10mg/mL). Mix was denatured by heating for 5 minutes at 80ºC and then quenched for 5 minutes at 4ºC. 120 µL of 5x hybridization buffer, 6 µL of dithiothreitol (DTT) (100 mM) and 6 µL of protector ribonuclease (RNase) inhibitor were mixed with 96 µL MilliQ H_2O. 50 µL of probe mix were added to each section, covered with a coverslip and incubated O/N at 55ºC in a humidified incubator.

Then, sections were washed with 2x SSC and 10 mM Tris pH 7.5 for 15 minutes at RT with stirring, followed by 0.1x SSC and 10 mM Tris pH 7.5 for additional 15 minutes. Next, sections were washed with 30% formamide, 0.1x SSC and 10 mM Tris pH 7.5 for 30 minutes at 58ºC. Finally, sections were rinsed in 0.1x SSC and 10 mM Tris pH 7.5 for 5 minutes at RT with stirring. The detection of the hybridized probe was performed with alkaline phosphatase (AP)-conjugated anti-DIG antibody (GE Healthcare). Sections were rinsed for 5 minutes, with stirring, in buffer 1 (100 mM Tris pH 7.5 and 150 mM NaCl in dH_2O), and then blocked by incubation in blocking buffer (1% Boehringer Blocking Reagent, Roche, in buffer 1) for 30 minutes at RT.

The next step was to dry the sections in the edges and incubate with 120 µL of anti-DIG-AP antibody (1:750 in blocking buffer) for 1 hour at RT in a humidified chamber. Unbound antibody was removed by washing twice with buffer 1 for 15 minutes at RT.

Next, detection with nitroblue tetrazolium chloride (NBT) was able to reveal the bound antibodies by colorimetric. Sections were rinsed in buffer 3 (100 mM Tris pH 9.5, 100 mM NaCl and 50 mM $MgCl_2$ in dH_2O) for 10 minutes at RT. Colour development was performed in the dark by incubation O/N of sections with X-Phos and NBT (Roche) in buffer 3. Reaction was stopped by rising in dH_2O (Simas *et al*., 1999). Sections were counterstained with 10% Mayer's Haemalum, rinsed in tap H_2O, mounted with Aquatex (Merck) and scanned with NanoZoomer-SQ (Hamamatsu). The analysis was performed with Fiji (ImageJ) software.

3.4. Statistical Analysis

Statistical analysis was performed with GraphPad Prism Software. All the statistical results were obtained by t-test (except the section 3.2.4. in which was performed a One-way ANOVA).

The frequency of genome positive cells was calculated from a regression plot of input cell number against the fraction of negative samples as described by Marques and colleagues (Marques *et al.*, 2003). The calculation was performed using the single-hit Poisson model (SHPM) by maximum likelihood estimation. The method developed by

Bonnefoix and colleagues consists in modelling the limiting dilution data according to the linear log-log regression model fitting the SHPM:

$$\left(-log\left(log(\mu_i)\right)\right) = log(f) + log(x_i)\ ,$$

where μ_i is the theoretical fraction of negative wells and x_i is the number of cells plated in each replicate well. f is the frequency of DNA positive cells and the maximum likelihood of f is the value that maximizes the function of SHPM. The model assumes that one cell of one cell subset is necessary and enough for generating a positive response (Bonnefoix *et al*., 2001).

4. Results

4.1. *In vitro* assays

4.1.1. Viral stock

A working stock of v-kLANA.yfp was prepared from media of infected cell monolayers (section 3.2.1.) and the titre was determined as described in section 3.2.2.. The value of the titre was 4.95×10^6 PFU/mL, which is within the range usually obtained in the laboratory ($> 10^6$ PFU/mL). This viral stock was used in all experiments.

4.1.2. Protein expression analysis

To confirm that the viral stocks expressed kLANA, expression of kLANA, YFP, and a housekeeping protein, actin, was assessed by Western blot using infected BHK-21 cell lysates (section 3.2.3.) (Figure 4.1.).

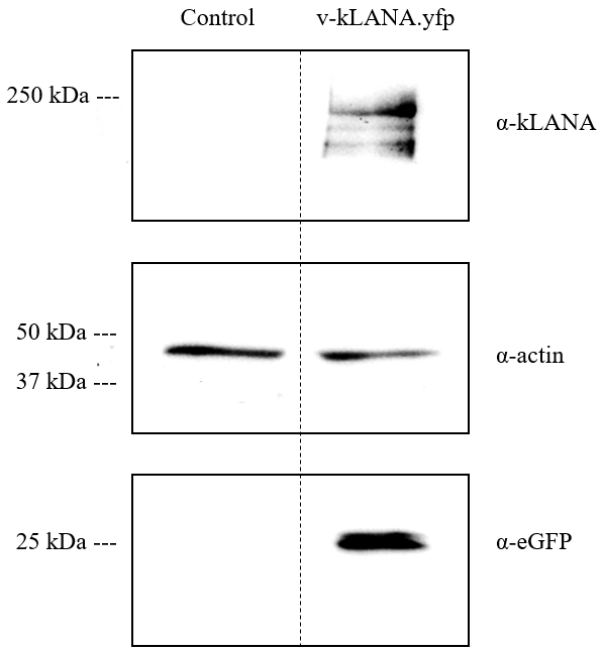

Figure 4. 1. Western blot analysis of proteins in total cellular lysate of infected cells with v-kLANA.yfp (molecular weight indicated on the left). 2.5×10^5 BHK-21 cells were infected with v-kLANA.yfp with a MOI of 3 PFU/cell for 6 hours. Control is a sample from uninfected cells.

LN53 was the antibody used to detect kLANA. It recognizes the repetitive glutamic motifs EQEQE in the glutamate and glutamine domain of kLANA. kLANA was observed at below the 250 kDa marker, as expected (Figure 4.1., top panel, lane 2). Other bands observed (Figure 4.1., top panel, lane 2) correspond to lower molecular weight isoforms of kLANA, which arise due to an alternative poly adenylation signal and different initiation of translation (Toptan *et al*., 2013). As expected, kLANA was not detected in the uninfected cell lysates (control) (Figure 4.1., top panel, lane 1).

Since this virus expresses YFP, an anti-eGFP antibody that recognizes GFP and variants, including YFP, was used to detect the YFP (Collins *et al*., 2009). A band corresponding to the expected size of YFP was observed at ≈ 25 kDa and was not observed in the control (uninfected cells) (Figure 4.1., middle panel).

Actin is a structural protein and is the main protein present in eukaryotic cells (Dominguez and Holmes, 2011). Both the samples, of cell lysates infected with kLANA and uninfected cell lysates (control) presented a band at ≈ 43 kDa, correspondent to actin of similar intensity, indicating equivalent loading of samples (Figure 4.1., bottom panel).

4.1.3. Effect of the studied drugs during lytic replication

A one-step growth curve was performed to identify potential alterations in the replication of the virus in the presence of three drugs: sulfathiazole, sulfanilamide and glybenclamide (section 3.2.4.) (Figure 4.2.). Sulfathiazole was tested at 25.5 μg/mL while sulfanilamide was tested at 17.2 μg/mL, based on the work of Angius and collegues, that used these concentrations on a cell line latently infected (Angius *et al*., 2017). Glybenclamide was tested at two doses: 25 μg/mL, based on the work of Malaisse and Malaisse-Lagae about insulin secretion *in vitro* (Malaisse and Malaisse-Lagae, 1970), and a smaller dose, 5 μg/mL. This assay allows the evaluation of the effect of the drugs in the lytic phase of infection, since kLANA is also expressed in this phase and there is not any data concerning the effect of the drugs in the lytic phase.

Moreover, it is important to validate the kinetics of the virus growth to confirm if the virus can grow properly from low dilutions and thus, corroborate the fitness of the viral stock to use *in vivo*.

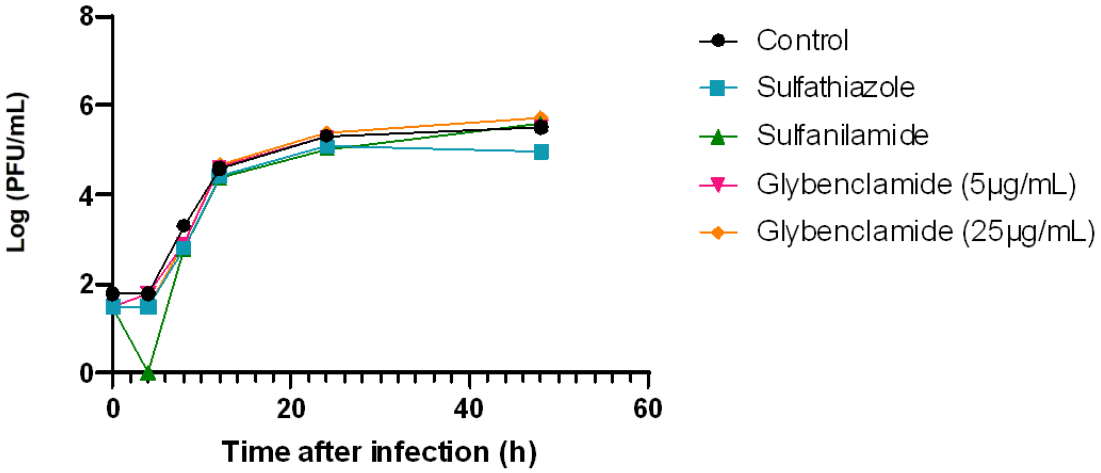

Figure 4. 2. One-step growth curve of v-kLANA.yfp in presence of sulfathiazole (25.5 µg/mL, blue), sulfanilamide (17.2 µg/mL, green), and glybenclamide (5 and 25 µg/mL, pink and orange, respectively). $5x10^4$ BHK-21 cells were infected with 5 PFU per cell of v-kLANA.yfp and at the indicated times, in hours, post-infection (0, 4, 8, 12, 24 and 48), cells and respective media were harvested, freeze-thawed and titrated by plaque assay. There was no statistically significant difference between experimental groups (One-way ANOVA statistical test).

The growth exhibited by the four experimental groups was similar to the untreated samples (control) (Figure 4.2.). Small differences observed did not reach statistical significance in One-way ANOVA statistical test. Thus, the assayed drugs, at the indicated concentrations, had no effect in virus replication.

In addition, this assay demonstrated that the viral stock used has a normal growth kinetics, showing that the virus can replicate efficiently. Therefore, the viral stock is fit for use *in vivo*.

4.2. *In vivo* assays

4.2.1. Effect of Sulfathiazole and Sulfanilamide in latent infection

Due to the very well documented toxicity and side effects of sulfonamides, and the lack of recent and consistent information about the doses in the literature, the starting point was to try a low dose. Therefore, on a first experiment, both drugs were tested at 0.25 mg/g of body weight. After the first experiment, the dose of both drugs was increased to 1 mg/g and an additional experimental group was administered with 0.5 mg/g of sulfathiazole, since sulfathiazole is more toxic than sulfanilamide (data obtained from an experiment not shown). The dose of both drugs was always equal so it could be compared. Mice were intranasally inoculated with 10^4 PFU of v-kLANA.yfp and the drugs were administered from 9 to 13 dpi (sections 3.3.3., 3.3.4. and 3.3.4.1.).

4.2.1.1. Toxicity

Considering all the performed experiments, the survival rate of mice administered with sulfathiazole and sulfanilamide was evaluated. Both drugs at 0.25 mg/g had a survival of 100% (n= 5 mice) with no signs of toxicity, as well as sulfathiazole at 0.5 mg/g (n= 5 mice). The dose of 1 mg/g was tested in two experiments and both experiments contribute to the survival rate obtained (n=10 mice, 5 mice from each experiment). A first experiment to check the toxicity of both drugs at 1 mg/g was performed and the results revealed the necessity of the addition of an experimental group treated with half of that dose of sulfathiazole in the next experiment. The increase to 1 mg/g, lead to a death rate of 10% in the case of sulfanilamide died. On the other hand, only 30% of mice administered with sulfathiazole had survived. Mice treated with sulfanilamide at 1 mg/g presented signs of toxicity, such as bristly and slow movements, since the second day of treatment, while mice treated with sulfathiazole only showed similar signs right before death, allied to muscle spasms. The deaths associated with the administration of sulfathiazole started on the second day of treatment – three mice died on the second day; one died on the third day; two died on the fourth day; and one died on the fifth day. In the case of sulfanilamide, the only death occurred on the fourth day. Given this, data of sulfathiazole at 1 mg/g is only data of three mice, while data of sulfanilamide at the same dose is constituted by four mice.

4.2.1.2. Infectious Centre Assay

To assess if the drugs can affect the establishment of latency of the virus in the spleen, infectious centre assay was performed.

This assay, also named *ex vivo* reactivation assay, consists in measuring latent virus reactivating from splenocytes, by co-culturing them with permissive BHK-21 cells. Virus reactivating from splenocytes form viral plaques, which were quantified (section 3.3.6.) (Figures 4.3. and 4.4., closed symbols). In parallel, it is necessary to verify that there are no lytic preformed infectious viruses in the spleen that could contribute to the number of viral plaques determined in the reactivating assay. To this end, an aliquot of the splenocyte suspensions was frozen - thus killing cells -, and thawed samples were titrated in BHK-21 cells (Figures 4.3. and 4.4., open symbols).

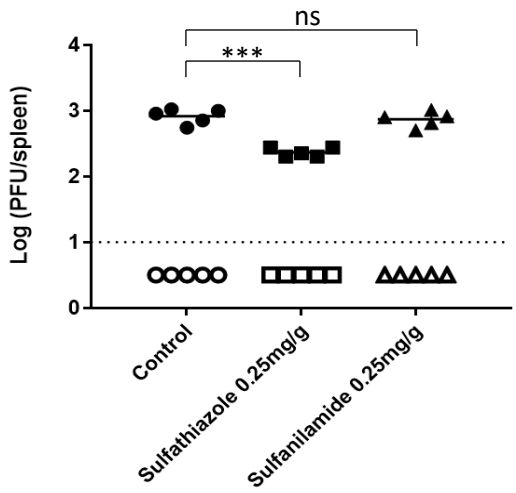

Figure 4. 3. Quantification of latent infection in the spleen, 14 dpi, by *ex vivo* reactivation assay. BALB/c mice were intranasally inoculated with 10^4 PFU of v-kLANA.yfp. At day 9 post-infection, groups of four mice were treated with: 0.25 mg/g/day of sulfathiazole in water (■); 0.25 mg/g/day of sulfathiazole in 17% DMSO/water (▲); or PBS (control, ●) by intraperitoneal injection. A daily dose was administered until mice were sacrificed at day 14 post-infection. Spleens were dissected, single splenocyte suspensions were prepared and latent viruses were titrated by *ex vivo* co-culture assay (closed symbols). Titres of infectious viruses were determined in freeze-thawed splenocyte suspensions (open symbols). Each circle represents the titre of an individual mouse and the horizontal bars denote mean values. The dashed line represents the limit of detection of the assay. (***: p-value<0.001; non-significant (ns): p-value>0.05, by unpaired t-test).

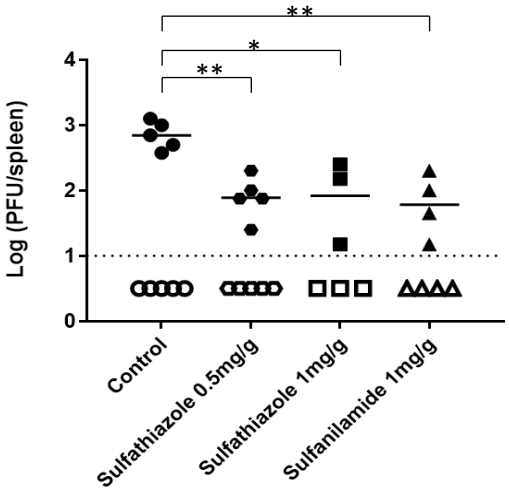

Figure 4. 4. Quantification of latent infection in the spleen, 14 dpi, by *ex vivo* reactivation assay. BALB/c mice were intranasally inoculated with 10^4 PFU of v-kLANA.yfp. At day 9 post-infection, four groups of mice were treated with: 0.5 mg/g/day of sulfathiazole in water (⬣); 1 mg/g/day of sulfathiazole in water (■); 1 mg/g/day of sulfanilamide in 17% DMSO/water (▲); or PBS (control, ●) by intraperitoneal injection. A daily dose was administered until mice were sacrificed at day 14 post-infection. Spleens were dissected, single splenocyte suspensions were prepared and latent viruses were titrated by *ex vivo* co-culture assay (closed symbols). Titres of infectious viruses were determined in freeze-thawed splenocyte suspensions (open symbols). Each circle represents the titre of an individual mouse and the horizontal bars denote mean values. The dashed line represents the limit of detection of the assay. (*: p-value<0.05; **: p-value<0.01, by unpaired t-test).

Untreated mice (control) presented an average of reactivating titres of $10^{2.95}$ PFU/mL and $10^{2.85}$ PFU/mL (Figures 4.3. and 4.4., respectively), which is in accordance with the previously described (data not published).

As observed, when mice are treated with sulfathiazole, latency is affected, being statistically significant the decrease with any of the doses, comparatively with the control (Figures 4.3. and 4.4.). A reduction of 0.6 log at 0.25 mg/g (Figure 4.3.), 1 log at 0.5 mg/g and 0.7 log at 1 mg/g (Figure 4.4.) was observed. Nevertheless, it is important to note that, at 1 mg/g, the group only has three mice, giving less credibility to the obtained results.

On the other hand, even though sulfanilamide did not show any effect at 0.25 mg/g, with a decrease of 0.05 log (Figure 4.3.), when the dose was increased to 1 mg/g, a reduction of 1 log was observed, being statistically significant (Figure 4.4.). However, at 1 mg/g, the experimental group is only constituted by four mice.

4.2.1.3. Frequency of DNA positive cells in total splenocytes

Additionally, a limiting dilution assay to quantify viral DNA positive cells in total splenocytes was performed. Real time PCR analysis using specific probe and primers for MHV-68 *M9* gene was done as described (section 3.3.7.). This assay does not depend on the ability of the virus to reactivate *ex vivo* as the infectious centre assay, and thus constitutes a complementary and independent measure of latent virus (Figure 4.5., and Tables 4.1. and 4.2.)

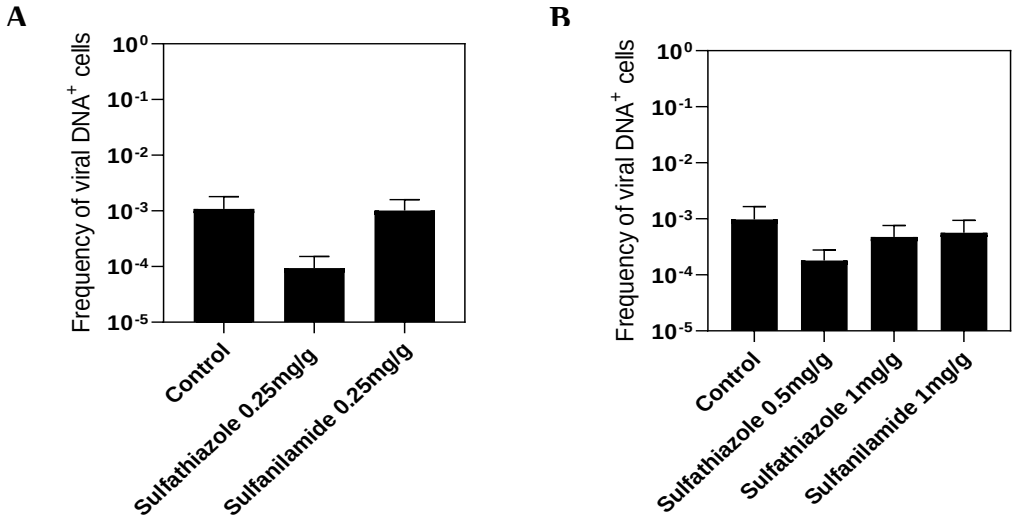

Figure 4. 5. Frequency of viral DNA positive cells in total splenocytes, obtained by limiting dilution assay and real-time PCR. Bars represent frequency of viral DNA positive cells with 95% confidence intervals. a) Data obtained from pools of five mice. b) Data obtained from pools of three (sulfathiazole 1 mg/g); four (sulfanilamide 1 mg/g); and five (sulfathiazole 0.5 mg/g) mice.

Table 4. 1. Reciprocal frequency of viral DNA positive cells in total splenocytes related to Figure 4.5.A..

Cell Population	Experimental group	Reciprocal frequency of viral DNA positive cells	95% confidence interval
Total Splenocytes	**Control**	925.39	(556.20; 2752.29)
	Sulfathiazole 0.25mg/g	10612.27	(6582.75; 27360.60)
	Sulfanilamide 0.25mg/g	987.56	(625.62; 2343.14)

Table 4. 2. Reciprocal frequency of viral DNA positive cells in total splenocytes related to Figure 4.5.B..

Cell Population	Experimental group	Reciprocal frequency of viral DNA positive cells	95% confidence interval
Total Splenocytes	**Control**	1027.91	(603.04; 3479.05)
	Sulfathiazole 0.5mg/g	5545.76	(3592.04; 12159.17)
	Sulfathiazole 1mg/g	2101.14	(1309.91; 5306.31)
	Sulfanilamide 1mg/g	1771.28	(1062.58; 5318.65)

Untreated mice (control) presented a reciprocal frequency of viral DNA positive cells of 925.39 and 1027.91 (Tables 4.1. and 4.2., respectively), which is concordant with the previously described (data not published).

Sulfathiazole showed to be able to decrease the frequency of infection, at any of the doses, when compared with the control. A decrease of 11.5-fold at 0.25 mg/g (Figure 5.A. and Table 4.1.), 5.4-fold at 0.5 mg/g and 2-fold at 1 mg/g (Figure 5.B. and Table 4.2.) was reached. Thus, according to this assay, an increase of the frequency of infection is related with an increase of the dose.

Sulfanilamide at 0.25 mg/g exhibited a 1-fold decrease, not displaying any effect (Figure 5.A. and Table 4.1.). At 1mg/g, there was a decrease of 1.7-fold relatively to control (Figure 4.5.B. and Table 4.2.).

4.2.1.4. Flow Cytometry

GC B cells are the main target of the virus to establish latency. Flow cytometry allows the quantification of the latent infection in B cells of the spleen, after incubation with specific antibodies (section 3.3.8.1.) (Figures 4.6., 4.7. and 4.8.; Appendix I). First, the percentage of GC B cells was determined (Figure 4.6.; Appendix I). The data represented on Appendix I refers to an experiment from which there were not acquired enough events so that the results could be significant. Due to this, the results are just indicative, being necessary to repeat the experiment.

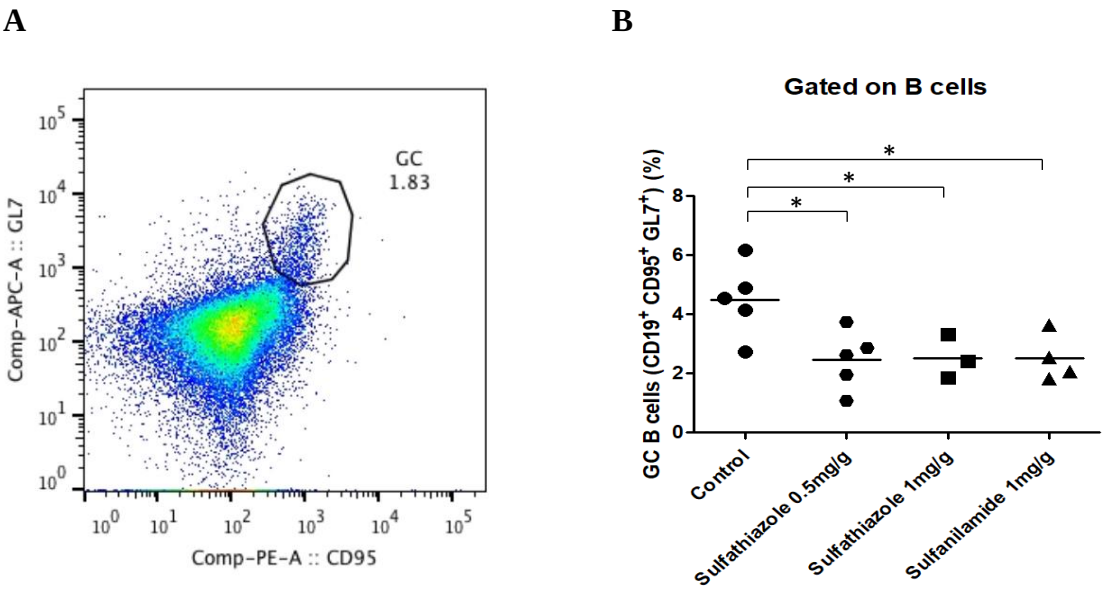

Figure 4. 6. Flow cytometry analysis. Percentage quantification of GC B cells ($CD19^+$ $GL7^+$ $CD95^+$). a) Representative flow cytometry plot gated on B cells. The indicated value refers to a percentage. b) Each dot represents an individual mouse and the horizontal bars denote mean values. (*: p-value<0.05, by unpaired t-test).

Untreated mice (control) presented a mean percentage of GC B cells of 4.5% (Figure 4.6.), which is in accordance with the previously described (data not published).

Gated on B cells, the percentage of GC B cells decreased when compared to the control (Figure 4.6.). While the mean percentage of GC B cells of the control is 4.5%, mice treated with sulfathiazole presented a decrease of 2.1% (1.5-fold decrease) at 0.5 mg/g and 2% (1.8-fold decrease) at 1mg/g (Figure 4.6.), comparing with the respective control. Mice treated with sulfanilamide also showed a decrease of 2% (1.8-fold decrease) at 1 mg/g (Figure 4.6.).

The next step was to determine the percentage of infected cells in GC B cells, through YFP protein expression (Figure 4.7.; Appendix I).

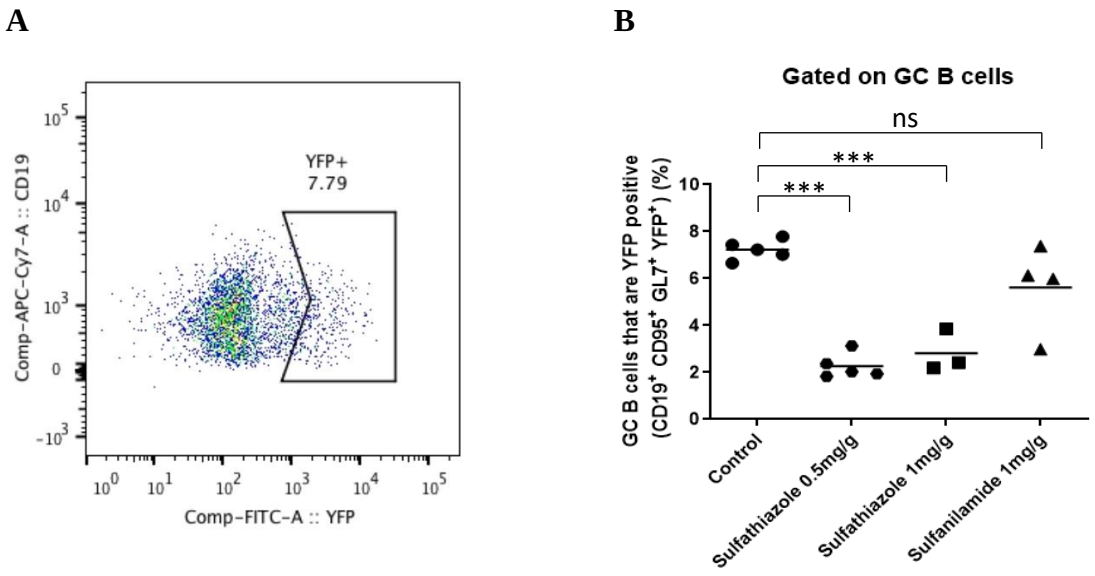

Figure 4. 7. Flow cytometry analysis. Percentage quantification of infected GC B cells ($CD19^+$ $GL7^+$ $CD95^+$ YFP^+). a) Representative flow cytometry plot gated on GC B cells. The indicated value refers to a percentage. b) Each dot represents an individual mouse and the horizontal bars denote mean values. (***: p-value<0.001; ns: p-value>0.05, by unpaired t-test).

Untreated mice (control) presented a percentage of infected GC B cells of 7.2% (Figure 4.7.), which is in accordance with the previously described (data not published).

The gate on GC B cells associated with the expression of YFP protein allows the identification of the percentage of infected GC B cells (Figure 4.7.). When compared with the control, sulfathiazole had a decrease of 4.9% (3.1-fold) at 0.5 mg/g and 4.4% (2.6-fold) at 1 mg/g (Figure 4.7.), with the same statistical significance for both. Sulfanilamide also presented a decrease, in this case a decrease of 1.6% (1.3-fold) at 1 mg/g (Figure 4.7.), even though it did not reach statistical significance.

The frequency of infected B cells with GC phenotype was also determined (Figure 4.8.; Appendix I).

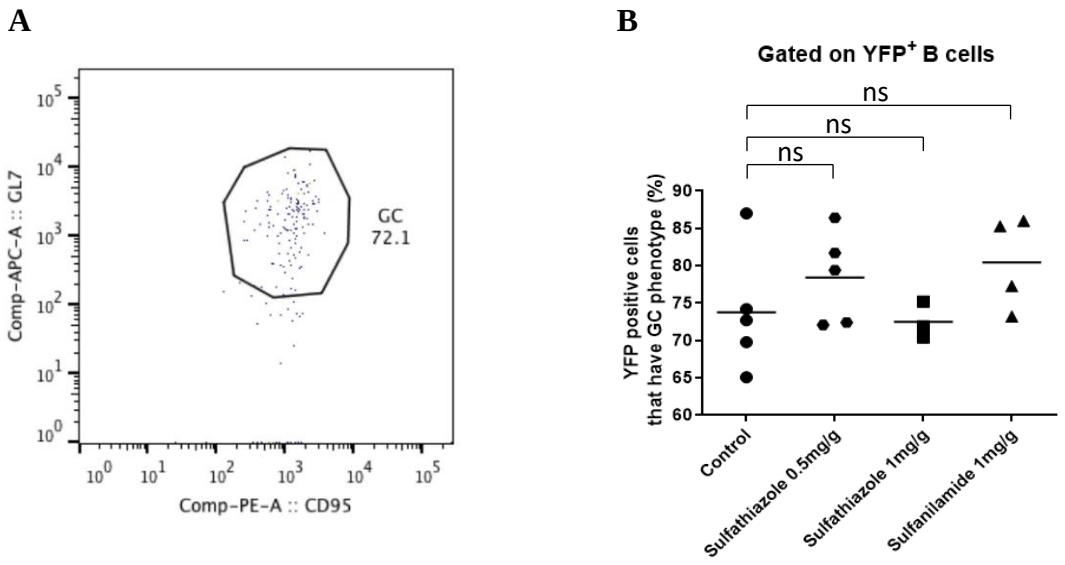

Figure 4. 8. Flow cytometry analysis. Percentage quantification of infected B cells with GC phenotype ($CD19^+$ YFP^+). a) Representative flow cytometry plot gated on YFP positive B cells. The indicated value refers to a percentage. b) Each dot represents an individual mouse and the horizontal bars denote mean values. (ns: p-value>0.05, by unpaired t-test).

Untreated mice (control) presented a percentage of infected B cells with GC phenotype of 73% (Figure 4.8.), which is concordant with the previously described (data not published).

Despite of the high discrepancy between the individual values of each group, all of the experimental groups presented similar values comparatively to the control, not reaching statistical significance (Figure 4.8.).

4.2.2. Effect of Glybenclamide in latent infection

Glybenclamide is a very effective hypoglycemic drug that acts on the stimulation of insulin secretion. Nowadays, this drug is used to control glycemia in diabetics with an oral posology up to 5 mg/day/person (Aurobindo Pharma Limited, 2011). Therefore, it would be safer to administrate to mice a lower dose comparing to sulfathiazole and sulfanilamide, in order to avoid the lethality of the hypoglycemic effect. Mice were intranasally inoculated with 10^4 PFU of v-kLANA.yfp and glybenclamide was administered from 9 to 13 dpi, at 0.005 mg/g (sections 3.3.3., 3.3.4. and 3.3.4.2.).

4.2.2.1. Toxicity

The toxicity associated with the administration of glybenclamide was evaluated and at 0.005 mg/g the survival rate was 100%, even though the mice presented slow movements from day two.

4.2.2.2. Infectious Centre Assay

An infectious centre assay was performed to evaluate if glybenclamide, at 0.005 mg/g, can affect the establishment of latency of the virus in the spleen (section 3.3.6.) (Figure 4.12.).

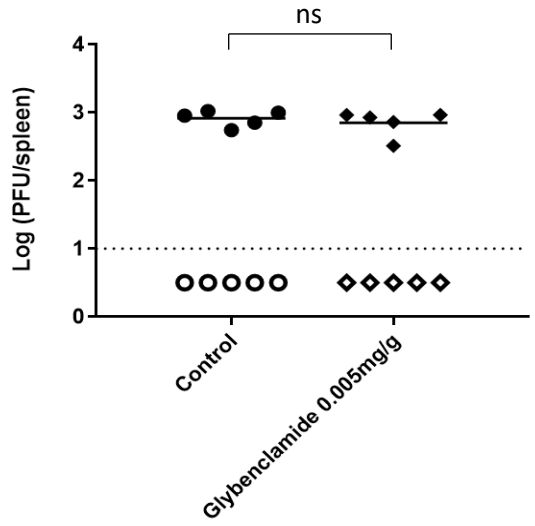

Figure 4. 9. Quantification of latent infection in the spleen, 14 dpi, by *ex vivo* reactivation assay. BALB/c mice were intranasally inoculated with 10^4 PFU of v-kLANA.yfp. At day 9 post-infection, four groups of mice were treated with: 0.005 mg/g/day of glybenclamide (◆); or PBS (control, ●) by intraperitoneal injection. A daily dose was administered until mice were sacrificed at day 14 post-infection. Spleens were dissected, single splenocyte suspensions were prepared and latent viruses were titrated by *ex vivo* co-culture assay (closed symbols). Titres of infectious viruses were determined in freeze-thawed splenocyte suspensions (open symbols). Each circle represents the titre of an individual mouse and the horizontal bars denote mean values. The dashed line represents the limit of detection of the assay. (ns: p-value>0.05, by unpaired t-test).

Untreated mice (control) presented an average of reactivating titres of $10^{2.95}$ PFU/mL (Figure 4.9.).

As observed, at this dose, glybenclamide did not affect latency, presenting a value similar to the control, with a decrease of only 0.02 log (Figure 4.9.).

4.2.2.3. Frequency of DNA positive cells in total splenocytes

A limiting dilution assay was performed to determine the frequency of DNA positive cells in total splenocytes (section 3.3.7.) (Figure 4.10. and Table 4.3.).

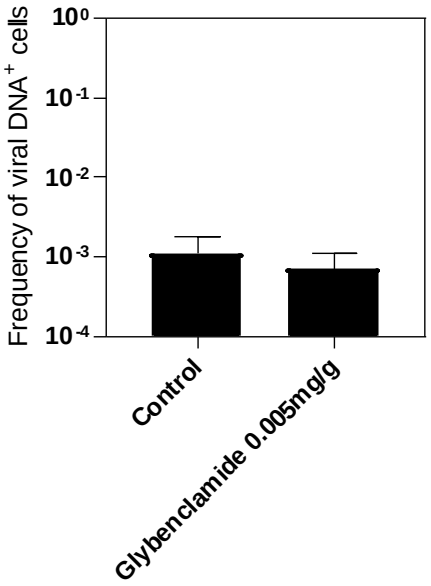

Figure 4. 10. Frequency of viral DNA positive cells in total splenocytes, obtained by limiting dilution assay and real-time PCR. Bars represent frequency of viral DNA positive cells with 95% confidence intervals. Data was obtained from pools of five mice.

Table 4. 3. Reciprocal frequency of viral DNA positive cells in total splenocytes related to Figure 4.10..

Cell Population	Experimental group	Reciprocal frequency of viral DNA positive cells	95% confidence interval
Total Splenocytes	**Control**	925.39	(556.20; 2752.29)
	Glybenclamide 0.005mg/g	1424.38	(925.07; 3094.81)

Untreated mice (control) presented a reciprocal frequency of viral DNA positive cells of 925.39 (Table 4.3.).

A 1.5-fold decrease was observed in the frequency of infection in mice treated with glybenclamide, when compared with the control (Figure 4.10. and Table 4.3.).

4.2.2.4. Flow Cytometry

The latent infection in B cells of the spleen was analysed by flow cytometry (section 3.3.8.) (Appendix II). The data represented on Appendix II refers to an experiment from which there were not acquired enough events so that the results could be significant. Due to this, the results are just indicative, being necessary to repeat the experiment.

4.2.3. Effect of JQ1 in latent infection

There are several studies with different doses with JQ1. Peirs and colleagues performed *in vivo* experiments with JQ1 at 0.05 mg/g in DMSO/10% 2-hydropropil-β-ciclodextrin via intraperitoneal and both the survival rate and the results involving c-Myc were satisfactory. Therefore, the chosen dose and vehicle were based on this work (Peirs *et al.*, 2017). Mice were intranasally inoculated with 10^4 PFU of v-kLANA.yfp and JQ1 was administered from 9 to 13 dpi, at 0.05 mg/g (sections 3.3.3., 3.3.4. and 3.3.4.3.).

4.2.3.1. Toxicity

There were no signs of toxicity associated with the administration of JQ1 at 0.05 mg/g, as the mice maintained normal behaviour throughout the experiments.

4.2.3.2. Infectious Centre Assay

To evaluate if JQ1 affected the establishment of latency of the virus in the spleen, infectious centre assay was performed (section 3.3.6.) (Figure 4.11.).

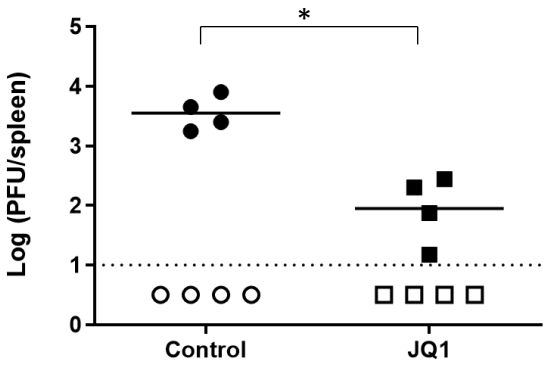

Figure 4. 11. Quantification of latent infection in the spleen, 14 dpi, by *ex vivo* reactivation assay. BALB/c mice were intranasally inoculated with 10^4 PFU of v-kLANA.yfp. At day 9 post-infection, four groups of mice were treated with: 0.05 mg/g of JQ1 in a solution of DMSO and 10% 2-hydropropil-β-ciclodextrin, in 1:10 (■); or 1:10 DMSO/10% 2-hydropropil-β-ciclodextrin (control, ●) by intraperitoneal injection. A daily dose was administered until mice were sacrificed at day 14 post-infection. Spleens were dissected, single splenocyte suspensions were prepared and latent viruses were titrated by *ex vivo* co-culture assay (closed symbols). Titres of infectious viruses were determined in freeze-thawed splenocyte suspensions (open symbols). Each circle represents the titre of an individual mouse and the horizontal bars denote mean values. The dashed line represents the limit of detection of the assay. (*: p-value<0.05, by unpaired t-test).

Untreated mice (control) presented an average of reactivating titres of $10^{3.53}$ PFU/mL (Figure 4.11.).

The results of the administration of JQ1 to mice showed that the drug affects viral latency, being observed a statistically significant decrease of 1.4 log (Figure 4.11.).

4.2.3.3. Frequency of DNA positive cells in total splenocytes

To determine the frequency of DNA positive cells in total splenocytes, a limiting dilution assay was performed (section 3.3.7.) (Figure 4.12. and Table 4.4.).

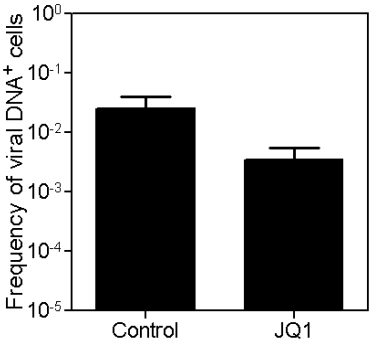

Figure 4. 12. Frequency of viral DNA positive cells in total splenocytes, obtained by limiting dilution assay and real-time PCR. Bars represent frequency of viral DNA positive cells with 95% confidence intervals. Data was obtained from pools of four mice.

Table 4. 4. Reciprocal frequency of viral DNA positive cells in total splenocytes related to Figure 4.15..

Cell Population	Experimental group	Reciprocal frequency of viral DNA positive cells	95% confidence interval
Total Splenocytes	**Control**	39.60	(24.91; 96.59)
	JQ1	292.19	(183.71; 713.56)

Untreated mice (control) presented a reciprocal frequency of viral DNA positive cells of 39.60 (Table 4.4.), which is lower than expected (data not published). Thus, further experiments are necessary to confirm this value.

Mice treated with JQ1 exhibited a 7.4-fold decrease in frequency of infection, when compared with the control (Figure 4.12. and Table 4.4.).

4.2.3.4. Flow Cytometry

The quantification of the latent infection in B cells of the spleen was performed by flow cytometry (section 3.3.8.) (Figures 4.13., 4.14. and 4.15.). Gated on B cells, the percentage of GC B cells was determined (Figure 4.13.).

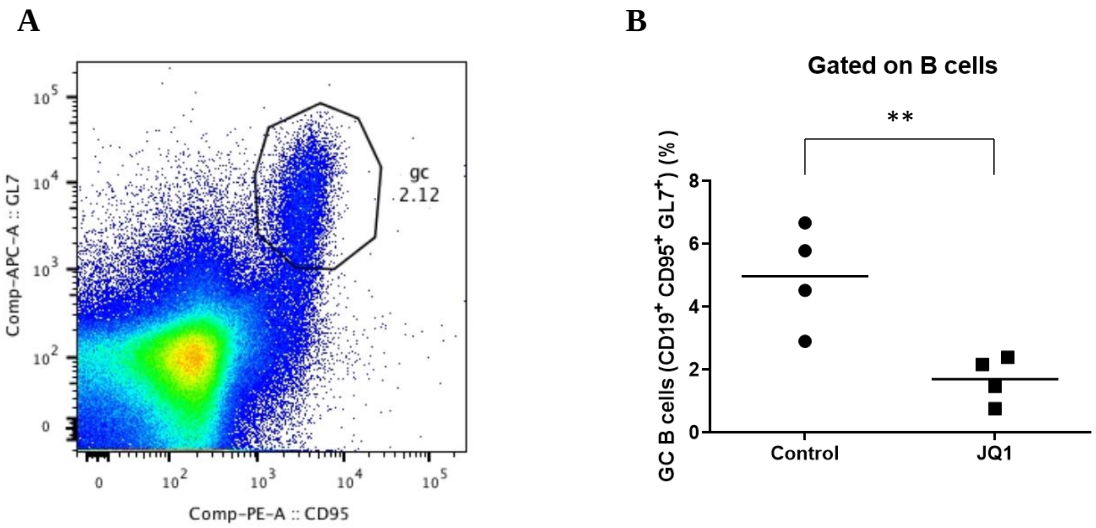

Figure 4. 13. Flow cytometry analysis. Percentage quantification of GC B cells ($CD19^+$ $GL7^+$ $CD95^+$). a) Representative flow cytometry plot gated on B cells. The indicated value refers to a percentage. b) Each dot represents an individual mouse and the horizontal bars denote mean values. (**: p-value<0.01, by unpaired t-test).

Untreated mice (control) presented a percentage of GC B cells of 5.2% (Figure 4.13.).

A decrease of the percentage of GC B cells to less than half was detected (Figure 4.13.). The control presented 4.9% of GC B cells and, mice treated with JQ1, decreased that percentage to 1.7%, exhibiting a reduction of 3.2% (1.5-fold). To note that the control presents high discrepancy between the individual values.

Next, the percentage of infected GC B cells was analysed (Figure 4.14.).

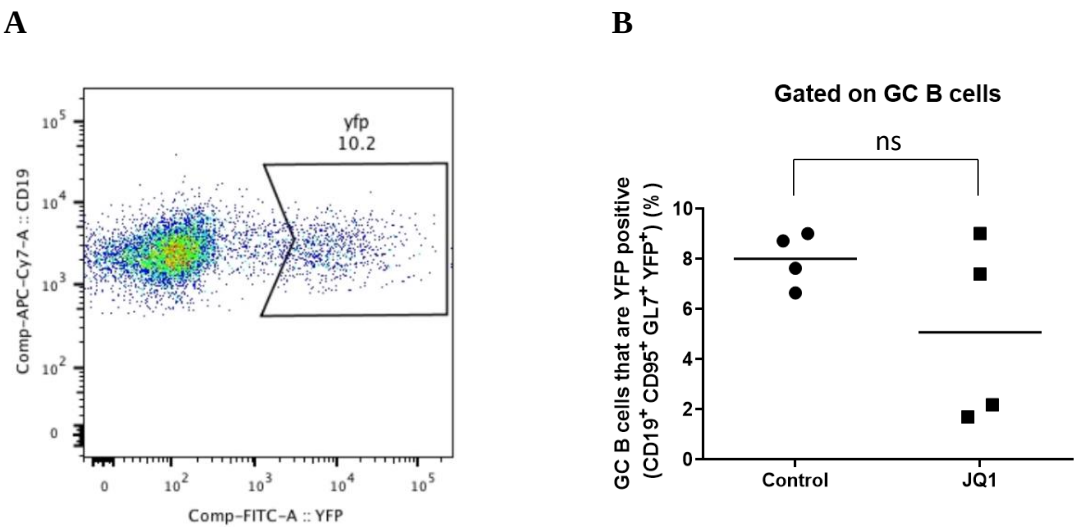

Figure 4. 14. Flow cytometry analysis. Percentage quantification of infected GC B cells ($CD19^+$ $GL7^+$ $CD95^+$ YFP^+). a) Representative flow cytometry plot gated on GC B cells. The indicated value refers to a percentage. b) Each dot represents an individual mouse and the horizontal bars denote mean values. (ns: p-value>0.05, by unpaired t-test).

Untreated mice (control) presented a percentage of infected GC B cells of 8.2% (Figures 4.14.).

The percentage of infected GC B cells was identified with the gate on GC B cells allied with the expression of YFP protein (Figure 4.14.). Although mice treated with the drug had a decrease of 3.3% (1.7-fold) when compared with the control, it does not reach statistical significance, since there is a high dispersion between the values.

The frequency of infected B cells with GC phenotype was also determined (Figure 4.15.).

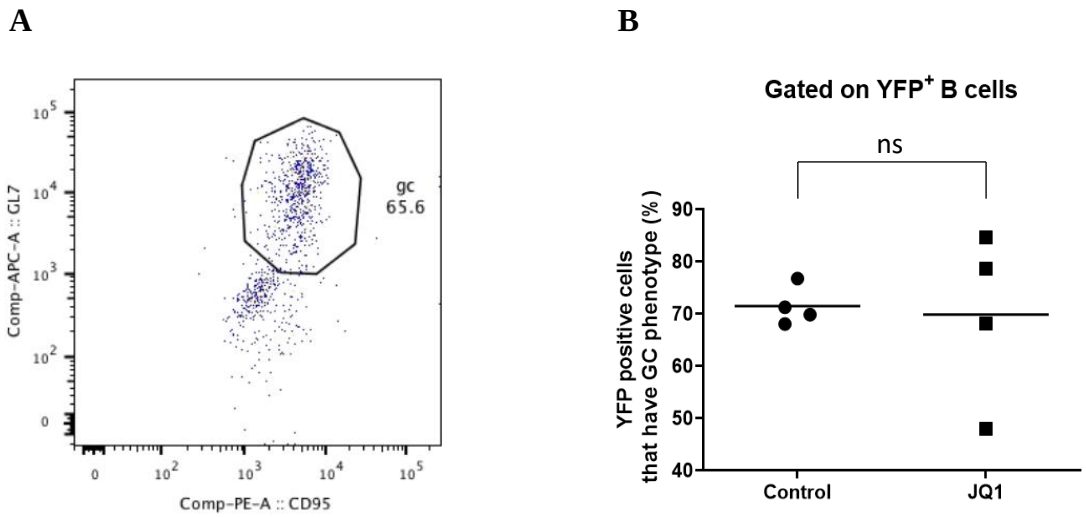

Figure 4. 15. Flow cytometry analysis. Percentage quantification of infected B cells with GC phenotype ($CD19^+$ YFP^+). a) Representative flow cytometry plot gated on YFP positive B cells. The indicated value refers to a percentage. b) Each dot represents an individual mouse and the horizontal bars denote mean values. (ns: p-value>0.05, by unpaired t-test).

Untreated mice (control) presented a percentage of infected B cells with GC phenotype of 71% (Figures 4.15.).

The result obtained in mice treated with JQ1 was not statistically significant, presenting values comparable to the control.

The number of total splenocytes was also determined, by counting cells on the haemocytometer, and the number of GC B cells was obtained based on the percentage obtained by flow cytometry and total cell count (Figure 4.16.).

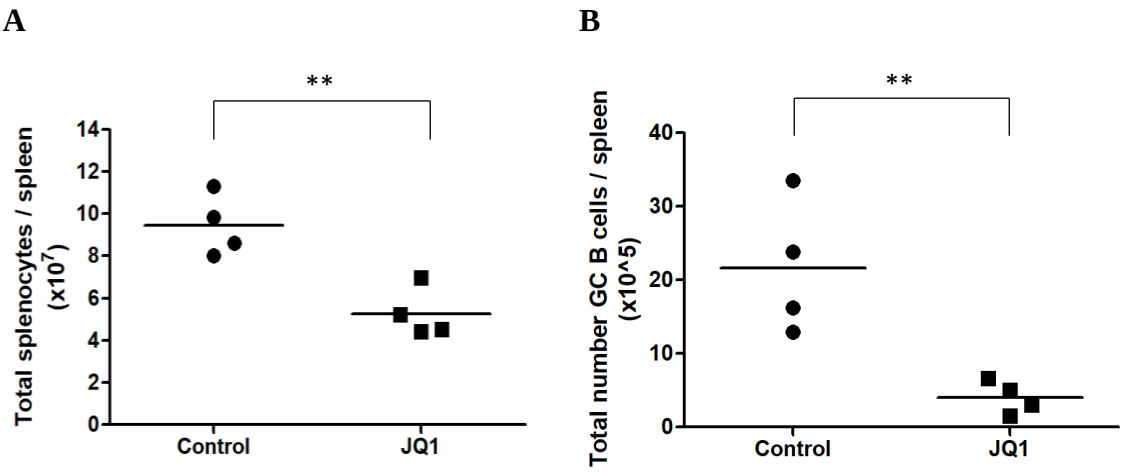

Figure 4. 16. Quantification of cells per spleen, each dot represents an individual mouse and the horizontal bars denote mean values. a) Quantification of total splenocytes per spleen estimated by trypan blue exclusion. b) Quantification of the total number of GC B cells ($CD19^+$ $GL7^+$ $CD95^+$) per spleen, calculated through the counted cells and the parental percentage, acquired by flow cytometry. (**: p-value<0.01, by unpaired t-test).

Untreated mice (control) presented a total number of splenocytes of $9.2x10^7$ (Figure 4.16.A.) and a total number of GC B cells of $20x10^5$ (Figure 4.16.B.), which is in accordance with the previously described (data not published).

As observed, mice treated with JQ1 showed a statistically significant decrease of $4.4x10^7$ of total splenocytes (1.9-fold) and of $15.9x10^5$ (4.9-fold) of GC B cells. Therefore, Figure 4.16.B. presented a result concordant with the Figure 4.13., highlighting the efficacy of JQ1 in reducing GC B cells.

4.2.3.5. Frequency of viral DNA positive cells in GC B cells

The promising results of JQ1 in ICA and in limiting dilution assay (sections 4.2.3.2. and 4.2.3.3.), allied to the results obtained in flow cytometry (section 4.2.3.4.), encouraged further study about this drug. The results obtained previously showed that JQ1 was able to affect viral latency, as well as to decrease the frequency of infection in total splenocytes. However, in cytometry analysis, it was showed that, gated on GC B cells, there was not a significant decrease in the percentage of infected GC B cells, and there was also a significant decrease of GC B cells, even though the percentage of infected cells that are GC B cells remained similar, when compared to the control.

Therefore, the next step was sorting the GC B cells from splenocyte suspensions (section 3.3.8.2.) and, then, determinate the frequency of viral DNA positive cells in GC B cells, by limiting dilution assay (section 3.3.9.) (Figure 4.17. and Table 4.5.).

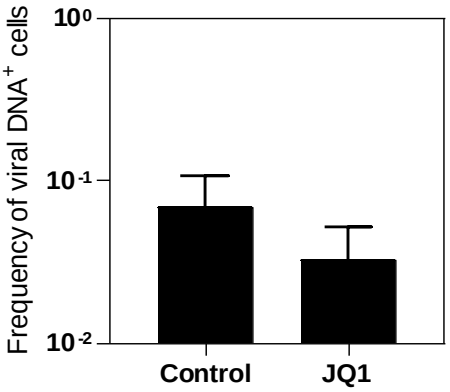

Figure 4. 17. Frequency of viral DNA positive cells in GC B cells, obtained by limiting dilution assay and real-time PCR. Data were obtained from pools of five mice. Bars represent frequency of viral DNA positive cells with 95% confidence intervals.

Table 4. 5. Reciprocal frequency of viral DNA positive cells in GC B cells related to Figure 4.20..

Cell Population	Experimental group	Reciprocal frequency of viral DNA positive cells	95% confidence interval
GC^+	**Control**	14.54	(9.35; 32.70)
	JQ1	30.57	(19.48; 71.02)

Untreated mice (control) presented a reciprocal frequency of viral DNA positive cells of 14.54 (Table 4.5.).

The decrease observed was only of 2.1-fold, being much less significative than the 7.4-fold determined in limiting dilution assay in total splenocytes (section 4.2.3.3.) (Figure 4.17. and Table 4.5.).

4.2.3.6. *In situ* hybridization to detect virally infected cells in spleen sections

Follicles are sites where there are T, B and GC B cells, and were occurs GC reaction. *In situ* hybridization using probe specific for MHV-68 and RNAs, transfer RNAs (tRNA) and miRNAs, was performed to detect infected cells in spleen sections. Analysis of the spleen sections also allow identification and quantification of the number and size of follicles (section 3.3.10.) (Figures 4.18. to 4.24.).

A

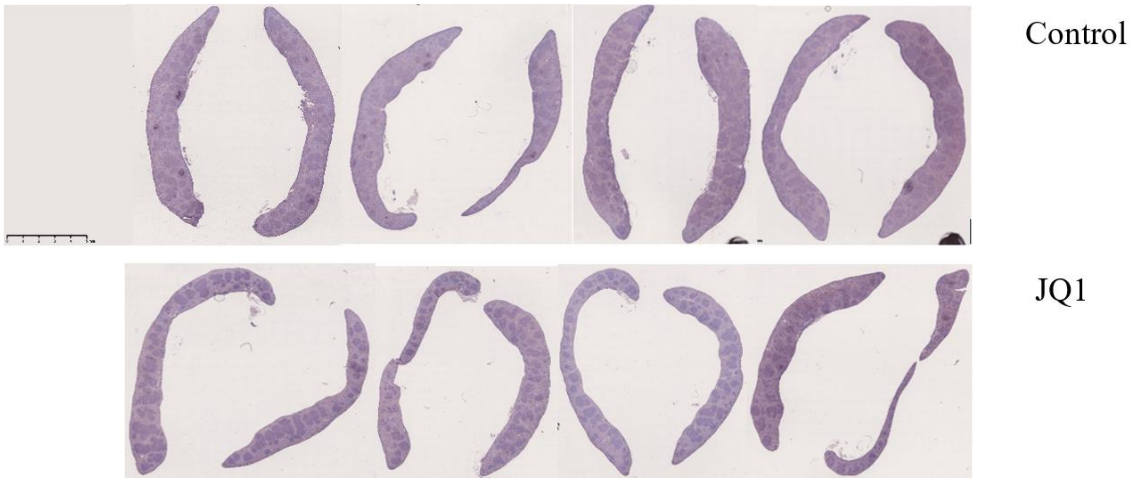

B

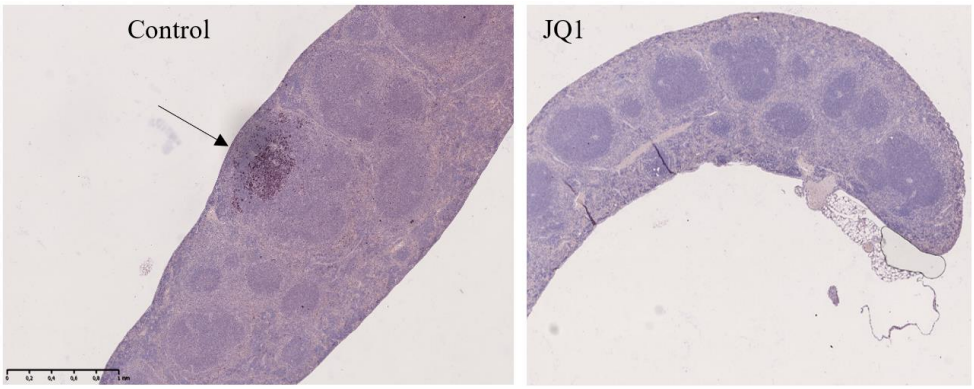

Figure 4. 18. Analysis of spleen sections of untreated (control) and treated (JQ1) mice after *in situ* hybridization (20x). a) Spleen sections of the four mice of each experimental group. Brown dots indicate infected follicles. Unspecific background is observed in the spleen sections. Scale bar: 5 mm. b) Representative spleen sections of the control group (left) and JQ1 group (right), highlighting the infection (brown dots, indicated by the arrow). Scale bar: 1 mm.

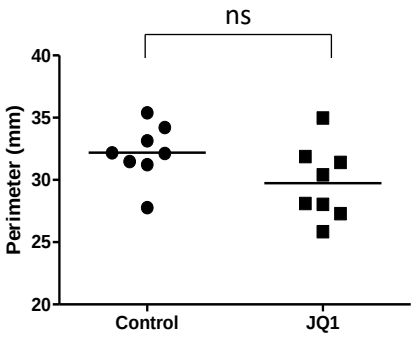

Figure 4. 19. Analysis of spleen sections of untreated (control) and treated (JQ1) mice after *in situ* hybridization. Quantification of the perimeter (mm) of the spleen sections. Each dot represents an individual mouse and the horizontal bars denote mean values. (ns: p-value>0.05, by unpaired t-test).

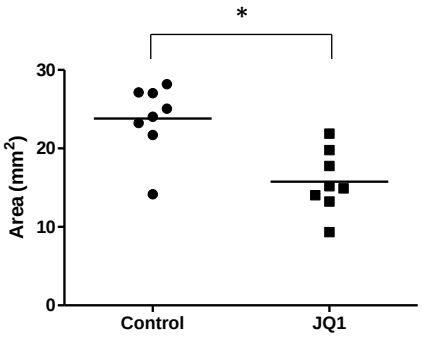

Figure 4. 20. Analysis of spleen sections of untreated (control) and treated (JQ1) mice after *in situ* hybridization. Quantification of the area (mm^2) of the spleen sections. Each dot represents an individual mouse and the horizontal bars denote mean values. (*: p-value<0.05, by unpaired t-test).

On the naked eye, a clear decrease in size of the spleen sections of mice treated with JQ1 is observed, mostly in width (Figure 4.18.A.). With Fiji (ImageJ) software was possible to determine the perimeter and area of the spleen sections (Figures 4.19. and 4.20., respectively). While the perimeter of the spleen sections of treated mice did not show statistical significance with a reduction of 1.1-fold, the area was affected, presenting a 1.6-fold decrease.

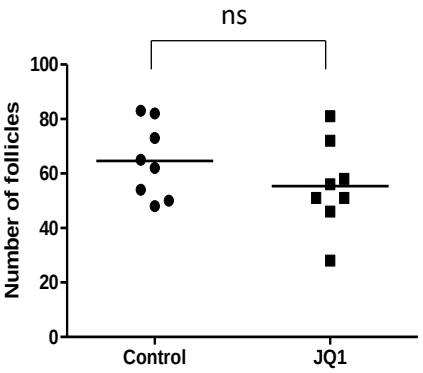

Figure 4. 21. Analysis of spleen sections of untreated (control) and treated (JQ1) mice after *in situ* hybridization. Quantification of the number of follicles per spleen section. Each dot represents an individual mouse and the horizontal bars denote mean values. (ns: p-value>0.05, by unpaired t-test).

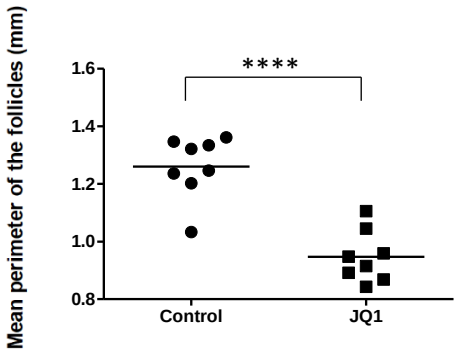

Figure 4. 22. Analysis of spleen sections of untreated (control) and treated (JQ1) mice after *in situ* hybridization. Quantification of the mean perimeter (mm) of the follicles of the spleen sections. Each dot represents an individual mouse and the horizontal bars denote mean values. (****: p-value<0.0001, by unpaired t-test).

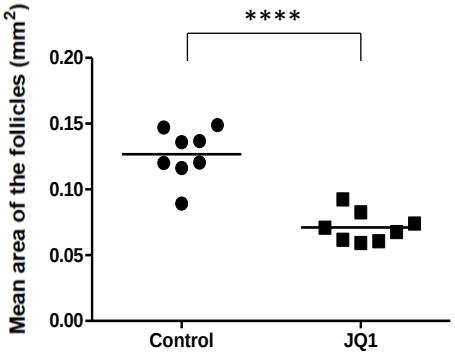

Figure 4. 23. Analysis of spleen sections of untreated (control) and treated (JQ1) mice after *in situ* hybridization. Quantification of the mean area (mm^2) of the follicles of the spleen sections. Each dot represents an individual mouse and the horizontal bars denote mean values. (****: p-value<0.0001, by unpaired t-test).

Both number and size (mean perimeter and mean area) of follicles were also quantified (Figures 4.21., 4.22. and 4.23., respectively). The number of follicles was similar to the control, with a 1.2-fold decrease. Nevertheless, the size of follicles was significantly lower (1.4-fold decrease in perimeter and 1.9-fold decrease in area), as expected, since the mice treated with JQ1 presented less GC B cells.

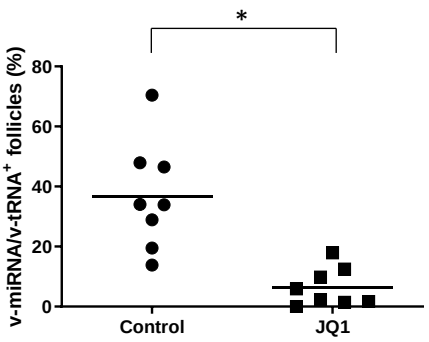

Figure 4. 24. Analysis of spleen sections of untreated (control) and treated (JQ1) mice after *in situ* hybridization. Quantification of the percentage of viral miRNA (v-miRNA) or viral tRNA (v-tRNA) positive follicles of the spleen sections. Each dot represents an individual mouse and the horizontal bars denote mean values. (**: p-value<0.01, by unpaired t-test).

Lastly, the percentage of v-miRNA/v-tRNA positive follicles was quantified. The follicles were considered positive if they had at least one v-miRNA/v-tRNA positive cell (brown points, Figures 4.18.A. and 4.18.B.). As expected, since the size of the follicles was low, a statistically significant decrease of v-miRNA/v-tRNA positive follicles was observed in mice treated with JQ1, when compared with the control (8.3-fold decrease) (Figure 4.24.).

5. Discussion

Kaposi's sarcoma-associated herpesvirus is a gammaherpesvirus that is able to establish a lifelong infection, where B cells are the main site of latent infection (Damania, 2004; Barton *et al*., 2011). Furthermore, the infection is constituted by two phases: lytic, responsible for the reactivation of the virus, leading to the replication of the viral genome and the production of infectious viral progeny, and latent, characterized by circularization of the genome, downregulation of cell surface markers and restriction of gene expression, with the objective of hiding itself from the immune system and establishing a long-term infection (Deshmane and Fraser, 1989; Jenner *et al*., 2001; Traylen *et al.*, 2011; Grinde, 2013). Although gene expression is limited, kLANA is abundantly expressed in this phase of infection. It is an essential protein that regulates the latent phase, controlling the transcription of both virus and host DNA, viral genome replication, episomal maintenance, tumorigenesis, viral latency and lytic reactivation (Ballestas *et al*., 1999; Lan *et al.*, 2004; Ye *et al*., 2004; Verma *et al*., 2007; Sun *et al*., 2014). Therefore, kLANA has been referred to as the best potential target to clear the latent infection. Nowadays, there is not a treatment for KSHV latent infection, and it is imperative to discover effective drugs, since this virus is related to several malignancies worldwide.

In this study, sulfathiazole, sulfanilamide and glybenclamide, which have already shown efficacy in clearing the KSHV infection *in vitro,* were tested *in vivo* (Angius *et al.*, 2017). Moreover, JQ1, which interferes with molecules that play an essential role in the persistence of latent infection, and has previously shown to reduce the number of GC B cells *in vivo,* was also tested *in vivo* to evaluate the effect on the viral infection (Ottinger *et al.*, 2009; Calado *et al*., 2012; Hellert *et al*., 2013; Stanlie *et al*., 2014; Uppal, 2014; Xu and Vakoc, 2017; Wang *et al*., 2018). Since there is not any appropriate small animal model to study KSHV *in vivo*, the experiments were performed using a chimeric virus mouse model. This chimera is a virus in which mLANA was replaced by kLANA, in the MHV-68 genome, enabling the study of the effect of drugs on kLANA, *in vivo*. Although the levels of latency of the chimeric virus are lower when compared with MHV-68, the copy number of the episome is similar in both viruses. The chimera used in this work was generated in a MHV-68 YFP background, expressing the YFP, allowing a direct identification of infected cells.

A viral stock of the chimeric YFP virus was produced to be used in all of the experiments described in this thesis. *In vitro* assays were executed to corroborate that the viral stock was appropriate for use *in vivo*. A Western blot confirmed that kLANA was expressed in infected cells while a one-step growth curve demonstrated a normal growth kinetics and replication. Therefore, the viral stock met all the requirements needed to be used *in vivo.*

The one-step growth curve was also performed to identify potential alterations in the replication of the virus in the presence of sulfathiazole, sulfanilamide and

glybenclamide. It was important to evaluate the effect in the lytic phase, since kLANA is also expressed in this phase. The results showed that, at the indicated concentrations, the drugs had no effect in virus replication *in vitro*.

In vivo assays using mice infected with kLANA.yfp virus were performed to assess latently-infected cells. ICA, which measures latency through *ex vivo* reactivation, was performed, and both frequency of DNA positive cells in total splenocytes and percentage of infected cells in GC B cells by YFP expression were determined. A summary of the results of treated mice relatively to untreated mice is shown in Table 5.1..

Table 5. 1. Summary of both the decrease observed in the assays in treated mice comparing with the control (untreated mice) and the survival rate, after treatment with the drugs at all of the tested doses.

	Dose (mg/g of body weight)	ICA (log decrease)	Frequency of Infection (fold decrease)	Flow Cytometry: GC B cells YFP positive (fold decrease)		Toxicity: Survival Rate (%)
Sulfathiazole	0.25	0.6	11.5	-		100
	0.5	1	5.4	3.1		100
	1	0.7	2	2.6		30
Sulfanilamide	0.25	0.05	1.5	-		100
	1	1	1.7	1.3		90
Glybenclamide	0.005	0.02	1.5	-		100
JQ1	0.05	1.4	7.4	1.7		100

At 0.25 mg/g, the survival rate after administration with sulfathiazole was 100%, with no signs of toxicity. Frequency of infection and capacity to establish latency, evaluated by ICA, significantly decreased. This demonstrated that, at this dose, sulfathiazole is an effective drug in diminishing viral infection. The dose of sulfathiazole was increased to 0.5 mg/g and 1 mg/g, to test if higher doses were more effective in decreasing the infection, and still safe at the same time. At 0.5 mg/g, mice treated with sulfathiazole did not show signs of toxicity and presented a survival rate of 100%. However, the increase to 1mg/g caused a death rate of 70%. The administration of both doses, 0.5 mg/g and 1 mg/g, resulted in a consistent decrease in latent infection in all of the three assays, proving the efficacy of the drug at these doses, too. Concluding, sulfathiazole showed to be a potent drug, being able to decrease the infection of v-kLANA.yfp at all of the tested doses. Therefore, this is in concordance with the results obtained by Angius and colleagues, which demonstrated the efficacy of this drug in latent infection *in vitro* (Angius *et al*., 2017). All three viral assays showed a decrease in infection of treated mice versus untreated controls. Nevertheless,

discrepancies in the level of decrease, between frequency of infection and both reactivation assay and quantity of GC B cells that are YFP positive, were observed, when comparing different doses (Table 5.1.). The reduction of latency, as measured by ICA and flow cytometry, was higher in mice treated with this drug at 0.5 mg/g, followed by 1 mg/g and finally 0.25 mg/g (summarized in Table 5.1.), whereas the frequency of infection markedly increased with higher drug doses. These results need to be confirmed in further experiments, but do not alter the main conclusions. Taking into account that the dose of sulfathiazole must be less than 1 mg/g, given the associated toxicity, and according to the results obtained at 0.25 mg/g and 0.5 mg/g, the ideal dose is ≥ 0.25 mg/g and < 1 mg/g, which should be assessed in further experiments.

Sulfanilamide was firstly administered at 0.25 mg/g and no signs of toxicity were registered. The results obtained in the assays in mice treated with this drug at this dose presented similar values, when compared to the control. Along with the increase of the dose to 1 mg/g, the survival rate dropped down to 90%. Nevertheless, the results were significantly better than with only 0.25 mg/g, having been obtained a significant decrease in reactivation assay. On the other hand, the frequency of infection presented a marginal decrease and the percentage of infected cells in GC B cells also had a small reduction, that did not reach statistical significance. These results suggest that, at 1 mg/g, this drug did not display an effect in clearing the infection, but it can largely affect the capacity of reactivation of the virus. It is known that RTA triggers DE and L genes, stimulating virus reactivation (Traylen *et al.*, 2011). Given this, it is possible that sulfanilamide interferes with RTA, decreasing the capacity of reactivation, even though further studies are necessary. In conclusion, at 1 mg/g, sulfanilamide is toxic and did not show high efficacy in diminishing latent infection and, at 0.25 mg/g, it had no toxicity or effect in viral infection. Then, the appropriate dose for further studies is > 0.25 mg/g and < 1 mg/g.

A decrease of GC B cells after administration with sulfathiazole and sulfanilamide was detected, regardless of the dose. Gene *BCL6* is essential to the GC reaction and may act by inhibiting the growth arrest and apoptosis of GC B cells (Phan and Dalla-Favera, 2004). One of the mechanisms is the repression of the transcription of p53. Since sulfathiazole and sulfanilamide impair the formation of the MDM2-p53 complex, a major quantity of p53 will be active, which can lead to a decrease of GC B cells (Phan and Dalla-Favera, 2004). Even though the effect of sulfanilamide, presumably acting on the MDM2-p53 complex, was not sufficient to affect the virus, it may have been sufficient to cause a deregulation of p53 and, consequently, affect GC B cells. Noteworthy, the decrease of GC B cells is related to a reduction of the level of systemic infection, since the number of infected GC B cells diminishes. Furthermore, in all the assays, the percentage of infected cells that have GC phenotype was also evaluated, since there are infected cells that are not GC B cells. The value did not suffer any alteration, indicating that the percentage of infected cells that are GC B cells remained similar.

Glybenclamide was tested at a low dose, since it is a very effective hypoglycemic drug that acts by stimulating insulin secretion. To avoid the lethality due to the hypoglycemic effect, the maximum dose used was 0.005 mg/g. Although the survival rate was 100%, there were signs of toxicity at this dose. No significant results were observed in any of the three viral assays performed, which indicates that the drug had no effect in latent infection. Although there is the possibility that increasing the dose would lead to a major effect of the drug on the virus, the hypoglycemic effect becomes a barrier to study the drug at higher doses *in vivo*.

The starting point for JQ1 studies was the *in vivo* assays. JQ1 was administered at 0.05 mg/g and the survival rate was 100%, with no signs of toxicity. Mice treated with this drug showed a high decrease in the capacity of the virus to establish latency, demonstrated in all the performed assays. The number of total splenocytes and GC B cells also presented a diminishment. However, when evaluating the percentage of infected cells in GC B cells, a statistically non-significant reduction was observed, and the percentage of infected cells with GC phenotype remained similar. Based on this, and knowing that JQ1 affects the transcription of *c-myc*, which is essential for GC formation and maintenance (Ember *et al*., 2014), it was thought that the administration of JQ1 decreased the number of GC B cells and consequently, the frequency of infection in total splenocytes, since the global number of infected GC B cells was diminished. Nevertheless, the number of infected GC B cells was not affected, as well as the viral infection itself. Following these results, GC B cells were sorted by flow cytometry from splenocyte suspensions and, then, the frequency of viral DNA positive cells in GC B cells was determined, by limiting dilution assay. A decrease of 2.1-fold in the frequency of infection was observed in treated mice, a result less significative than the 7.4-fold decrease observed in total splenocytes. This was also in concordance with the reduction obtained in the quantification of GC B cells, presenting a similar value (1.5-fold decrease). For this reason, it was clarified that the frequency of infection was not significantly affected, only the number of GC B cells. This fact led to a consequent decrease of the infection, due to a reduction in the global number of infected GC B cells, even though the frequency of infection, as well as the virus and infectivity, were not affected. An *in situ* hybridization to detect viral RNAs was also performed with the purpose of analysing GC B and infected cells. A decrease in size of the spleen sections of mice treated with JQ1 was observed in the measured area of the spleen section, even though the perimeter was not affected, since the decrease was mostly in width. Although the number of follicles registered in treated mice was similar to the control group, their size was significantly lower (for both area and perimeter), as expected, since the mice treated with JQ1 presented less GC B cells. Finally, a statistically significant decrease in the v-miRNA/v-tRNA positive follicles was observed, showing that the infection had diminished, since there were less GC B cells. Thus, it was concluded that JQ1 mainly affects the number of GC B cells, which leads to a consequent decrease of the magnitude of systemic infection, even though it does not appear to affect the virus and the latent infection. This result is in agreement with what was previously described concerning the decrease of GC B cells caused by JQ1 (Stanlie

et al., 2014). Moreover, it is also in concordance with the fact that JQ1 was not able to disrupt the interaction of BRD proteins with kLANA (Chen *et al.*, 2017).

In summary, even though not all the results are in concordance with the previously obtained *in vitro*, the study remains relevant, since it is also important to know that, even though a drug has a potent action *in vitro*, the effect on a living organism may be different. The action of JQ1 on the virus was unveiled and, even though the virus appears not to be affected, the decrease of GC B cells might be promising in infected patients. Additionally, sulfathiazole revealed to be a very effective drug against the viral infection, giving highlights about a possible way to clear KSHV infection.

6. Conclusions and Future Perspectives

Herpesviruses are a massive cause of disease, with a large percentage of infected people worldwide, and are among the most successful human pathogens with the capacity of a lifelong infection. Adding to the fact that, currently, there is no treatment that can clear the KSHV infection, in this study several drugs were tested *in vivo.*

Sulfathiazole, impairing the formation of the MDM2-p53 complex, allows the detachment of viral genome from the cellular DNA. This study revealed that it leads to the decrease of v-kLANA.yfp latency at all the tested doses. Thus, this drug showed to be promising in the treatment of KSHV infection. To guarantee the efficacy demonstrated, additional studies must be performed. First, it is imperative to do repeat experiments, to resolve inconsistencies between the different virological assays. Second, it is necessary to increase the number of mice assessed, to guarantee the same statistical efficacy in sizable populations. It would also be interesting to increase the number of days of treatment, to evaluate the effect in a larger time period. Next, since the drug causes a decrease of GC B cells, it would be relevant to perform a complementary confirmatory assay. Similarly to what was done for JQ1, GC B cells may be sorted by flow cytometry and, then, the frequency of viral DNA positive cells in GC B cells determined, in order to understand the importance of this decrease and the consequences to the virus. Finally, it is essential to understand the associated toxicity, through necropsy analysis. Blood and organ failure should be examined to check any pathologies occurring in mice. After that, it will be possible to create a carrier or an antibody that, coupled with the drug, could turn it into a safer alternative.

Sulfanilamide appears to only have an effect in decreasing the capacity of virus reactivation. Thus, it is necessary to clarify how it affects the virus and how it diminishes the capacity of reactivation, starting with the evaluation of the influence of sulfanilamide on RTA. Then, like with sulfathiazole, it is important to unveil its role in decreasing the number of GC B cells and to clarify the associated toxicity. Assessing the effect of the expansion of the period of treatment would also be interesting.

Glybenclamide had no effect *in vivo* at the tested dose. Although the hypoglycemic effect is a limitation when studying this drug at higher doses, future studies could be performed with more time of treatment.

JQ1, interfering with *c-myc*, demonstrated to be effective in reducing GC B cells *in vivo*, even though it does not appear to affect the virus or the latent infection. However, JQ1 is able to significantly reduce the level of systemic infection, since it decreases the number of GC B cells, including the infected cells, which can be useful to the patients infected with KSHV. Nevertheless, the majority of these patients is also infected with HIV and, consequently, have a compromised immune system. Due to that, being treated with a drug that decreases the number of cells of the immune system even more, particularly GC B cells, where B cells maturate, could bring additional

complications to the patients. Thus, one of the future perspectives for JQ1 is to test the consequences associated with the decrease of GC B cells *in vivo*. Another problem is that JQ1 has a short half-life of one hour, leading to a short period of effect, and limiting its clinical use (Moyer, 2011). It will be necessary to overcome this, searching new formulations that increase the half-life of this drug.

Concluding, the main objective of this work was achieved, since the therapeutic potential of these drugs was evaluated. Moreover, it was important to define the threshold of the doses, both the associated toxicity and the effect on the virus. Although several studies are still necessary, this was a significant starting point that can provide new ways to treat the KSHV infection.

References

Ackermann, M. (2006). Pathogenesis of gammaherpesvirus infections. *Veterinary Microbiology*, *113*(3-4), 211-222.

Aliye, N., Fabbretti, A., Lupidi, G., Tsekoa, T., & Spurio, R. (2015). Engineering color variants of green fluorescent protein (GFP) for thermostability, pH-sensitivity, and improved folding kinetics. *Applied Microbiology and Biotechnology*, *99*(3), 1205-1216.

Amon, W., & Farrell, P. J. (2005). Reactivation of Epstein-Barr virus from latency. *Reviews in Medical Virology*, *15*(3), 149–156.

Angius, F., Piras, E., Uda, S., Madeddu, C., Serpe, R., Bigi, R., Chen, W., Dittmer, D. P., Pompei, R., & Ingianni, A. (2017). Antimicrobial sulfonamides clear latent Kaposi Sarcoma Herpesvirus infection and impair MDM2-p53 complex formation. *The Journal of Antibiotics (Tokyo)*, *70*(9), 962–966.

Baer, R., Bankier, A. T., Biggin, M. D., Deininger, P. L., Farrell, P. J., Gibson, T. J., Hatfull, G., Hudson, G. S., Satchwell, S. C., Seguin, C., Tuffnell, E. S., & Barrell, B. G. (1984). DNA sequence and expression of the B95-8 Epstein-Barr virus genome. *Nature*, *310* (5974), 207-211.

Bagni, R. & Whitby, D. (2009). Kaposi's sarcoma-associated herpesvirus transmission and primary infection. *Current Opinion in HIV and AIDS*, *4*(1), 22-26.

Ballestas, M. E. & Kaye, K. M. (2001). Kaposi's Sarcoma-Associated Herpesvirus Latency-Associated Nuclear Antigen 1 Mediates Episome Persistence through cis-Acting Terminal Repeat (TR) Sequence and Specifically Binds TR DNA Kaposi's Sarcoma-Associated Herpesvirus Latency. *Journal of Virology*, *75*(7), 3250–3258.

Ballestas, M. E., Chatis, P. A., & Kaye, K. M. (1999). Efficient persistence of extrachromosomal KSHV DNA mediated by latency-associated nuclear antigen. *Science*, *284*(5414), 641–644.

Ballon, G., Akar, G., & Cesarman, E. (2015). Systemic Expression of Kaposi Sarcoma Herpesvirus (KSHV) Vflip in Endothelial Cells Leads to a Profound Proinflammatory Phenotype and Myeloid Lineage Remodeling *In Vivo*. *PLoS Pathogens*, *11*(1), 1–20.

Baltimore, D. (1971). Expression of animal virus genomes. *Bacteriological Reviews*, *35*(3), 235–241.

Bândea, C. (1983). A new theory on the origin and the nature of viruses. *Journal of Theoretical Biology*, *105*(4), 591-602.

Barbera, A. J. (2006). The Nucleosomal Surface as a Docking Station for Kaposi's Sarcoma Herpesvirus LANA. *Science*, *311*(5762), 856–861.

Barton, E., Mandal, P., & Speck, S. H. (2011). Pathogenesis and Host Control of Gammaherpesviruses: Lessons from the Mouse. *Annual Review of Immunology*, *29*, 351–397.

Bechtel, J. T., Liang, Y., Hvidding, J., & Ganem, D. (2003). Host Range of Kaposi's Sarcoma-Associated Herpesvirus in Cultured Cells. *Journal of Virology*, *77*(11), 6474–6481.

Bellare, P. & Ganem, D. (2009). Regulation of KSHV lytic switch protein expression by a virus- encoded microRNA: an evolutionary adaptation that fine- tunes lytic reactivation. *Cell Host Microbe*, *6*(6), 570–575.

Bhatt, S., Ashlock, B. M., Toomey, N. L., Diaz, L. A., Mesri, E. A., Lossos, I. S., & Ramos, J. C. (2013). Efficacious proteasome/HDAC inhibitor combination therapy for primary effusion lymphoma. *The Journal of Clinical Investigation*, *123*(6), 2616–2628.

Blasdell, K., McCracken, C., Morris, A., Nash, A. A., Begon, M., Bennett, M., & Stewart, J. P. (2003). The wood mouse is a natural host for Murine herpesvirus 4. *The Journal of General Virology*, *84*(1), 111–113.

Blaskovic, D., Stancekova, M., Svobodova, J., & Mistrikova, J. (1980). Isolation of five strains of herpesviruses from two species of free-living small rodents. *Acta Virologica*, *24*(6), 468.

Bodsworth, N. J., Bloch, M., Bower, M., Donnell, D., Yocum, R., International Panretin Gel KS Study Group. (2001). Phase III vehicle- controlled, multi- centered study of topical alitretinoin gel 0.1% in cutaneous AIDS- related Kaposi's sarcoma. American *Journal of Clinical Dermatology*, *2*(2), 77–87.

Bonnefoix, T., Bonnefoix, P., Callanan, M., Verdiel, P., & Sotto, J. J. (2001). Graphical representation of a generalized linear model-based statistical test estimating the fit of the single-hit Poisson model to limiting dilution assays. *Journal of Immunology*, *167*(10), 5725-5730.

Bower, M., Dalla Pria, A., Coyle, C., Andrews, E., Tittle, V., Dhoot, S., & Nelson, M. (2014). Prospective stage- stratified approach to AIDS- related Kaposi's sarcoma. *Journal of Clinical Oncology*, *32*(5), 409–414.

Bower, M., Newsom-Davis, T., Naresh, K., Merchant, S., Lee, B., Gazzard, B., Stebbing, J., & Nelson, M. (2011). Clinical features and outcome in HIV- associated multicentric Castleman's disease. *Journal of Clinical Oncology*, *29*(18), 2481–2486.

Cai, Q., Verma S. C., Lu, J., & Robertson, E. S. (2010). Molecular Biology of Kaposi's Sarcoma Herpesvirus and Related Oncogenesis. *Advances in Virus Research*, *78*, 87–142.

Cai, X., Lu, S., Zhang, Z., Gonzalez, C. M., Damania, B., & Cullen, B. R. (2005). Kaposi's sarcoma-associated herpesvirus expresses an array of viral microRNAs in latently infected cells. *Proceedings of the National Academy of Sciences of the United States of America*, *102*(15), 5570–5575.

Calado, D. P., Sasaki, Y., Godinho, S. A., Pellerin, A., Kochert, K., Sleckman, B. P., De Alborán, I. M., Janz, M., Rodig, S., & Rajewsky, K. (2012). The cell-cycle regulator c-Myc is essential for the formation and maintenance of germinal centers. *Nature Immunology*, *13*(11), 1092–1100.

Calderwood, M. A., Venkatesan, K., Xing, L., Chase, M. R., Vazquez, A., Holthaus, A. M., Ewence, A. E., Li, N., Hirozane-Kishikawa, T., Hill, D. E., Vidal, M., Kieff, E., & Johannsen, E. (2007). Epstein-Barr virus and virus human protein interaction maps. *Proceedings of the National Academy of Sciences of the United States of America*, *104*(18), 7606–7611.

Cesarman, E. (2011). Gammaherpesvirus and lymphoproliferative disorders in immunocompromised patients. *Cancer Letters*, *305*(2), 163–174.

Cesarman, E., Damania, B., Krown, S. E., Martin, J., Bower, M., & Whitby, D. (2019). Kaposi Sarcoma. *Nature Reviews Disease Primers*, *5*(1), 9-56.

Chadburn, A., Hyjek, E., Mathew, S., Cesarman, E., Said, J., & Knowles, D.M. (2004). KSHV- positive solid lymphomas represent an extra- cavitary variant of primary effusion lymphoma. *The American Journal of Surgical Pathology*, *28*(11), 1401–1416.

Chakraborty, S., Veettil, M. V., & Chandran, B. (2012). Kaposi's sarcoma associated herpesvirus entry into target cells. *Frontiers in Microbiology*, *3*(6), 1–13.

Chang, K., Kim, Y., Lovell, S., Rathnayake, A. D., & Groutas, W. C. (2019). Antiviral Drug Discovery: Norovirus Proteases and Development of Inhibitors. *Viruses*, *11*(2), 197-210.

Chang, Y., Cesarman, E., Pessin, M. S., Lee, F., Culpepper, J., Knowles, D. M., & Moore, P. S. (1994). Identification of herpesvirus-like DNA sequences in AIDS-associated Kaposi's sarcoma. *Science*, *266*(5192), 1865–1869.

Chen, H. S., De Leo, A., Wang, Z., Kerekovic, A., Hills, R., & Lieberman, P. M. (2017). BET-Inhibitors Disrupt Rad21-Dependent Conformational Control of KSHV Latency. *PLoS Pathogens*, *13*(1), 1–22.

Collins, C. M., Boss, J. M., & Speck, S. H. (2009). Identification of Infected B-Cell Populations by Using a Recombinant Murine Gammaherpesvirus 68 Expressing a Fluorescent Protein. *Journal of Virology*, *83*(13), 6484–6493.

Correia, B., Cerqueira, S. A., Beauchemin, C., Pires de Miranda, M., Li, S., Ponnusamy, R., Rodrigues, L., Schneider, T. R., Carrondo, M. A., Kaye, K. M., Simas, J. P., McVey, C. E. (2013). Crystal Structure of the Gamma-2 Herpesvirus LANA DNA Binding Domain Identifies Charged Surface Residues Which Impact Viral Latency. *PLoS Pathogens*, *9*(10), 1-16.

Coscoy, L. (2007). Immune evasion by Kaposi' s sarcoma-associated herpesvirus. *Nature Reviews Immunology*, *7*(5), 391–401.

Damania, B. & Cesarman, E. (2013). Kaposi's Sarcoma–Associated Herpesvirus. In Knipe, D. M. & Howley, P. M. (Eds.), *Field's Virology*, 2nd ed., Chapter 65, 2080–2128.

Damania, B. (2004). Oncogenic γ-herpesviruses: Comparison of viral proteins involved in tumorigenesis. *Nature Reviews Microbiology*, *2*(8), 656–668.

Davison, A. J. (2002). Evolution of the herpesviruses. *Veterinary Microbiology*, *86*(1-2), 69–88.

Davison, A. J. (2010). Herpesvirus systematics. *Veterinary Microbiology*, *143*(1), 52–69.

Davison, A. J., Eberle, R., Ehlers, B., Hayward, G. S., Mcgeoch, D. J., Minson, A. C., Pellett, P. E., Roizman, B., Studdert, M. J., & Thiry, E. (2009). The order *Herpesvirales*. *Archives of Virology*, *154*, 171–177

Davison, A. J., Kurobe, T., Gatherer, D., Cunningham, C., Korf, I., Fukuda, H., Hedrick, R. P., & Waltzek, T. B. (2013). Comparative Genomics of Carp Herpesviruses. *Journal of Virology*, *87*(5), 2908–2922.

De Clercq, E. (2004). Antivirals and antiviral strategies. *Nature Reviews Microbiology*, *2*(9), 704–720.

De Leon Vazquez, E., Carey, V., & Kaye, K. (2013). Identification of Kaposi's Sarcoma-Associated Herpesvirus LANA Regions Important for Episome Segregation, Replication, and Persistence. *Journal of Virology*, *87*(22), 12270–12283.

Decker, L. L., Shankar, P., Khan, G., Freeman, R. B., Dezube, B. J., Lieberman, J., & Thorley-Lawson, D. A. (1996). The Kaposi Sarcoma-associated Herpesvirus (KSHV) Is Present as an Intact Latent Genome in KS Tissue but Replicates in the Peripheral Blood Mononuclear Cells of KS Patients. *The Journal of Experimental Medicine*, *184*(7), 283-288.

Deshmane, S. L., & Fraser, N. W. (1989). During Latency, Herpes Simplex Virus Type 1 DNA Is Associated with Nucleosomes in a Chromatin Structure. *Journal of Virology*, *46*(2), 498–512.

Di Domenico, E. G., Toma, L., Bordignon, V., Trento, E., D'Agosto, G., Cordiali-Fei, P., & Ensoli, F. (2016). Activation of DNA damage response induced by the Kaposi's sarcoma-associated herpes virus. *International Journal of Molecular Sciences*, *17*(6), 854-870.

Dittmer, D., Lagunoff, M., Renne, R., Staskus, K., Haase, A., & Ganem, D. (1998). A cluster of latently expressed genes in Kaposi's sarcoma-associated herpesvirus. *Journal of Virology*, *72*(10), 8309–8315.

Dominguez, R. & Holmes, K. C. (2011). Actin structure and function. Annual Review of *Biophysics*, *40*, 169-186.

Duvic, M., Friedman-Kien, A. E., Looney, D. J., Miles, S. A., Myskowski, P. L., Scadden, D. T., Von Roenn, J., Galpin, J. E., Groopman, J., Loewen, G., Stevens, V., Truglia, J. A., & Yocum, R. C. (2000). Topical treatment of cutaneous lesions of acquired immunodeficiency syndrome- related Kaposi sarcoma using alitretinoin gel: results of phase 1 and 2 trials. *Archives of Dermatology*, *136*(12), 1461–1469.

Efstathiou, S., Ho, Y.M., & Minson, A. C. (1990). Cloning and molecular characterization of the murine herpesvirus 68 genome. *The Journal of General Virology*, *71*(6), 1355–1364.

Ember, S. W., Zhu, J. Y., Olesen, S. H., Martin, M. P., Becker, A., Berndt, N., Georg, G. I., & Schonbrunn, E. (2014). Acetyl-lysine binding site of bromodomain-containing protein 4 (BRD4) interacts with diverse kinase inhibitors. *ACS Chemical Biology*, *9*(5), 1160-1171.

Feibelman, K.M., Fuller, B. P., Li, L., LaBarbera, D. V., & Geiss, B. J. (2018). Identification of small molecule inhibitors of the Chikungunya virus nsP1 RNA capping enzyme. *Antiviral Research*, *154*, 124-131.

Ferri, E., Petosa, C., & Mckenna, C. E. (2015). Bromodomains: Structure , function and pharmacology of inhibition. *Biochemical Pharmacology*, *106*, 1-18.

Filippakopoulos, P., Qi, J., Picaud, S., Shen, Y., Smith, W. B., Fedorov, O., Morse, E. M., Keates, T., Hickman, T. T., Felletar, I., Philpott, M., Munro, S., McKeown, M. R., Wang, Y., Christie, A. L., West, N., Cameron, M. J., Schwartz, B., Heightman, T. D., La Thangue, N., French, C. A., Wiest, O., Kung, A. L., Knapp, S., & Bradner, J. E. (2010). Selective inhibition of BET bromodomains. *Nature*, *468*(7327), 1067-1073.

Flaño, E., Husain, S. M., Sample, J. T., Woodland, D. L., & Blackman, M. A. (2000). Latent murine gamma-herpesvirus infection is established in activated B-cells, dendritic cells, and macrophages. *Journal of Immunology*, *165*(2), 1074–1081.

Flaño, E., Kim, I. J., Woodland, D. L., & Blackman, M. A. (2002). Gamma-herpesvirus latency is preferentially maintained in splenic germinal center and memory B-cells. *The Journal of Experimental Medicine*, *196*(10), 1363–1372.

Forterre, P. (2010). Giant viruses: Conflicts in revisiting the virus concept. *Intervirology*, *53*(5), 362–378.

Fowler, P., Marques, S., Simas, J. P., & Efstathiou, S. (2003). ORF73 of murine herpesvirus-68 is critical for the establishment and maintenance of latency. *The Journal of General Virology*, *84*(12), 3405–3416.

Frederico, B., Chao, B., May, J. S., Belz, G. T., & Stevenson, P. G. (2014). A Murine gamma-herpesviruses exploits normal splenic immune communication routes for systemic spread. *Cell Host & Microbe*, *15*(4), 457–470.

Gao, S. J., Zhang, Y. J., Deng, J. H., Rabkin, C. S., Flore, O., & Jenson, H. B. (1999). Molecular polymorphism of Kaposi's sarcoma-associated herpesvirus (Human herpesvirus 8) latent nuclear antigen: evidence for a large repertoire of viral genotypes and dual infection with different viral genotypes. *The Journal of Infectious Diseases*, *180*(5), 1466–1476.

Giffin, L. & Damania, B. (2014). KSHV: pathways to tumorigenesis and persistent infection. *Advances in Virus Research*, *88*, 111-159.

Glibenclamide 5 mg Tablets (glybenclamide) [package leaflet]. United Kingdom: Aurobindo Pharma Limited; 2011.

Göko, E. & Esra, Y. (2014). Fluorescence Interaction and Determination of Sulfathiazole with Trypsin. *Journal of Fluorescence*, *24*(5), 1439–1445.

Goncalves, P. H., Uldrick, T. S., & Yarchoan, R. (2017). HIV- associated Kaposi sarcoma and related diseases. *AIDS*, *31*(14), 1903–1916.

Grinde, B. (2013). Herpesviruses: latency and reactivation – viral strategies and host response. *Journal of Oral Microbiology*, *5*(1), 22766.

Grulich, A. E., Beral, V., & Swerdlow, A. J. (1992). Kaposi's sarcoma in England and Wales before the AIDS epidemic. *British Journal of Cancer*, *66*(6), 1135–1137.

Habison, A. C., Beauchemin, C., Simas, J. P., Usherwood, E. J., & Kaye, K. M. (2012). Murine Gammaherpesvirus 68 LANA Acts on Terminal Repeat DNA To Mediate Episome Persistence. *Journal of Virology*, *86*(21), 11863–11876.

Habison, A. C., Pires de Miranda, M., Beauchemin, C., Tan, M., Cerqueira, S. A., Correia, B., Ponnusamy, R., Usherwood, E. J., McVey, C. E., Simas, J. P., & Kaye, K. M. (2017). Cross-species conservation of episome maintenance provides a basis for *in vivo* investigation of Kaposi's sarcoma herpesvirus LANA. *PLoS Pathogens*, *13*(9), 1-25.

Hansen, A., Henderson, S., Lagos, D., Nikitenko, L., Coulter, E., Roberts, S., Gratrix, F., Plaisance, K., Renne, R., Bower, M., Kellam, P., & Boshoff, C. (2010). KSHV-encoded miRNAs target MAF to induce endothelial cell reprogramming. *Genes and Development*, *24*(2), 195–205.

Harris, A. H., Osborne, R. H., Streeton, C. L., & McNeil, H. (2002). Quality of life and Kaposi sarcoma: using preference techniques to value the health gains from treatment. *Supportive Care in Cancer*, *10*(6), 486–493.

Hellert, J., Weidner-Glunde, M., Krausze, J., Richter, U., Adler, H., Fedorov, R., Pietrek, M., Rückert, J., Ritter, C., Schulz, T. F., & Luhrs, T. (2013). A structural basis for BRD2/4-mediated host chromatin interaction and oligomer assembly of Kaposi sarcoma-associated herpesvirus and murine gammaherpesvirus LANA proteins. *PLoS Pathogens*, *9*(10), 1-19.

Hengel, H., Koszinowski, U. H., & Conzelmann, K. K. (2005). Viruses know it all: new insights into IFN networks. *Trends in Immunololy*, *26*(7), 396–401.

Hu, M., Wang, C., Li, W., Lu, W., Bai, Z., Qin, D., Yan, Q., Zhu, J., Krueger, B. J., Renne, R., Gao, S., & Lu, C. (2015). A KSHV microRNA Directly Targets G Protein-Coupled Receptor Kinase 2 to Promote the Migration and Invasion of Endothelial Cells by Inducing CXCR2 and Activating AKT Signaling. *PLoS Pathogens*, *11*(9), 1–27.

Jenner, R. G., Albà, M. M., Boshoff, C., & Kellam, P. (2001). Kaposi's sarcoma-associated herpesvirus latent and lytic gene expression as revealed by DNA arrays. *Journal of Virology*, *75*(2), 891-902.

Juillard, F., Tan, M., Li, S., & Kaye, K. M. (2016). Kaposi's sarcoma herpesvirus genome persistence. *Frontiers in Microbiology*, *7*(1149), 1–15.

Klein, E., Kis, L. L., & Klein, G. (2007). Epstein-Barr virus infection in humans: From harmless to life endangering virus-lymphocyte interactions. *Oncogene*, *26*(9), 1297–1305.

Komatsu, T., Ballestas, M. E., Barbera, A. J., Kelley-Clarke, B., & Kaye, K.M. (2004). KSHV LANA1 binds DNA as an oligomer and residues N-terminal to the oligomerization domain are essential for DNA binding, replication, and episome persistence. *Virology*, *319*(2), 225–236.

Komatsu, T., Barbera A. J., Ballestas, M. E., & Kaye, K. M. (2001). The Kaposi's Sarcoma-Associated Herpesvirus Latency-Associated Nuclear Antigen. *Viral Immunology*, *14*(4), 311–317.

Koon, H. B., Krown, S. E., Lee, J. Y., Honda, K., Rapisuwon, S., Wang, Z., Aboulafia, D., Reid, E. G., Rudek, M. A., Dezube, B. J., & Noy, A. (2014). Phase II trial of imatinib in AIDS- associated Kaposi's sarcoma: AIDS malignancy consortium protocol 042. *Journal of Clinical Oncology*, *32*(5), 402–408.

Krown, S. E. (2007). AIDS-associated Kaposi's sarcoma: is there still a role for interferon alfa?. *Cytokine & Growth Factor Reviews*, *18*(5-6), 395-402.

Krown, S. E., Roy, D., Lee, J. Y., Dezube, B. J., Reid, E. G., Venkataramanan, R., Han, K., Cesarman, E., & Dittmer, D. P. (2012). Rapamycin with antiretroviral therapy in AIDS- associated Kaposi sarcoma. *Journal of Acquired Immune Deficiency Syndromes*, *59*(5), 447–454.

Kumar, B. & Chandran, B. (2016). KSHV entry and trafficking in target cells—Hijacking of cell signal pathways,actin and membrane dynamics. *Viruses*, *8*(11), 305-327.

Kwun, H. J., da Silva, S. R., Shah, I. M., Blake, N., Moore, P. S., & Chang, Y. (2007). Kaposi's Sarcoma-Associated Herpesvirus Latency-Associated Nuclear Antigen 1 Mimics Epstein-Barr Virus EBNA1 Immune Evasion through Central Repeat Domain Effects on Protein Processing. *Journal of Virology*, *81*(15), 8225–8235.

Lan, K., Kuppers, D. A., Verma, S. C., & Robertson, E. S. (2004). Kaposi's sarcoma-associated herpesvirus-encoded latency-associated nuclear antigen inhibits lytic replication by targeting Rta: a potential mechanism for virus-mediated control of latency. *Journal of Virology*, *78*(12), 6585–6594.

Lichterfeld, M., Qurishi, N., Hoffmann, C., Hochdorfer, B., Brockmeyer, N. H., Arasteh, K., Mauss, S., Rockstroh, J. K. & German Clinical AIDS Working Group (KAAD). (2005). Treatment of HIV-1-associated Kaposi's sarcoma with pegylated liposomal doxorubicin and HAART simultaneously induces effective tumor remission and CD4+ T cell recovery. *Infection*, *33*(3), 140–147.

Lovén, J., Hoke, H. A., Lin, C. Y., Lau, A., Orlando, D. A., Vakoc, C. R., Bradner, J. E., Lee, T. I., & Young, R. A. (2013). Selective inhibition of tumor oncogenes by disruption of super-enhancers. *Cell*, *153*(2), 320-334.

Luzi, L. and Pozza, G. (1997). Glibenclamide: an old drug with a novel mechanism of action?. *Acta Diabetologica*, *34*(4), 239-244.

Macpherson, I. & Stoker, M. (1962). Polyoma transformation of hamster cell clones--an investigation of genetic factors affecting cell competence. *Virology*, *16*, 147-151.

Malaisse, W. & Malaisse-Lagae, F. (1970). Effects of glycodiazin and glybenclamide upon insulin secretion *in vitro*. *European Journal of Pharmacology*, *9*(1), 93-98.

Mariggiò, G., Koch, S., & Schulz, T. F. (2017). Kaposi sarcoma herpesvirus pathogenesis. *Philosophical Transactions of the Royal Society B: Biological Sciences*, *372*(1732), 1-20.

Marques, S., Efstathiou, S., Smith, K. G., Haury, M., & Simas, J. P. (2003). Selective gene expression of latent murine gammaherpesvirus 68 in B lymphocytes. *Journal of Virology*, *77*(13), 7308–7318.

Mbulaiteye, S., Marshall, V., Bagni, R. K., Wang, C. D., Mbisa, G., Bakaki, P. M., Owor, A. M., Ndugwa, C. M., Engels, E. A., Katongole-Mbidde, E., Biggar, R. J., & Whitby, D. (2006). Molecular evidence for mother-to-child transmission of Kaposi sarcoma-associated herpesvirus in Uganda and K1 gene evolution within the host. *The Journal of Infectious Diseases*, *193*(9), 1250-1257.

McAllister, S. C., Hanson, R. S., & Manion, R. D. (2015). Propranolol decreases proliferation of endothelial cells transformed by Kaposi's sarcoma- associated herpesvirus and induces lytic viral gene expression. *Journal of Virology*, *89*(21), 11144–11149.

Mesri, E. A., Cesarman, E., & Boshoff, C. (2010). Kaposi's sarcoma and its associated herpesvirus. *Nature Reviews Cancer*, *10*(10), 707–719.

Mettenleiter, T. C., Klupp, B. G., & Granzow, H. (2009). Herpesvirus assembly: An update. *Virus Research*, *143*, 222–234.

Miller, D. M., Thomas, S. D., Islam, A., Muench, D., & Sedoris, K. (2012). c-Myc and cancer metabolism. *Clinical Cancer Research*, *18*(20), 5546–5553.

Moll, U. M. & Petrenko, O. (2003). The MDM2-p53 Interaction. *Molecular Cancer Research*, *1*(14), 1001-1008.

Moore, P. S. & Chang, Y. (2003). Immunoevasion and Tumorigenesis: Two Sides of the Same Coin ?. *Annual Review of Microbiology*, *57*(20), 609–639.

Moorman, N.J., Willer, D.O., & Speck, S.H. (2003). The gammaherpesvirus 68 latency-associated nuclear antigen homolog is critical for the establishment of splenic latency. *Journal of Virology*, *77*(19), 10295–10303.

Moyer, M. W. (2011). First drugs found to inhibit elusive cancer target. *Nature Medicine*, *17*(11), 1325.

Mui, U. N., Haley, C. T., & Tyring, S. K. (2017). Viral Oncology: Molecular Biology and Pathogenesis. *Journal of Clinical Medicine*, *6*(12), 111-168.

Muller, B. & Krausslich, H. G. (2009). Antiviral strategies. *Handbook of Experimental Pharmacology*, *189*, 1–24.

Muller, K. H., Kakkola, L., Nagaraj, A. S., Cheltsov, A. V., Anastasina, M., & Kainov, D. E. (2012). Emerging cellular targets for influenza antiviral agents. *Trends in Pharmacological Sciences*, *33*(2), 89-99.

Nador, R. G., Cesarman, E., Chadburn, A., Dawson, D. B., Ansari, M. Q., Sald, J., & Knowles, D.M. (1996). Primary effusion lymphoma: a distinct clinicopathologic entity associated with the Kaposi's sarcoma- associated herpesvirus. *Blood*, *88*(2), 645–656.

Narkhede, M., Arora, S., & Ujjani, C. (2018). Primary effusion lymphoma: current perspectives. *OncoTargets and Therapy*, *11*, 3747–3754.

Nash, A. A., Dutia, B. M., Stewart, J. P., & Davison, A. J. (2001). Natural history of murine gamma-herpesvirus infection. *Philosophical Transactions of the Royal Society B: Biological Sciences*, *356*(1408), 569–579.

Ohsaki, E. & Ueda, K. (2012). Kaposi's Sarcoma-Associated Herpesvirus Genome Replication, Partitioning, and Maintenance in Latency. *Frontiers in Microbiology*, *3*(7), 1-12.

Ottinger, M., Pliquet, D., Christalla, T., Frank, R., Stewart, J. P., & Schulz, T. F. (2009). The Interaction of the Gammaherpesvirus 68 orf73 Protein with Cellular BET Proteins Affects the Activation of Cell Cycle Promoters. *Journal of Virology*, *83*(9), 4423–4434.

Patick, A. K. & Potts, K. E. (1998). Protease Inhibitors as Antiviral Agents. *Clinical Microbiology Reviews*, *11*(4), 614–627.

Paul, A. G., Sharma-Walia, N., & Chandran, B. (2011). Targeting KSHV/HHV-8 latency with COX-2 selective inhibitor nimesulide: A potential chemotherapeutic modality for primary effusion lymphoma. *PLoS ONE*, *6*(9), 1-19.

Peirs, S., Frismantas, V., Matthijssens, F., Van Loocke, W., Pieters, T., Vandamme, N., Lintermans, B., Dobay, M. P., Berx, G., Poppe, B., Goossens, S., Bornhauser, B. C., Bourquin, J. P., Van Vlierberghe, P. (2017). Targeting BET proteins improves the therapeutic efficacy of BCL-2 inhibition in T-cell acute lymphoblastic leukemia. *Leukemia*, *31*(10), 2037–2047.

Petre, C. E., Sin, S., & Dittmer, D. P. (2007). Functional p53 Signaling in Kaposi's Sarcoma-Associated Herpesvirus Lymphomas: Implications for Therapy. *Journal of Virology*, *81*(4), 1912–1922.

Phan, R. T. & Dalla-Favera, R. (2004). The BCL6 proto-oncogene suppresses p53 expression in germinal-centre B cells. *Nature*, *432*(7017), 635-639.

Piolot, T., Tramier, M., Coppey, M., Nicolas, J., & Marechal, V. (2001). Close but Distinct Regions of Human Herpesvirus 8 Latency-Associated Nuclear Antigen 1 Are Responsible for Nuclear Targeting and Binding to Human Mitotic Chromosomes. *Journal of Virology*, *75*(8), 3948–3959.

Polizzotto, M. N., Uldrick, T. S., Wyvill, K. M., Aleman, K., Marshall, V., Wang, V., Whitby, D., Pittaluga, S., Jaffe, E. S., Millo, C., Tosato, G., Little, R. F., Steinberg, S. M., Sereti, I., & Yarchoan, R. (2016a). Clinical features and outcomes of patients with symptomatic Kaposi sarcoma herpesvirus (KSHV)-associated Inflammation: prospective characterization of KSHV inflammatory cytokine syndrome (KICS). *Clinical Infectious Diseases*, *62*(6), 730–738.

Polizzotto, M. N., Uldrick, T. S., Wyvill, K. M., Aleman, K., Peer, C. J., Bevans, M., Sereti, I., Maldarelli, F., Whitby, D., Marshall, V., Goncalves, P. H., Khetani, V., Figg, W. D., Steinberg, S. M., Zeldis, J. B., & Yarchoan, R. (2016b). Pomalidomide for Symptomatic Kaposi's Sarcoma in People With and Without HIV Infection: A Phase I/II Study. *Journal of Clinical Oncology*, *34*(34), 4125-4131.

Polizzotto, M. N., Uldrick, T.S., Wang, V., Aleman, K., Wyvill, K.M., Marshall, V., Pittaluga, S., O'Mahony, D., Whitby, D., Tosato, G., Steinberg, S. M., Little, R. F., & Yarchoan, R. (2013). Human and viral interleukin-6 and other cytokines in Kaposi sarcoma herpesvirusassociated multicentric Castleman disease. *Blood*, *122*(26), 4189–4198.

Ponnusamy, R., Petoukhov, M. V., Correia, B., Custodio, T. F., Juillard, F., Tan, M., Pires de Miranda, M., Carrondo, M. A., Simas, J. P., Kaye, K. M., Svergun, D. I., & McVey, C. E. (2015). KSHV but not MHV-68 LANA induces a strong bend upon binding to terminal repeat viral DNA. *Nucleic Acids Research*, *43*(20), 10039–10054.

Prasad, B. V. & Schmid, M. F. (2012). Principles of Virus Structural Organization. *Advances in Experimental Medicine and Biology*, *726*, 17–47.

Purushothaman, P., Dabral, P., Gupta, N., Sarkar, R., & Verma, S. C. (2016). KSHV genome replication and maintenance. *Frontiers in Microbiology*, *7*(54), 1–14.

Renne, R., Lagunoff, M., Zhong, W., & Ganem, D. O. N. (1996). The Size and Conformation of Kaposi ' s Sarcoma-Associated Herpesvirus (Human Herpesvirus 8) DNA in Infected Cells and Virions, *70*(11), 8151–8154.

Russo, J. J., Bohenzky, R. A., Chien, M. C., Chen, J., Yan, M., Maddalena, D., Parry, J. P., Peruzzi, D., Edelman, I. S., Chang, Y., & Moore, P. S. (1996). Nucleotide sequence of the Kaposi sarcoma-associated herpesvirus (HHV8). *Proceedings of the National Academy of Sciences of the United States of America*, *93*(25), 14862–14867.

Sanz, D., Claramunt, R. M., Alkorta, I., Sánchez-Sanz, G., & Elguero, J. (2012). The structure of glibenclamide in the solid state. *Magnetic Resonance in Chemistry*, *50*(3), 246–255.

Sarid, R., Flore, O., Bohenzky, R. A., Chang, Y., & Moore, P. S. (1998). Transcription mapping of the Kaposi's sarcoma- associated herpesvirus (human herpesvirus 8) genome in a body cavity- based lymphoma cell line (BC-1). *Journal of Virology*, *72*(2), 1005–1012.

Shi, F., Xie, Y., Shi, L., & Xu, W. (2013). Viral RNA polymerase: a promising antiviral target for influenza A virus. *Currently Medicinal Chemistry*, *20*(31):3923-3934.

Simas, J. P. & Efstathiou, S. (1998). Murine gammaherpesvirus 68: A model for the study of gammaherpesvirus pathogenesis. *Trends in Microbiology*, *6*(7), 276–282.

Simas, J. P., Swann, D., Bowden, R., & Efstathiou, S. (1999). Analysis of murine gammaherpesvirus-68 transcription during lytic and latent infection. *The Journal of General Virology*, *80*(1), 75–82.

Skold, O. (2000). Sulfonamide resistance: mechanisms and trends. *Drug Resistance Updates*, *3*(3), 155-160.

Spear, P. G. & Longnecker, R. (2003). Herpesvirus Entry: an Update. *Journal of Virology*, *77*(19), 10179–10185.

Speck, S. H. & Ganem, D. (2010). Viral latency and its regulation: lessons from the gammaherpesviruses. *Cell Host Microbe*, *8*(1), 100–115.

Stallone, G., Schena, A., Infante, B., Di Paolo, S., Loverre, A., Maggio, G., Ranieri, E., Gesualdo, L., Schena, F. P., & Grandaliano, G. (2005). Sirolimus for Kaposi's sarcoma in renal- transplant recipients. *The New England Journal of Medicine*, *352*(13), 1317–1323.

Stanlie, A., Yousif, A. S., Akiyama, H., Honjo, T., & Begum, N. A. (2014). Chromatin Reader Brd4 Functions in Ig Class Switching as a Repair Complex Adaptor of Nonhomologous End-Joining. *Molecular Cell*, *55*(1), 97-110.

Stewart, J. P., Usherwood, E. J., Ross, A., Dyson, H, & Nash, T. (1998). Lung Epithelial Cells Are a Major Site of Murine Gammaherpesvirus Persistence. *The Journal of Experimental Medicine*, *187*(12), 1941–1951.

Sun, Q., Tsurimoto, T., Juillard, F., Li, L., Li, S., De León Vázquez, E., Chen, S., & Kaye, K. (2014). Kaposi's sarcoma-associated herpesvirus LANA recruits the DNA polymerase clamp loader to mediate efficient replication and virus persistence. *Proceedings of the National Academy of Sciences of the United States of America*, *111*(32), 11816–11821.

Sunil-Chandra, N. P., Efstathiou, S., & Nash, A. A. (1992b). Murine gammaherpesvirus 68 establishes a latent infection in mouse B lymphocytes *in vivo*. *The Journal of General Virology*, *73*(12), 3275-3279.

Sunil-Chandra, N. P., Efstathiou, S., Arno, J., & Nash, A. A. (1992a). Virological and pathological features of mice infected with murine gamma-herpesvirus 68. *The Journal of General Virology*, *73*(9), 2347-2356.

Thakker, S. & Verma, S. C. (2016). Co-infections and pathogenesis of KSHV-associated malignancies. *Frontiers in Microbiology*, *7*(151), 1–14.

Toptan, T., Fonseca, L., Kwun, H. J., Chang, Y., & Moore, P. S. (2013). Complex Alternative Cytoplasmic Protein Isoforms of the Kaposi's Sarcoma-Associated Herpesvirus Latency-Associated Nuclear Antigen 1 Generated through Noncanonical Translation Initiation. *Journal of Virology*, *87*(5), 2744–2755.

Traylen, C. M., Patel, H. R., Fondaw, W., Mahatme, S., Williams, J. F., Walker, L. R., Dyson, O. F., Arce, S., & Akula, S. M. (2011). Virus reactivation: A panoramic view in human infections. *Future Virology*, *6*(4), 451–463.

Trontelj, Z., Lužnik, J., Pirnat, J., Jazbinšek, V., Lavrič, Z., & Srčič, S. (2019). Polymorphism in Sulfanilamide: 14N Nuclear Quadrupole Resonance Study. *Journal of Pharmaceutical Sciences*, *108*(9), 1–6.

Tsai, C. H., Lee, P. Y., Stollar, V., & Li, M. L. (2006). Antiviral therapy targeting viral polymerase. *Current Pharmaceutical Design*, *12*(11), 1339-1355.

Ueda, K. (2012). For the future studies of Kaposi's sarcoma-associated herpesvirus. *Frontiers in Microbiology*, *3*(237), 1–2.

Uldrick, T. S., Wyvill, K. M., Kumar, P., O'Mahony, D., Bernstein, W., Aleman, K., Polizzotto, M. N., Steinberg, S. M., Pittaluga, S., Marshall, V., Whitby, D., Little, R. F., & Yarchoan, R. (2012). Phase II study of bevacizumab in patients with HIV- associated Kaposi's sarcoma receiving antiretroviral therapy. *Journal of Clinical Oncology*, *30*(13), 1476–1483.

Uppal, T., Banerjee, S., Sun, Z., Verma, S. C., & Robertson, E. S. (2014). KSHV LANA — The Master Regulator of KSHV Latency. *Viruses*, *6*(12), 4961–4998.

Uppal, T., Jha, H. C., Verma, S. C., & Robertson, E. S. (2015). Chromatinization of the KSHV genome during the KSHV life cycle. *Cancers*, *7*(1), 112–142.

Verma, S. C., Lan, K., & Robertson, E. (2007). Structure and function of latency-associated nuclear antigen. *Current Topics in Microbiology and Immunology*, 312, 101–136.

Virgin IV, H. W., Latreille, P., Wamsley, P., Hallsworth, K., Weck, K. E., Canto, A. J. D. A. L., & Speck, S. H. (1997). Complete Sequence and Genomic Analysis of Murine Gammaherpesvirus 68. *Journal of Virology*, *71*(8), 5894–5904.

Vitale, F., Briffa, D. V., Whitby, D., Maida, I., Grochowska, A., Levin, A., Romano, N., & Goedert, J. J. (2001). Kaposi's sarcoma herpes virus and Kaposi's sarcoma in the elderly populations of 3 Mediterranean islands. *Internation Journal of Cancer*, *91*(4), 588-591.

Wakeham, K., Webb, E. L., Sebina, I., Muhangi, L., Miley, W., Johnson, W. T., Ndibazza, J., Elliott, A. M., Whitby, D., & Newton, R. (2011). Parasite infection is associated with Kaposi's sarcoma associated herpesvirus (KSHV) in Ugandan women. *Infectious Agents and Cancer*, *6*(1), 15-21.

Wang, J., Liu, Z., Wang, Z., Wang, S., Chen, Z., Li, Z., Zhang, M., Zou, J., Dong, B., Gao, J., Shen, L. (2018). Targeting c-Myc: JQ1 as a promising option for c-Myc-amplified esophageal squamous cell carcinoma. *Cancer Letters*, *419*, 64–74.

Weck, K. E., Kim, S. S., Virgin IV, H. W., & Speck, S. H. (1999). B-cells regulate murine gammaherpesvirus 68 latency. *Journal of Virology*, *73*(6), 4651– 4661.

Wen, K. W. & Damania, B. (2010). Kaposi sarcoma-associated herpesvirus (KSHV): Molecular biology and oncogenesis. *Cancer Letters*, *289*(2), 140–150.

Wilson, A. C., & Mohr, I. (2012). A cultured affair: HSV latency and reactivation in neurons. *Trends in Microbiology*, *20*(12), 604–611.

Xiao, Y., Chen, J., Liao, Q., Wu, Y., Peng, C., & Chen, X. (2013). Lytic infection of Kaposi's sarcoma-associated herpesvirus induces DNA double-strand breaks and impairs non-homologous end joining. *The Journal of General Virology*, *94*, 1870–1875.

Xu, Y. & Vakoc, C. R. (2017). Targeting Cancer Cells with BET Bromodomain Inhibitors. *Cold Spring Harbor Perspectives in Medicine*, *7*(7), 1-17.

Yarchoan, R., Pluda, J. M., Wyvill, K. M., Aleman, K., Rodriguez-Chavez, I. R., Tosato, G., Catanzaro, A. T., Steinberg, S. M., & Little, R. F. (2007). PART IV. Cytokine and hormone immunotherapy treatment of AIDS- related Kaposi's sarcoma with interleukin-12: rationale and preliminary evidence of clinical activity. *Critical Reviews in Immunology*, *27*(5), 401–414.

Ye, F. C., Zhou, F. C., Yoo, S. M., Xie, J. P., Browning, P. J., & Gao, S. J. (2004). Disruption of Kaposi's sarcoma-associated herpesvirus latent nuclear antigen leads to abortive episome persistence. *Journal of Virology*, *78*(20), 11121–11129.

Appendix I – Sulfathiazole and Sulfanilamide (0.25 mg/g)

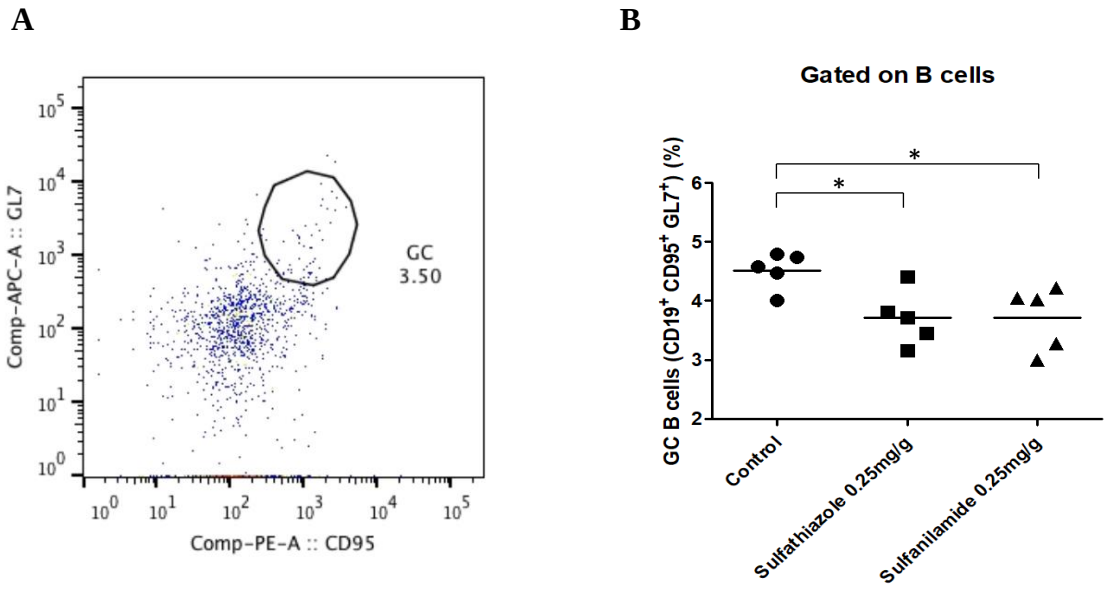

Appendix I. 1. Flow cytometry analysis. Percentage quantification of GC B cells ($CD19^+$ $GL7^+$ $CD95^+$). a) Representative flow cytometry plot gated on B cells. The indicated value refers to a percentage. b) Each dot represents an individual mouse and the horizontal bars denote mean values. (*: p-value<0.05, by unpaired t-test).

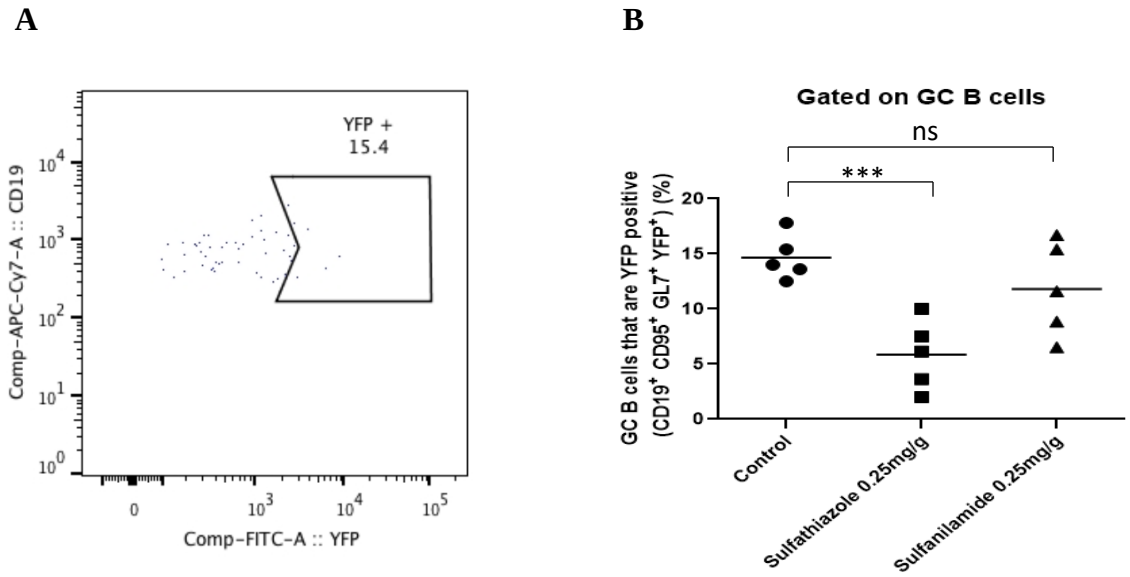

Appendix I. 2. Flow cytometry analysis. Percentage quantification of infected GC B cells ($CD19^+$ $GL7^+$ $CD95^+$ YFP^+). a) Representative flow cytometry plot gated on GC B cells. The indicated value refers to a percentage. b) Each dot represents an individual mouse and the horizontal bars denote mean values. (***: p-value<0.001; ns: p-value>0.05, by unpaired t-test).

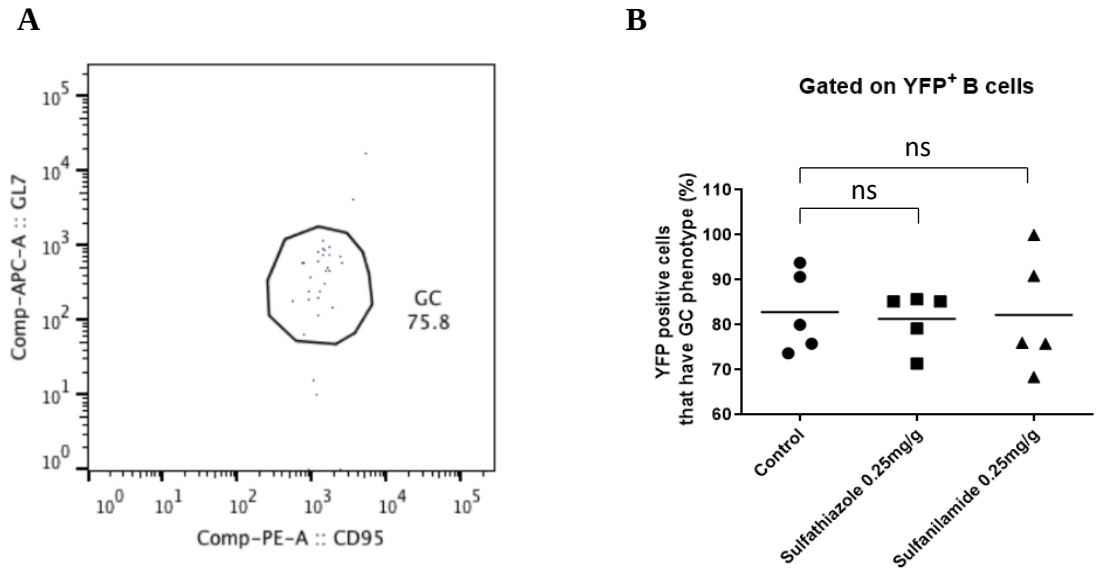

Appendix I. 3. Flow cytometry analysis. Percentage quantification of infected B cells with GC phenotype ($CD19^+$ YFP^+). a) Representative flow cytometry plot gated on YFP positive B cells. The indicated value refers to a percentage. b) Each dot represents an individual mouse and the horizontal bars denote mean values. (ns: p-value>0.05, by unpaired t-test).

Appendix II – Glybenclamide

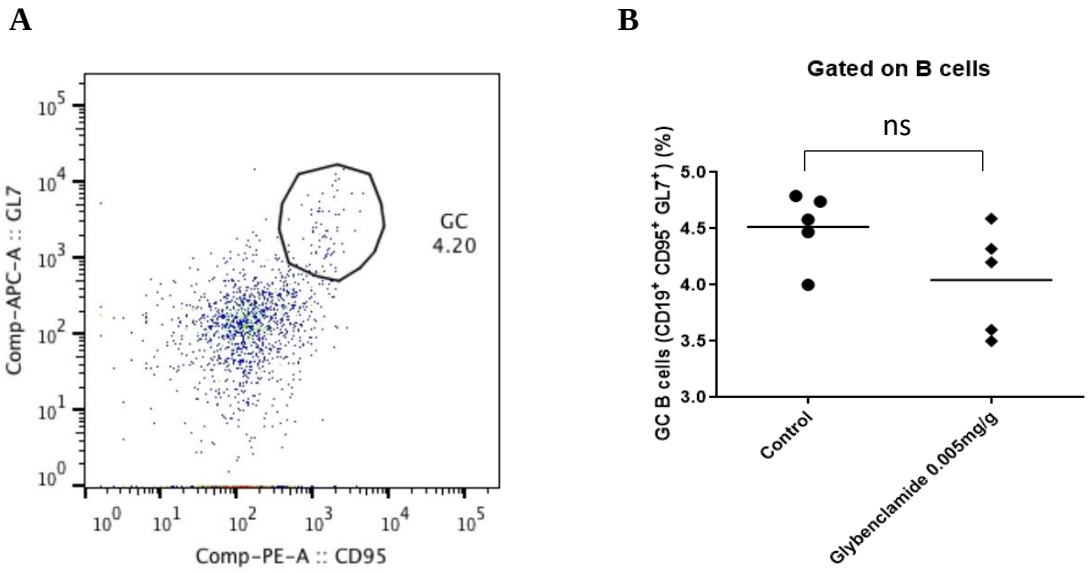

Appendix II. 1. Flow cytometry analysis. Percentage quantification of GC B cells ($CD19^+$ $GL7^+$ $CD95^+$). a) Representative flow cytometry plot gated on B cells. The indicated value refers to a percentage. b) Each dot represents an individual mouse and the horizontal bars denote mean values. (ns: p-value>0.05, by unpaired t-test).

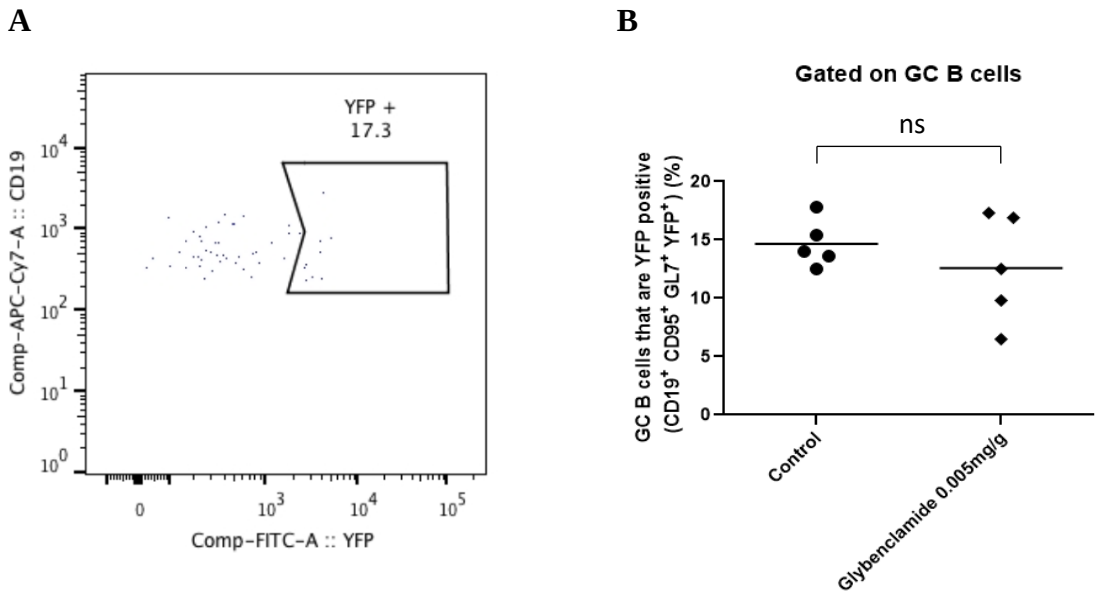

Appendix II. 2. Flow cytometry analysis. Percentage quantification of infected GC B cells ($CD19^+$ $GL7^+$ $CD95^+$ YFP^+). a) Representative flow cytometry plot gated on GC B cells. The indicated value refers to a percentage b) Each dot represents an individual mouse and the horizontal bars denote mean values. (ns: p-value>0.05, by unpaired t-test).

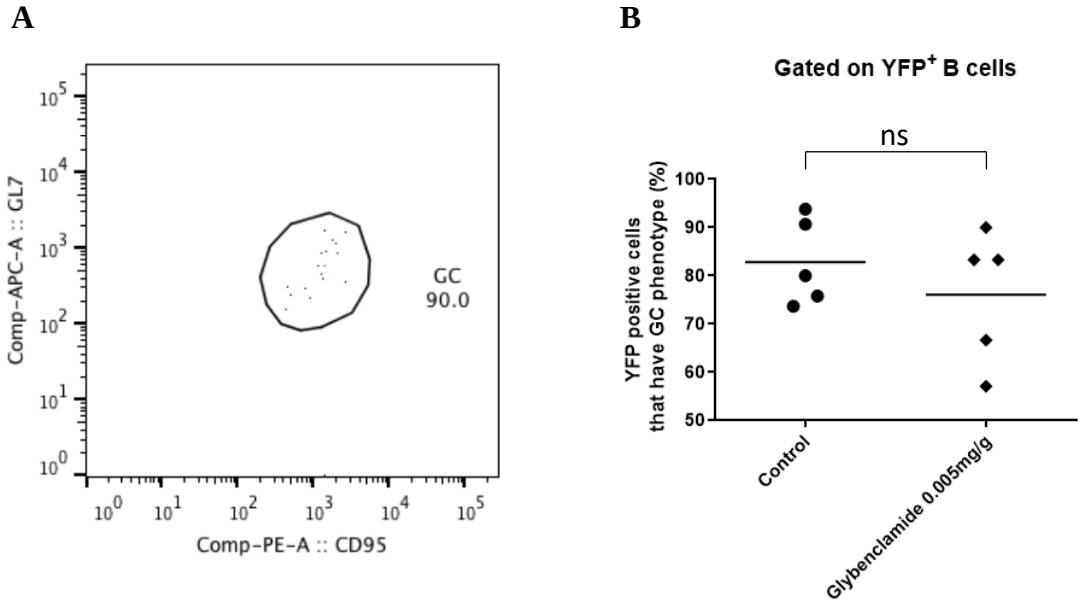

Appendix II. 3. Flow cytometry analysis. Percentage quantification of infected B cells with GC phenotype ($CD19^+$ YFP^+). a) Representative flow cytometry plot gated on YFP positive B cells. The indicated value refers to a percentage. b) Each dot represents an individual mouse and the horizontal bars denote mean values. (ns: p-value>0.05, by unpaired t-test).